UFCG

PPGECA

Universidade Federal de Campina Grande

OBTENÇÃO DE EQUAÇÕES IDF PARA ESTUDOS DE CHUVAS INTENSAS NO BRASIL: ABORDAGEM ANALÍTICA, USO DE SENSORIAMENTO REMOTO E PROPOSTA DE FERRAMENTA

Fagner França da Costa

Universidade Federal de Campina Grande - UFCG
Centro de Tecnologia e Recursos Naturais - CTRN
Pós-Graduação em Engenharia Civil e Ambiental - PPGECA

FAGNER FRANÇA DA COSTA

OBTENÇÃO DE EQUAÇÕES IDF PARA ESTUDOS DE CHUVAS INTENSAS NO BRASIL: ABORDAGEM ANALÍTICA, USO DE SENSORIAMENTO REMOTO E PROPOSTA DE FERRAMENTA

Campina Grande – PB
2024

FAGNER FRANÇA DA COSTA

OBTENÇÃO DE EQUAÇÕES IDF PARA ESTUDOS DE CHUVAS INTENSAS NO BRASIL: ABORDAGEM ANALÍTICA, USO DE SENSORIAMENTO REMOTO E PROPOSTA DE FERRAMENTA

Tese apresentada ao Programa de Pós-Graduação em Engenharia Civil e Ambiental da Universidade Federal de Campina Grande, como requisito para obtenção do título de Doutor em Engenharia Civil e Ambiental, com ênfase em Recursos Hídricos.

Orientadores: Drª Iana Alexandra Alves Rufino
Dr. Ricardo de Aragão

Campina Grande – PB
2024

C837o Costa, Fagner França da.
Obtenção de equações IDF para estudos de chuvas intensas no Brasil: abordagem analítica, uso de sensoriamento remoto e proposta de ferramenta / Fagner França da Costa. – Campina Grande, 2024.
121 f. : il. color.

Tese (Doutorado em Engenharia Civil e Ambiental) – Universidade Federal de Campina Grande, Centro de Tecnologia e Recursos Naturais, 2024.
"Orientação: Profa. Dra. Iana Alexandra Alves Rufino, Prof. Dr. Ricardo de Aragão".
Referências.

1. Chuvas Intensas. 2. Mudanças Climáticas. 3. Inundações. 4. Sensoriamento Remoto. 5. Recursos Hídricos. I. Rufino, Iana Alexandra Alves. II. Aragão, Ricardo de. III. Título.

CDU 551.578.1(043)

FICHA CATALOGRÁFICA ELABORADA PELA BIBLIOTECÁRIA SEVERINA SUELI DA SILVA OLIVEIRA CRB-15/225

MINISTÉRIO DA EDUCAÇÃO
UNIVERSIDADE FEDERAL DE CAMPINA GRANDE
POS-GRADUACAO ENGENHARIA CIVIL AMBIENTAL
Rua Aprigio Veloso, 882, - Bairro Universitario, Campina Grande/PB, CEP 58429-900

REGISTRO DE PRESENÇA E ASSINATURAS

1. **ATA DA DEFESA PARA CONCESSÃO DO GRAU DE DOUTOR EM ENGENHARIA CIVIL E AMBIENTAL**

2. **ALUNO(A): FAGNER FRANÇA DA COSTA / COMISSÃO EXAMINADORA: DR.ª IANA ALEXANDRA ALVES RUFINO - PPGECA/UFCG (PRESIDENTE) - ORIENTADORA, DR. RICARDO DE ARAGÃO – UFCG – COORIENTADOR, DR. CARLOS DE OLIVEIRA GALVÃO – PPGECA/UFCG – EXAMINADOR INTERNO, DR. CRISTIANO DAS NEVES ALMEIDA - UFPB – EXAMINADOR EXTERNO, DR. MARCO AURÉLIO HOLANDA DE CASTRO - UFC - EXAMINADOR EXTERNO, DR.ª ANDRÉA SOUSA FONTES - UFBA - EXAMINADORA EXTERNA (PORTARIA 26/2024). / TITULO DA TESE: "OBTENÇÃO DE EQUAÇÕES IDF PARA ESTUDOS DE CHUVAS INTENSAS NO BRASIL: ABORDAGEM ANALÍTICA, USO DE SENSORIAMENTO REMOTO E PROPOSTA DE FERRAMENTA" / ÁREA DE CONCENTRAÇÃO: RECURSOS HÍDRICOS E SANEAMENTO AMBIENTAL / HORA DE INICIO: 08:30 HORAS / FORMA DA SESSÃO: POR VIDEOCONFERÊNCIA.**

3. **EM SESSÃO REALIZADA POR VIDEOCONFERÊNCIA, APÓS EXPOSIÇÃO DE CERCA DE 40 MINUTOS, O(A) ALUNO(A) FOI ARGUIDO(A) ORALMENTE PELOS MEMBROS DA COMISSÃO EXAMINADORA, TENDO DEMONSTRADO SUFICIÊNCIA DE CONHECIMENTO E CAPACIDADE DE SISTEMATIZAÇÃO NO TEMA DE SUA TESE, SENDO-LHE ATRIBUÍDO O CONCEITO "EM EXIGÊNCIA", SENDO QUE A POSSIBILIDADE DE APROVAÇÃO ESTÁ CONDICIONADA À AVALIAÇÃO DA NOVA VERSÃO DO TRABALHO FINAL, SEGUINDO PROCEDIMENTOS PREVISTOS NA RESOLUÇÃO DO PROGRAMA. O PRESIDENTE DA COMISSÃO EXAMINADORA, OUVIDOS OS DEMAIS MEMBROS, DEVERÁ FICAR RESPONSÁVEL POR ATESTAR QUE AS CORREÇÕES SOLICITADAS NA LISTA DE EXIGÊNCIAS FORAM ATENDIDAS NA VERSÃO FINAL DO TRABALHO. A COMISSÃO EXAMINADORA, CUMPRINDO OS PRAZOS REGIMENTAIS, ESTABELECE UM PRAZO MÁXIMO DE 30 DIAS PARA QUE SEJAM FEITAS AS ALTERAÇÕES EXIGIDAS. APÓS O DEPÓSITO FINAL DO DOCUMENTO DE TESE, DEVIDAMENTE REVISADO E MEDIANTE ATESTADO DO ORIENTADOR, O CONCEITO "EM EXIGÊNCIA" PASSARÁ IMEDIATAMENTE PARA O DE "APROVADO". NA FORMA REGULAMENTAR, FOI LAVRADA A PRESENTE ATA, QUE É ASSINADA POR MIM, FLÁVIO PEREIRA DA CUNHA, SECRETÁRIO(A), ALUNO(A) E OS MEMBROS DA COMISSÃO EXAMINADORA PRESENTES.**

4. **CAMPINA GRANDE, 28 DE AGOSTO DE 2024**

5.

6. gov.br Documento assinado digitalmente
CRISTIANO DAS NEVES ALMEIDA
Data: 04/09/2024 04:57:41-0300
Verifique em https://validar.iti.gov.br

7.

8. _____

9. **DR. CRISTIANO DAS NEVES ALMEIDA – EXAMINADOR EXTERNO**

10.

11. gov.br Documento assinado digitalmente
MARCO AURELIO HOLANDA DE CASTRO
Data: 02/09/2024 19:39:17-0300
Verifique em https://validar.iti.gov.br

12.

13. _____

14. **DR. MARCO AURÉLIO HOLANDA DE CASTRO – EXAMINADOR EXTERNO**

15.

16. gov.br Documento assinado digitalmente
ANDREA SOUSA FONTES
Data: 04/09/2024 09:49:59-0300
Verifique em https://validar.iti.gov.br

17.

18. _____

19. **DR.ª ANDRÉA SOUSA FONTES - EXAMINADORA EXTERNA**

Documento assinado eletronicamente por **Fagner França da Costa**, **Usuário Externo**, em 29/08/2024, às 09:51, conforme horário oficial de Brasília, com fundamento no art. 8º, caput, da Portaria SEI nº 002, de 25 de outubro de 2018.

Documento assinado eletronicamente por **IANA ALEXANDRA ALVES RUFINO**, **PROFESSOR(A) DO MAGISTERIO SUPERIOR**, em 29/08/2024, às 16:51, conforme horário oficial de Brasília, com fundamento no art. 8º, caput, da Portaria SEI nº 002, de 25 de outubro de 2018.

Documento assinado eletronicamente por **CARLOS DE OLIVEIRA GALVAO**, **PROFESSOR(A) DO MAGISTERIO SUPERIOR**, em 30/08/2024, às 08:14, conforme horário oficial de Brasília, com fundamento no art. 8º, caput, da Portaria SEI nº 002, de 25 de outubro de 2018.

Documento assinado eletronicamente por **FLAVIO PEREIRA DA CUNHA**, **SECRETÁRIO (A)**, em 30/08/2024, às 09:22, conforme horário oficial de Brasília, com fundamento no art. 8º, caput, da Portaria SEI nº 002, de 25 de outubro de 2018.

Documento assinado eletronicamente por **RICARDO DE ARAGAO**, **PROFESSOR(A) DO MAGISTERIO SUPERIOR**, em 30/08/2024, às 14:50, conforme horário oficial de Brasília, com fundamento no art. 8º, caput, da Portaria SEI nº 002, de 25 de outubro de 2018.

A autenticidade deste documento pode ser conferida no site https://sei.ufcg.edu.br/autenticidade, informando o código verificador **4665051** e o código CRC **77A32AE7**.

Referência: Processo nº 23096.047999/2024-10 SEI nº 4665051

DEDICATÓRIA

"*Existe uma herança de deus separada para cada um de nós, existe um propósito, para mim e para você, creia*".

Regis Danese

AGRADECIMENTOS

Primeiramente agradeço a Deus pelo dom da vida e por me guiar para a realização deste sonho;

À minha família, em especial aos meus pais Martinho Costa e Margarida Costa;

Ao Conselho Nacional de Desenvolvimento Científico e Tecnológico (CNPq) pela concessão da bolsa;

Ao Laboratório de Hidráulica 2 pela infraestrutura fornecida;

Aos professores, Drª. Iana Rufino e Dr. Ricardo Aragão, pela paciência, amizade, confiança e orientação na realização desta pesquisa;

Aos professores da Pós-Graduação em Engenharia Civil e Ambiental (PPGECA/UFCG) pelos conhecimentos que transmitiram;

Aos meus colegas da turma de doutorado, especialmente Rivaildo e Mariano, pela convivência, ensinamentos e amizades; e

Por fim, a todos que direta ou indiretamente contribuíram para a conclusão deste trabalho, o meu muito obrigado.

RESUMO

Eventos extremos de precipitação e seus impactos nos sistemas hidrológicos e na sociedade são considerações críticas na engenharia e gestão de recursos hídricos. Com base no exposto, a presente tese tem como objetivo principal apresentar uma abordagem metodológica para a definição de equações IDF, de forma a contribuir com os estudos de chuvas intensas no Brasil. A principal hipótese desta tese é que os estudos e projetos que dependem diretamente de dados históricos de chuvas intensas devem considerar as mudanças nos padrões pluviométricos observados nos últimos anos, quer tenham sido efeitos de mudanças climáticas ou de ações antrópicas, e que, é preciso lançar mão de bases de dados, ferramentas e procedimentos analíticos capazes de dar um melhor suporte para os mesmos. Para responder as hipóteses, três etapas principais foram realizadas. Sendo cada etapa correspondente a um objetivo específico, detalhado da seguinte forma: (i) equações de Intensidade-Duração-Frequência (IDF) e regionalização de seus parâmetros; (ii) avaliação de desempenho de quatro produtos de sensoriamento remoto ao longo da estimativa de precipitação; e (iii) desenvolvimento de uma ferramenta para estudos de chuvas intensas no Brasil. As duas primeiras etapas foram aplicadas no Estado da Paraíba. A última etapa foi aplicada em todo o Brasil. Os resultados permitiram visualizar que o desempenho insatisfatório dos produtos de estimativa de precipitação deve ser atribuído principalmente a regiões de alta elevação e regiões costeiras. A ferramenta desenvolvida, denominada GEOT-IDF Equations, apresentou resultados promissores na definição de equações IDF. De forma geral, todos os estudos desenvolvidos demonstraram utilidade e elevado potencial de exploração na engenharia e gestão de recursos hídricos, como avaliação de eventos de chuvas intensas e definição de precipitação de projeto.

Palavras-chave: Chuvas intensas, mudanças climáticas, inundações, sensoriamento remoto.

ABSTRACT

Extreme precipitation events and their impacts on hydrological systems and society are critical considerations in water resources engineering and management. Based on the above, this thesis aims to present a methodological approach for defining IDF equations to contribute to studies of heavy rainfall in Brazil. The central hypothesis of this thesis is that studies and projects that directly depend on historical data on heavy rainfall should consider changes in rainfall patterns observed in recent years, whether they were effects of climate change or human actions, and that it is necessary to use databases, tools, and analytical procedures capable of providing better support for them. Three main steps were carried out to answer the hypotheses. Each step corresponds to a specific objective, detailed as follows: (i) Intensity-Duration-Frequency (IDF) equations and regionalization of their parameters; (ii) performance evaluation of four remote sensing products throughout the precipitation estimation; and (iii) development of a tool for heavy rainfall studies in Brazil. The first two stages were applied in the state of Paraíba. The last stage was applied throughout Brazil. The results showed that the unsatisfactory performance of the rainfall estimation products should be attributed mainly to high-elevation and coastal regions. The developed tool, GEOT-IDF Equations, showed promising results in defining IDF equations. In general, all the studies developed demonstrated usefulness and high potential for exploration in water resources engineering and management, such as assessing heavy rainfall events and defining design rainfall.

Keywords: Intense rains, climate change, floods, remote-sensing.

LISTA DE FIGURAS

LISTA DE TABELAS

LISTA DE EQUAÇÕES

LISTA DE ABREVIATURAS E SIGLAS

a, b, c, d, e, f.	parâmetros empíricos
AESA.	Agência Executiva de Gestão das Águas do Estado da Paraíba
AGRIAMBI.	Revista Brasileira de Engenharia Agrícola e Ambiental
ASCAT.	*Advanced Scatterometer*
CA.	coeficiente de ajuste
CETESB.	*Company Environmental Sanitation Technology of the State of São Paulo*
CHC.	*Climate Hazards Center*
CHIRPS.	*Climate Hazards Group InfraRed Precipitation*
CHRS.	*Center for Hydrometeorology and Remote Sensing*
CMR.	coeficiente de massa residual
D.	*adjustment distribution*
DMI.	Departamento Meteorológico Indiano
EUMETSAT.	*European Meteorological Satellite Organization*
FAR.	Taxa de Alarme Falso
FO.	Função objetivo
GEV.	*Generalized Extreme Values*
HCV.	*high-level cyclonic vortices*
IBGE.	Instituto Brasileiro de Geografia e Estatística
IDF.	Intensidade-Duração-Frequência
ITCZ.	*intertropical convergence zone*
KGE.	eficiência Kling-Gupta
KS.	Kolmogorov-Smirnov
LI.	*squall lines*
MAE.	Erro médio absoluto
MB.	máximo de bloco
MCG.	Modelos Climáticos Globais
MCR.	Modelos Climáticos Regionais
NEB.	*Northeast Brazil*
NOAA.	*National Oceanic and Atmospheric Administration*

NS.	eficiência de Nash-Sutcliffe
OMM.	Organização Meteorológica Mundial
PDIR-Now.	*Dynamic Infrared-Rain Rate*
POD.	Probabilidade de Detecção
POT.	*peak over threshold method*
R^2.	Coeficiente de determinação
RC.	*climatic region*
RMSE.	Raiz do erro quadrático médio
RS.	*remote-sensing*
SD.	desvio padrão
SM2RAIN.	*Soil Moisture to Rain*
SM2RAIN-ASCAT.	*Soil Moisture to Rain - Advanced SCATterometer*
SMA.	série máxima anual
SPPs.	*Satellite Precipitation Products*
SUDENE.	Superintendência do Desenvolvimento do Nordeste
t.	duração
T_r.	Período de retorno
TS.	Taxa de Sucesso
UCI.	*University of California, Irvine*
USGS.	*US Geological Survey*
VCAS.	*Cyclonic Vortices of High Level*
WMO.	*World Meteorological Organization*

SUMÁRIO

Capítulo

1

1. INTRODUÇÃO

1.1. Caracterização do problema

Entre as obras de engenharia de recursos hídricos utilizadas para mitigar ou controlar o excesso de escoamento superficial, as medidas estruturais intensivas (convencionais) mais utilizadas são a macro e a microdrenagem urbana, também denominados de sistemas de drenagem urbana.

Dados hidrológicos, como precipitação e vazão de projeto, são usados para dimensionar os elementos que fazem parte dos sistemas de drenagem urbana e devem ser bem caracterizados. Além disso, vale ressaltar, que para garantir a capacidade de suporte destas estruturas hidráulicas, são necessárias ações permanentes e continuadas de manutenção, bem como (e tão importante quanto), atualizações das equações empíricas utilizadas no projeto de possíveis novas estruturas e ou recuperações de infraestrutura antiga, como, por exemplo, as relações de Intensidade-Duração-Frequência (IDF).

Neste contexto, a chamada "vazão de projeto" é um dado de entrada essencial para o dimensionamento de obras hidráulicas e é obtida a partir da chuva de projeto, sendo a conversão

de chuva em vazão, efetuada através de um modelo chuva-vazão, como é o caso do método racional (Back e Cadorin, 2021). Sendo assim, é importante que as IDFs sejam o mais atualizadas e precisas possíveis, o que vai depender da qualidade dos dados de entrada (séries temporais de precipitação) e dos métodos de inferência estatística (Ombadi et al., 2018).

Até o ano de 2020, por exemplo, o Brasil havia catalogado cerca de 3.096 equações de chuvas intensas, publicadas em 118 artigos, sendo 10 artigos acadêmicos, teses e dissertações, 61 artigos publicados em revistas científicas, 27 artigos em eventos científicos e 20 artigos classificados como livros e relatórios técnicos (Back e Cadorin 2021), sendo o engenheiro Otto Pfafstetter (1957) o pioneiro dessas equações IDF no Brasil.

Este número de estudos mostra a importância de tais informações para um dimensionamento adequado de obras hidráulicas. No entanto, os estudos disponíveis podem ser considerados defasados tendo em vista a realidade cada vez mais plausível de mudanças nos regimes hidrológicos e a dificuldade de garantir através de uma relação matemática estas vazões de projeto em cenários de constante mudança climática e de uso e ocupação do solo.

Estas mudanças reforçam a necessidade de informações atualizadas com frequência sobre as equações IDF, tal como vários estudos argumentam (por exemplo, Pérez-Zanón et al., 2016; Hosseinzadehtalaei et al., 2019; Ren et al., 2019; Fowler et al., 2021a; Shabankareh e Abedini, 2023).

Outro desafio até então não resolvido é o de ter uma ferramenta capaz de gerar equações IDF para todos os estados do Brasil. A maioria das publicações apresenta soluções para uma aplicação local ou desatualizadas (Chang et al., 2013; Simonovic et al., 2015; Rodrigues et al., 2023; Vargas et al., 2023; GPRH, 2024).

Embora estas pesquisas contribuam enormemente para a gestão das águas pluviais urbanas e a mitigação de desastres, observa-se uma oportunidade de inovação. Por exemplo, a ausência de uma ferramenta conectada a um serviço contínuo e online de dados de precipitação é altamente relevante, principalmente nos dias de hoje, dada as mudanças nos padrões de precipitações verificados nos últimos anos.

Além disso, apesar dos recentes avanços na formulação de relações IDF, na grande maioria dos países, a definição/atualização de relações IDF continua sendo um grande desafio. Isso se deve principalmente à disponibilidade limitada de registros pluviométricos ou pluviográficos, como no Brasil. Daí, a importância também de uma ferramenta capaz de incorporar registros de

precipitações estimados a partir de produtos de sensoriamento remoto (SR), assim como a utilização de Modelos Climáticos Globais (MCG) e/ou Modelos Climáticos Regionais (MCR), dada as mudanças climáticas intensificadas pela ação antrópica (IPCC, 2023) e os efeitos de Ilha de Calor Urbana (Wang et al., 2020).

1.2. Justificativa

O aquecimento global colocou a ciência em alerta, pois é reconhecido como resultado do impacto causado por algumas atividades humanas (queima excessiva de combustíveis fósseis, desmatamento) (IPCC, 2023). O aquecimento global potencializa o efeito estufa, que deixa de ser apenas um fenômeno natural que torna possível a vida na Terra, para se tornar um risco para a humanidade.

De acordo com Guven et al. (2021), no próximo século, o clima testemunhará mudanças ameaçadoras à medida que os humanos continuarem as suas atividades que aumentam os gases do efeito estufa. Isto resultará em graves problemas globais, como alterações no ciclo hidrológico, que provocarão um aumento na intensidade de eventos extremos (secas prolongadas e chuvas intensas, por exemplo).

Além desse fato, as alterações nas características naturais do meio ambiente causadas pelo intenso desenvolvimento dos centros urbanos (remoção da vegetação, impermeabilização do solo, alteração das características naturais dos rios), também afetam diretamente o ciclo hidrológico local (Yulianto et al., 2020), como: alteração no grau de impermeabilização da bacia hidrográfica, o que, consequentemente, leva à diminuição do volume infiltrado e ao aumento da vazão superficial, principalmente em ruas sem infraestrutura de drenagem de águas pluviais.

A falta de infra-estruturas hidráulicas, a má concepção ou a falta de manutenção das obras já existentes, podem tornar os centros urbanos mais susceptíveis a desastres causados por alagamentos e inundações durante chuvas fortes ou de longa duração, causando graves impactos na população local.

O fato é que as inundações são hoje uns dos desastres mais recorrentes e destrutivos em todo o mundo, pois provocam perdas econômicas, geram mortes e interrompem os serviços públicos (Kind e Botzen, 2016; Yin et al., 2016). A frequência das inundações cresce à medida que a população urbana aumenta, visto que, mais áreas são impermeabilizadas e, como consequência, mais pessoas se tornam sujeitas a eventos extremos de inundação causados por chuvas cada vez

mais intensas e frequentes, em parte, devido as mudanças climáticas (Chang et al., 2021). Estudos mostram que as mudanças climáticas têm aumentado a frequência e a duração das precipitações e, por consequência, a incidência das inundações em muitas bacias hidrográficas impermeabilizadas e em áreas de baixadas e de fundo de vales (Bui et al., 2019).

Segundo dados de Donatti et al. (2024), 89.462 pessoas morreram entre 2000 e 2022 no mundo devido a essas catástrofes. América Central, Caribe, Leste da África, incluindo Madagascar, e Sul e Leste da Ásia foram as regiões que mais sofreram. Para o mesmo período, o Brasil está na segunda categoria mais crítica como um dos países que mais sofreram com enchentes. O alcance dos eventos varia de 58 a 108 (EM-DAT/CRED 2023). No ano de 2024, por exemplo, o país enfrenta um enorme desastre hidrológico que atingiu quase todo o estado do Rio Grande do Sul (478 de 497 municípios) e atualmente já registra 175 mortes e 38 desaparecidos, além de muitos outros feridos, prejuízos e tristes consequências (G1 RS, 2024).

1.3. Hipóteses

A principal hipótese desta tese é que os estudos e projetos que dependem diretamente de dados históricos de chuvas intensas devem considerar as mudanças nos padrões pluviométricos observados nos últimos anos, quer tenham sido efeitos de mudanças climáticas ou de ações antrópicas, e que, é preciso lançar mão de bases de dados, ferramentas e procedimentos analíticos capazes de dar um melhor suporte para os mesmos.

1.4. Objetivos

1.4.1. Objetivo geral

Apresentar uma abordagem metodológica para a definição de equações IDF, de forma a contribuir com os estudos de chuvas intensas no Brasil.

1.4.2. Objetivo específicos

- Atualizar e regionalizar as equações IDF para todo o território do Estado da Paraíba;
- Avaliar a aplicação de produtos de sensoriamento remoto na estimativa de totais precipitados no Estado da Paraíba; e
- Propor uma ferramenta para obtenção e atualização contínua das equações IDF.

1.5. Estrutura geral do documento da tese

Este documento tese está estruturado em oito capítulos. Para uma visão geral de como os objetivos da tese e publicações derivadas desta pesquisa se articulam é apresentada a Figura 1.

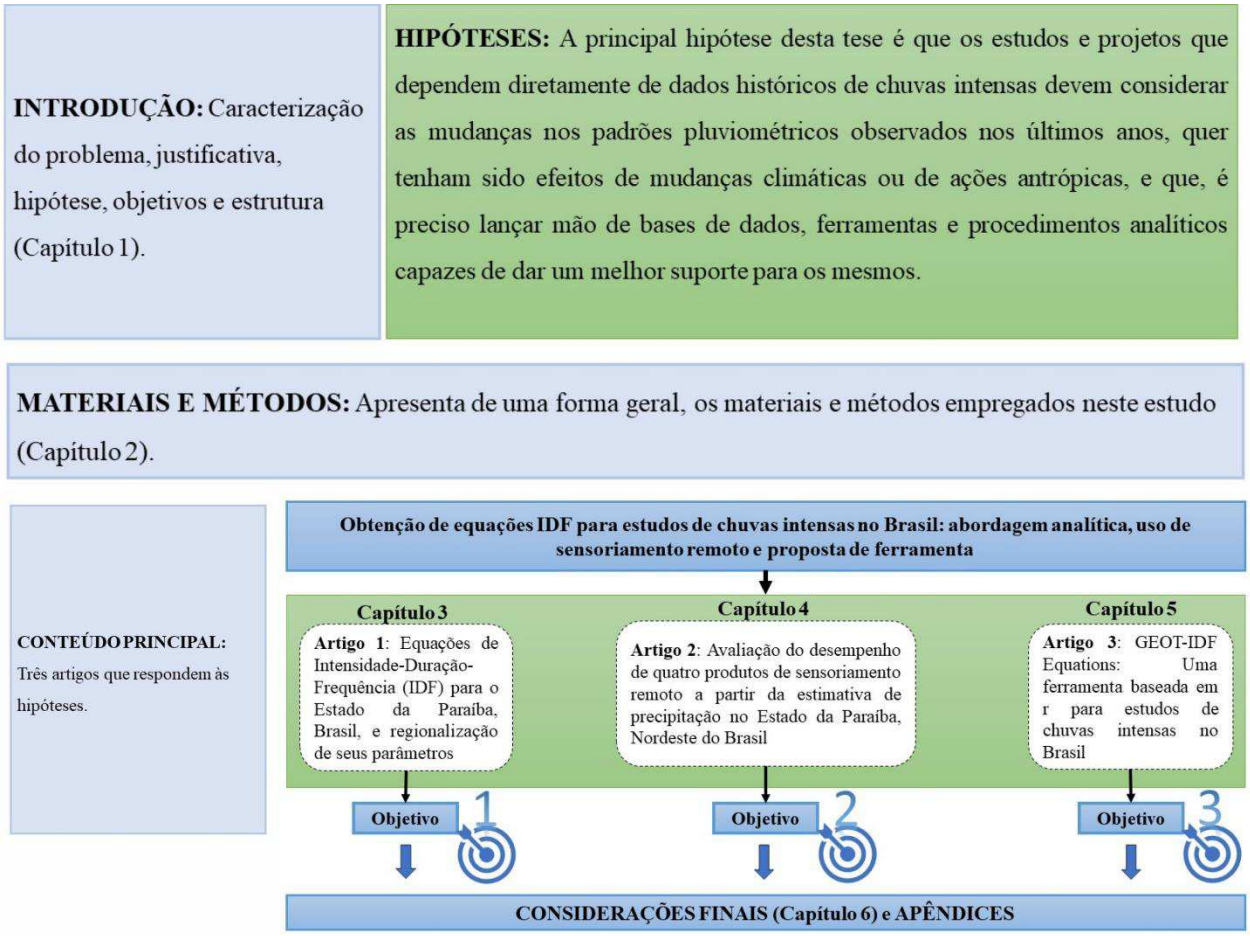

Figura 1 – Visão geral da Tese

Este capítulo (capítulo 1) apresenta a caracterização do problema, justificativa, hipóteses e os objetivos deste estudo, bem como a estrutura geral da tese. O segundo capítulo, apresenta de uma forma geral, os materiais e métodos empregados neste estudo.

O terceiro capítulo consiste na atualização e regionalização de equações IDF para o território estadual da Paraíba. A publicação derivada desta etapa da pesquisa já foi publicada na Revista Brasileira de Engenharia Agrícola e Ambiental – AGRIAMBI (https://www.agriambi.com.br/). Neste documento o artigo é apresentado exatamente da forma como foi publicado.

O quarto capítulo diz respeito a uma avaliação do desempenho de diferentes produtos de sensoriamento remoto na estimativa de totais precipitados. Os resultados desta avaliação foram

publicados na Revista Remote Sensing Applications: Society and Environment (https://www.sciencedirect.com/journal/remote-sensing-applications-society-and-environment). Neste documento o artigo é apresentado exatamente da forma como foi publicado.

O quinto capítulo consiste no desenvolvimento de uma ferramenta para obtenção e atualização automática e contínua de equações IDF para todo o país. Os resultados desta etapa da pesquisa foram submetidos em forma de artigo para a Revista Earth Science Informatics (https://link.springer.com/journal/12145) e, encontra-se (no momento da redação deste documento - Tese) com o status de aceite pela revista. É apresentado então, o texto referente à versão mais atual deste artigo.

Como sexto capítulo desta tese, são apresentadas considerações finais, de forma a percorrer os 3 artigos apresentados, identificando os objetivos alcançados, as limitações gerais da pesquisa e suas possibilidades de continuidade.

Ao final, há o apêndice A que contêm as equações IDF para todo o território do Estado da Paraíba.

Por fim, esclareço que ao optar pela apresentação dos artigos publicados e submetido em forma de capítulos, não há um capítulo final de referências bibliográficas, sendo estas apresentadas ao final de cada capítulo.

1.6. Referências

Back Á. J. S., Cadorin S. B. (2021). Heavy rain equations for Brazil. International Journal of Development Research. https://doi.org/10.37118/ijdr.20850.01.2021.

Bui D. T., Ngo P. T., Pham T. D., Jaafari A., Minh N. Q., Hoa P. V., Samui P. (2019). A novel hybrid approach based on a swarm intelligence optimized extreme learning machine for flash flood susceptibility mapping. Catena. http://dx.doi.org/10.1016/j.catena.2019.04.009.

Chang K. B., Lai S. H., Faridah O. (2013). RainIDF: automated derivation of rainfall intensity–duration–frequency relationship from annual maxima and partial duration series. Journal of Hydroinformatics. https://doi.org/10.2166/hydro.2013.192.

Chang H., Pallathadka A., Sauer J., Grimm N., Zimmerman R., Cheng C., Iwaniec D. M., Kim Y., Lloyd R., Mcphearson T., Rosenzweig B., Troxler T., Welty C., Brenner R., Herreros-Cantis P.

(2021). Assessment of Urban Flood Vulnerability Using the Social-Ecological-Technological Systems Framework in Six US cities. Sustainable Cities and Society. https://doi.org/10.1016/j.scs.2021.102786.

Donatti C. I., Nicholas K., Fedele G., Delforge D., Speybroeck N., Moraga P., Blatter J., Below R., Zvoleff A. (2024). Global hotspots of climate-related disasters. International Journal of Disaster Risk Reduction. http://dx.doi.org/10.1016/j.ijdrr.2024.104488.

EM-DAT/CRED (2023). Centre for Research on the Epidemiology of Disasters. Bruxelas, Bélgica. Retrieved from. www.emdat.be.

Fowler H. J., Lenderink G., Prein A. F., Westra S., Allan R. P., Ban N., Barbero R., Berg P., Blenkinsop S., Do H. X., Guerreiro S., Haerter J. O., Kendon E. J., Lewis E., Schaer C., Sharma A., Villarini G., Wasko C., Zhang X. (2021a). Anthropogenic intensification of short-duration rainfall extremes. Nature Reviews Earth & Environment. https://doi.org/10.1038/s43017-020-00128-6.

G1 RS - Globo news portal of Rio Grande do Sul (2024). A month of floods in RS: see the chronology of the disaster that hit 471 cities, killed more than 170 people and forced 600 thousand from their homes. Retrieved from. https://g1.globo.com/rs/rio-grande-do-sul/noticia/2024/05/29/um-mes-de-enchentes-no-rs-veja-cronologia-do-desastre.ghtml.

Guven A., Pala A., Sheikhvaisi M. (2021). Investigation of impact of climate change on small catchments using different climate models and statistical approaches. Water Supply. https://doi.org/10.2166/ws.2021.383.

GPRH. Water Resources Research Group – Federal University of Viçosa. Retrieved from. https://www.gprh.ufv.br/?area=softwares.

Hosseinzadehtalaei P., Tabari H., Willems P. (2019). Regionalization of anthropogenically forced changes in 3 hourly extreme rainfall over Europe. Environmental Research Letters. https://doi.org/10.1088/1748-9326/ab5638.

IPCC. Climate Change 2023: The Physical Science Basis. Disponível online: https://www.gov.br/mcti/pt-br/acompanhe-o-mcti/sirene/publicacoes/relatorios-do-ipcc/arquivos/pdf/copy_of_IPCC_Longer_Report_2023_Portugues.pdf. Acessado em 08 de agosto 2024.

Kind J., Botzen W. J. W., Aerts J. C. J. H. (2016). Accounting for risk aversion, income distribution and social welfare in cost-benefit analysis for flood risk management. Wires Climate Change. https://doi.org/10.1002/wcc.446.

Ombadi M., Nguyen P., Sorooshian S., Hsu Kuo-Lin (2018). Developing Intensity-Duration-Frequency (IDF) Curves From Satellite-Based Precipitation: Methodology and Evaluation. Water Resources Research. http://dx.doi.org/10.1029/2018WR022929.

Pfafstetter O. (1957). Chuvas Intensas no Brasil. Rio de Janeiro: DNOS. 419p.

Pérez-Zanón N., Casas-Castillo M. C., Rodríguez-Solà R., Peña J. C., Rius A., Solé J. G., Redaño Á. (2016). Analysis of extreme rainfall in the Ebre Observatory (Spain). Theoretical and Applied Climatology. http://dx.doi.org/10.1007/s00704-015-1476-0.

Ren H., Hou Z. J., Wigmosta M., Liu Y., Leung L. R. (2019). Impacts of spatial heterogeneity and temporal non-stationarity on intensity-duration-frequency estimates-A case study in a mountainous California-Nevada watershed. Water. https://doi.org/10.3390/w11061296.

Rodrigues et al., organizers (2023). IDFGeo: web tool for acquiring IDF equations and project rainfall for monitored and non-monitored locations in the state of Rio Grande do Sul, Brazil: technical manual. [electronic resource]. Pelotas: POU. 36p.

Shabankareh R. N. T., Abedini M. J. (2023). Implementation of a probability matching method in developing intensity–duration–frequency relationships for sub-daily durations using IMERG satellite-based data. Hydrological Sciences Journal. http://dx.doi.org/10.1080/02626667.2023.2229817.

Simonovic S. P., Schardong A., Sandink D., Srivastav R. (2015). A web-based tool for the development of Intensity Duration Frequency curves under changing climate. Environmental Modelling & Software. https://doi.org/10.1016/j.envsoft.2016.03.016.

Yin J., Yu D., Yin Z., Liu M., He Q. (2016). Evaluating the impact and risk of pluvial flash flood on intra-urban road network: a case study in the city center of shanghai, China. Journal of Hydrology. https://doi.org/10.1016/j.jhydrol.2016.03.037.

Yulianto F., Suwarsono, Nugroho U. C., Nugroho N. P., Sunarmodo W., Khomarudin M. R. (2020). Spatial-temporal dynamics land use/land cover change and flood hazard mapping in the upstream citarum watershed, west java, Indonesia. Quaestiones Geographicae. http://dx.doi.org/10.2478/quageo-2020-0010.

Vargas M. M., Beskow S., Moura M.M., Cunha Z. A., Beskow T. L. C., Silveira J. P. M. (2023). GAM-IDF: a web tool for fitting IDF equations from daily rainfall data. International Journal of Hydrology Science and Technology. https://doi.org/10.1504/IJHST.2023.131882.

Wang W., Wang L., Miao Y., Cheng C., Chen S. (2020). A survey on the influence of intense rainfall. Journal of Infrastructure Preservation and Resilience. https://doi.org/10.1186/s43065-020-00003-0.

Capítulo

2

2. MATERIAIS E MÉTODOS

São apresentados neste capítulo (Capítulo 2) todos os materiais e métodos inerentes à tese como um todo. Estes podem vir a ser reapresentados e descritos (mesmo que de forma suscinta) em cada um dos artigos, mas aqui são apresentados de forma reunida para uma compreensão de todos os procedimentos metodológicos da tese.

Com relação aos dados, observam-se duas tipologias distintas: (i) dados advindos de observações remotas da superfície da terra; (ii) dados de observações por instrumentos de campo ou "*ground truth*". Para os procedimentos metodológicos adotados ambos são relevantes sendo os resultados obtidos ora por validação e comparação dos mesmos, ora pelo uso combinado de diferentes bases de dados e tipologias.

O ambiente RStudio (R Core Team, 2024) é a ferramenta escolhida para as análises sendo alguns dos resultados finalizados em ambiente SIG (Sowftare QGIS), ambos são softwares livres. Quanto ao ambiente RStudio, foi considerada as seguintes configurações:

- Versão R = 4.4.1 (https://cran.r-project.org/);
- Versão Rtools = 4.4 (https://cran.r-project.org/bin/windows/Rtools/);

- Software RStudio (https://posit.co/downloads/); e
- Sistema operacional: Windows.

Os procedimentos metodológicos escolhidos também são apresentados e agrupados em:

- Obtenção do dado e análise de consistência
- Análises de frequência
- Operações de desagregação (downscaling)
- Parametrização de geração das curvas IDF
- Desenvolvimento de ferramenta opensource, que permitam o acesso a grandes serviços de dados
- Apresentação das IDF em diferentes formatos e plataformas

2.1. Aquisição de dados

Quatro produtos de estimativa de precipitação via sensoriamento remoto foram avaliados neste estudo (Tabela 1).

Tabela 1 - Resumo dos produtos de precipitação de detecção remota avaliados neste estudo

Produto	Baseado	Resolução		Cobertura temporal	Referência
		Espacial	Temporal		
CHIRPS	Satélite	0,05º	Diário	2000-2020	Funk et al. (2014)
MSWEP	Combinações	0,1º		2000-2020	Beck et al. (2019)
PDIR-Now	Satélite	0,04º		2001-2020	Nguyen et al. (2020)
SM2RAIN-ASCAT		0,1º		2007-2020	Brocca et al. (2019)

Para avaliar a precisão dos dados dos quatro produtos de precipitação mencionados acima, esses conjuntos de dados foram comparados com dados de precipitação total diário extraídos de pluviômetros, que fornecem informações locais relativamente precisas. Para tanto, observações diárias de registros pluviométricos foram fornecidas pela Agência Executiva de Gestão das Águas do Estado da Paraíba (AESA, 2021).

Neste estudo, também foram considerados registros de pluviômetros extraídos do site HidroWeb (https://www.snirh.gov.br/hidroweb/serieshistoricas).

A ferramenta considera uma série temporal mínima de 30 anos, conforme recomendado pela Organização Meteorológica Mundial (OMM), para definir as equações IDF aplicando a metodologia de série máxima anual (SMA), um tipo de máximo de bloco - MB (Tanaka, 2021). Quando a série temporal é inferior a 30 anos, a ferramenta trabalha com o método pico acima do

limite (POT) (Liu et al., 2023). Por fim, o algoritmo remove quaisquer outliers e verifica se a série tem uma tendência climática usando o teste de Mann-Kendall (Mann, 1945; Kendall, 1975) a um nível de significância de 5% (Barbero et al. 2017).

O critério de seleção é que a série temporal deve ter lacunas de dados baixas (não mais que 10% de dados ausentes), uma condição imposta por vários estudos relatados por Rodrigues et al. (2021). Quando a lacuna de dados excede 10%, a ferramenta aplica o método de regressão K-*Nearest Neighbors* (Aha et al., 1991), uma técnica de aprendizado de máquina usada para prever valores contínuos com base na similaridade de dados. A ideia básica é prever o valor de uma nova observação, os K vizinhos (estações pluviométricas vizinhas) preenchem as lacunas na série temporal.

Embora não seja o foco da ferramenta, ela também fornece a opção de usar o produto de estimativa de precipitação diária CLIMBra com correção de viés e redução de escala (Ballarin et al., 2023) e produtos de estimativa de precipitação diária de sensoriamento remoto, como o MSWEP que já vem com correção de viés (Beck et al., 2019), para definir equações IDF. No entanto, esses conjuntos de dados meteorológicos são baseados em interpolação de dados *in-situ*, o que introduz um erro embutido. Portanto, uma análise de desempenho deve ser conduzida para verificar se esses conjuntos de dados podem simular dados *in-situ* para os quais as equações IDF devem ser desenvolvidas.

2.2. Métodos

2.2.1. Análise de frequência

Foram consideradas diferentes distribuições de probabilidade (Tabela 2) para obter a precipitação máxima diária que poderia ser igualada ou superada a cada 5, 10, 15, 20, 25, 50 e 100 anos (Naghettini e Pinto, 2007).

Tabela 2 - Resumo das distribuições de probabilidade consideradas neste estudo

Distribuição	Equação
Normal	$f(x;\mu;\sigma) = \frac{1}{\sqrt{2\pi\sigma^2}} * e^{\left(-\frac{(x-\mu)^2}{2\sigma^2}\right)}$
Gamma	$f(x;\xi;\beta) = \frac{1}{\beta^{\xi}\Gamma(\xi)} * x^{(\xi-1)} * e^{-\frac{x}{\beta}}$
Exponencial	$f(x;\lambda) = \lambda * e^{-\lambda x}$
Log-Normal	$f(x;\mu;\sigma) = \frac{1}{x\sigma\sqrt{2\pi}} * e^{\left(-\frac{(\ln(x)-\mu)^2}{2\sigma^2}\right)}$
Gumbel	$f(x;\theta;\beta) = \frac{1}{\beta} * e^{-(z+e^{-z})}$ where $z = \frac{x-\theta}{\beta}$
Weibull	$f(x;\beta;\xi) = \frac{\xi}{\beta} * \left(\frac{x}{\beta}\right)^{\xi-1} * e^{-(\frac{x}{\beta})^{\xi}}$
GEV	$f(x;\theta;\beta;\xi) = \frac{1}{\beta}\left[1+\xi\left(\frac{x-\theta}{\beta}\right)\right]^{\frac{-1}{\xi}} * e^{\left[-\left\{1+\xi\left(\frac{x-\theta}{\beta}\right)\right\}^{\frac{-1}{\xi}}\right]}$ para $1+\xi\left(\frac{x-\theta}{\beta}\right) > 0$

Onde x é o conjunto de dados, μ é a média da série temporal, σ é o desvio padrão da série temporal, ξ é o parâmetro de forma, β é o parâmetro de escala, λ é o parâmetro de taxa, e θ é o parâmetro de localização

Após calcular os parâmetros das distribuições, é definida a melhor distribuição com base no teste não paramétrico de Kolmogorov-Smirnov (Equação 1) e a razão de verossimilhança (Equação 2), que é considerado o mais eficiente para amostras grandes por apresentar menor variância nos estimadores (Naghettini e Pinto, 2007). Também foi considero o teste de qui-quadrado (Equação 3) para escolher entre distribuições candidatas.

$$T_{ks} = \max_{1\leq j\leq N}\left(\left|F(Y_j) - \left(\frac{j}{N+1}\right)\right|\right)$$

Equação 1

$$\lambda = -2 * \left(\log{*}L(\hat{\theta}_{fit}) - \log{*}L(\hat{\theta}_{null})\right)$$

Equação 2

$$x^2 = \sum \frac{(O_i - E_i)^2}{E_i}$$

Equação 3

Onde $F(Y_j)$ é a distribuição teórica, j é o valor começando em 1 e se estendendo até N, N é o tamanho da série temporal de precipitação, n é o tamanho da amostra, λ é a razão de verossimilhança, $\log{*}L(\hat{\theta}_{fit})$ é o logaritmo da função de verossimilhança maximizada do modelo ajustado aos dados, $\log{*}L(\hat{\theta}_{null})$ é o logaritmo da função de verossimilhança maximizada do modelo nulo, $\hat{\theta}_{fit}$ é a estimativa dos parâmetros do modelo ajustado, $\hat{\theta}_{null}$ é a estimativa dos

parâmetros do modelo nulo, x^2 é a estatística do teste qui-quadrado, O_i é a frequência observada para a categoria i, e E_i é a frequência esperada para a categoria i sob a distribuição teórica.

Foi empregado o método Weibull (Makkonen, 2005), em conjunto com o teste não paramétrico de Kolmogorov-Smirnov (Equação 1), a um nível de significância de 5%, para definir a melhor distribuição, levando em consideração o menor valor de KS. Em situações de empate, aplica-se o critério da razão de verossimilhança (Equação 2), em conjunto com o teste qui-quadrado (Equação 3), ao nível de significância de 5%, para definir a melhor distribuição.

2.2.2. Desagregação da precipitação

Após identificar a distribuição de probabilidade adequada para a série temporal de chuvas, foram obtidos os valores máximos de precipitação para os seguintes períodos de retorno (T_r): 5, 10, 15, 20, 25, 50 e 100 anos. Em seguida, esses valores foram primeiramente transformados em precipitação pluviométrica de 24 horas (CETESB, 1986) e depois desagregados pelas durações listadas na Tabela 4 utilizando a equação exponencial (Equação 4) proposta por Silveira (2000). Também é possível desagregar a precipitação diária em intervalos através do método Isozona (Torrico, 1974) (Equação 5, Tabela 3 e Figura 2) e o proposto por Back (2020) (Equação 6). Para cada duração de chuva, foi considerado um valor mínimo (Tabela 4) acima do qual a precipitação pode ser considerada intensa, conforme indicado pela CETESB (1986). O algoritmo incorpora ainda o método de desagregação de precipitação (Equação 7) proposto pelo Departamento Meteorológico Indiano - DMI (Basumatary e Sil 2017; Sam et al. 2021; Shamkhi et al. 2022; Bibi 2023).

$$C_{24}(t) = e^{1,5\times\ln\left(\frac{\ln(t)}{7,3}\right)}$$

Equação 4

$$P_{24h} = 1,095 * P_{1\text{-day}}$$

Equação 5

$$h = \left(\frac{t}{27,9327+3,8346t^{0,7924}}\right) * P_{1\text{-day}}$$

Equação 6

$$P_t = P_{24h} * \sqrt[3]{\frac{t}{1440}}$$

Equação 7

Onde $C_{24(t)}$ é o coeficiente aplicado à precipitação de 24 horas durante "t" (minutos); t é a duração (minutos); h é a precipitação total para um determinado período (mm), P_{24h} e a precipitação de 24h, $P_{1\text{-day}}$ é a precipitação provável com duração de 1 dia para o local selecionado, e P_t é a precipitação na duração de t-minutos (mm).

Tabela 3 - Relações entre precipitação e o método Isozona

Isozona	**1h/24h**										**6min/24h**	
	T_r											
	5	10	15	20	25	30	50	100	1000	10000	5-50	100
A	0,362	0,358	0,356	0,355	0,354	0,353	0,350	0,347	0,336	0,336	0,070	0,063
B	0,381	0,378	0,375	0,374	0,373	0,372	0,369	0,366	0,354	0,343	0,084	0,075
C	0,401	0,397	0,395	0,393	0,392	0,391	0,388	0,384	0,372	0,360	0,098	0,088
D	0,420	0,416	0,414	0,412	0,411	0,410	0,407	0,403	0,390	0,378	0,112	0,100
E	0,440	0,436	0,433	0,432	0,430	0,429	0,426	0,422	0,409	0,396	0,126	0,112
F	0,460	0,455	0,453	0,451	0,449	0,448	0,445	0,441	0,427	0,413	0,139	0,124
G	0,479	0,474	0,472	0,470	0,468	0,467	0,464	0,459	0,445	0,431	0,154	0,137
H	0,499	0,494	0,491	0,489	0,486	0,486	0,483	0,478	0,463	0,448	0,167	0,149

Tabela 4 - Valores mínimos de precipitação adotados

Duração (minutos)	**Precipitação (mm)**
5	8
10	10
15	15
20	15
30	20
60	25
360	40
480	40
720	47
1440	55

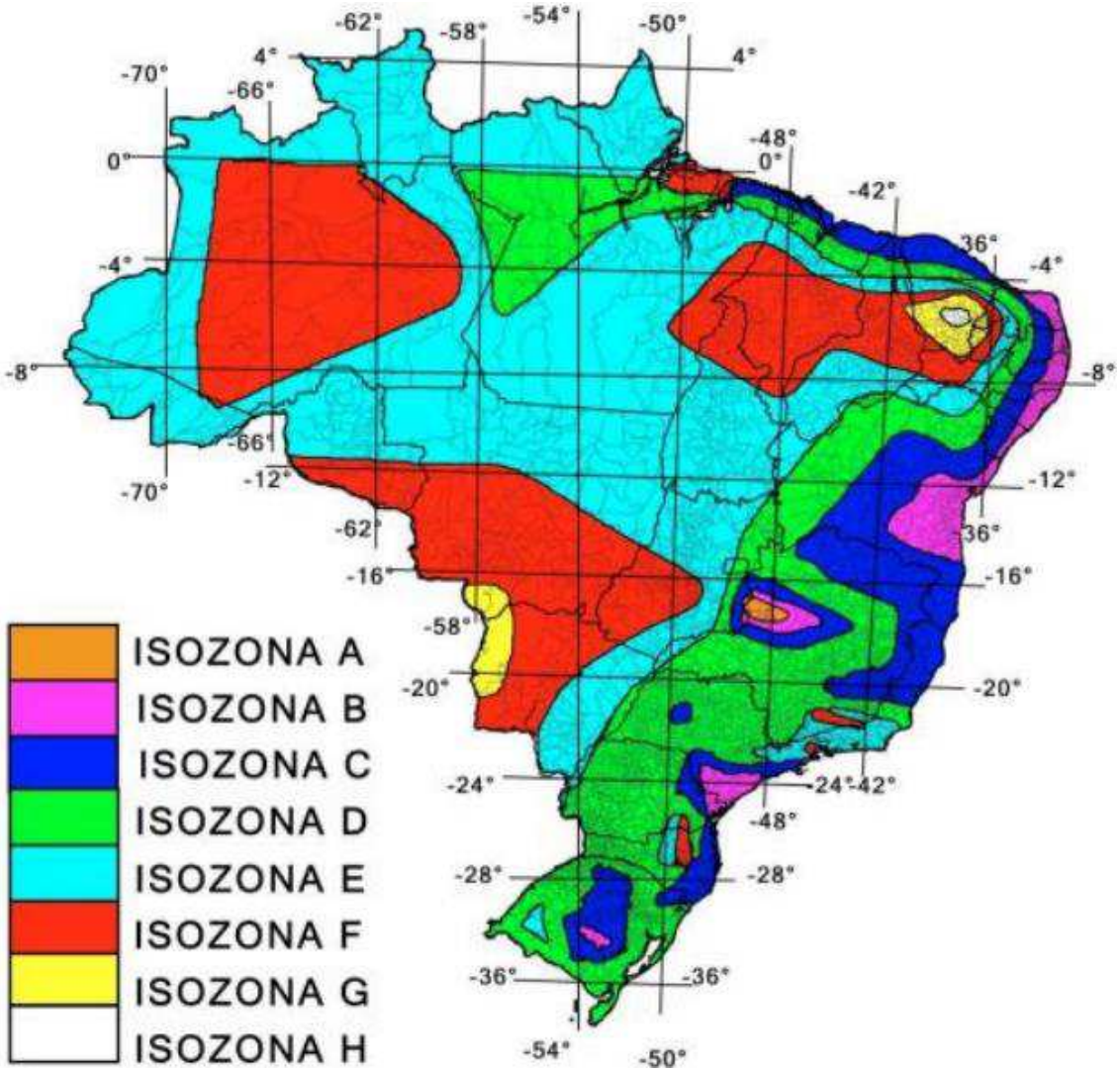

Figura 2 - Mapa de isozonas
Fonte: Torrico (1974) apud Santos (2015)

2.2.3. Determinação das equações IDF adequadas e seus parâmetros

A partir das precipitações desagregadas para diferentes T_r (5, 10, 15, 20, 25, 50 e 100 anos), a intensidade para durações de 6, 10, 15, 20, 30, 60, 360, 480, 600, 720 e 1440 min são calculados para diferentes tipos de equações IDF (Tabela 5).

Tabela 5 - Equações IDF adotadas neste estudo

ID	Equação
1	$i = \frac{a \times T_r^{\,b}}{(t + c)^d}$
2	$i = \frac{a \times T_r^{\,b}}{(t + c)^{d*T_r{}^e}}$
3	$i = \frac{a \times (T_r\text{-}b)^c}{(d \times t + e)^f}$
4	$i = \frac{a \times (T_r + b)^c}{(t + d)^e}$
5	$i = \frac{a \times T_r^{\,b}}{t^c}$

Onde i é a intensidade (mm/h), a, b, c, d, e, f são os parâmetros empíricos, que variam de acordo com os dados e a região onde os dados são obtidos

Para calibrar os parâmetros empíricos (Tabela 5), foram aplicadas duas funções objetivo (FO): FO1, uma função de minimização (Erro relativo), e a segunda (FO2), uma função de maximização (eficiência de Nash-Sutcliffe; NS). O valor de NS (Nash e Sutcliffe 1970) pode variar de -∞ a 1, e se o NS for igual a 1, há um ajuste perfeito aos dados observados (Moriasi et al., 2007). Portanto a abordagem utilizada foi aplicar F01 (Equação 8) para identificar os valores ótimos locais e a partir dos resultados utilizar F02 (Equação 9) para calcular os valores ótimos globais dos parâmetros da equação IDF.

$$FO1 = \min\left[\sum_{j=1}^{np}\sum_{j=1}^{nd}\left(\frac{T_j\text{-}M_j}{M_j}\right)\right]$$

Equação 8

$$FO2 = \max\left[1\text{-}\left(\frac{\sum_{j=1}^{np}(T_j\text{-}M_j)^2}{\sum_{j=1}^{n}(T_j\text{-}\overline{T})^2}\right)\right]$$

Equação 9

Onde np é o número de períodos de retorno, nd é o número de durações utilizadas para a desagregação da precipitação, T_j é o dado observado no instante do tempo j, M_j é o dado simulado no momento do tempo j, $\overline{T}$ é a média dos dados observados.

2.2.4. Análise do desempenho

Este estudo utilizou diferentes estatísticas (métricas contínuas e categóricas) para comparar os dados simulados *versus* dados *in-situ*. As métricas contínuas utilizadas foram: coeficiente de determinação - R^2 (Equação 10); raiz do erro quadrático médio - RMSE (Equação 11); erro médio absoluto - MAE (Equação 12); coeficiente de ajuste - CA (Equação 13); coeficiente de massa

residual - CMR (Equação 14); desvio padrão - SD (Equação 15); e eficiência Kling-Gupta - KGE (Equação 16).

$$R^2 = \frac{[N\times(\sum M_i\times T_i)]^2}{[N\times\sum T_i{}^2-(\sum T_i)^2]\times[N\times\sum M_i{}^2-(\sum M_i)^2]}$$

Equação 10

$$RMSE = \sqrt{\frac{1}{N}\sum_{i=1}^{N}(T_i-M_i)^2}$$

Equação 11

$$MAE = \frac{1}{N}\sum_{i=1}^{N}|T_i-M_i|$$

Equação 12

$$CA = \frac{\sum(M_i-\overline{M})^2}{\sum(T_i-\overline{M})^2}$$

Equação 13

$$CMR = \left[\frac{\sum M_i-\sum T_i}{\sum M_i}\right]$$

Equação 14

$$SD = \sqrt{\frac{1}{n}\sum_{i=1}^{n}(T_i-\overline{T})^2}$$

Equação 15

$$KGE = 1-\sqrt{(R-1)^2+(vr-1)^2+(\beta-1)^2}$$

Equação 16

Onde N é o número de observações na equação de regressão não-linear.

Quanto as métricas categóricas, foram consideradas as seguintes: Probabilidade de Detecção - POD (Equação 17), Taxa de Alarme Falso - FAR (Equação 18) e Taxa de Sucesso - TS (Equação 19) (Stanski et al., 1989; Nurmi, 2003). Essas métricas foram aplicadas à precipitação diária total, considerando um limiar de 1 mm/dia (Tan e Duan, 2017; Ziveh et al., 2022).

$$POD = \frac{hits}{(hits+misses)}$$

Equação 17

$$FAR = \frac{false\ alarms}{(hits+false\ alarms)}$$

Equação 18

$$TS = \frac{\text{hits}}{(\text{hits}+\text{misses}+\text{false alarms})}$$

Equação 19

Onde hits é o número de vezes que uma previsão "sim" foi seguida por uma ocorrência "sim", misses é o número de vezes que uma previsão "não" foi seguida por uma ocorrência "sim" e false alarms é o número de vezes que uma previsão "sim" foi seguida por uma ocorrência "não". De acordo com Bathelemy et al. (2022), os valores ideais de POD, FAR e TS são 1, 0 e 1, respectivamente.

2.2.5. Desenvolvimento de ferramenta para atualização e obtenção de equações IDFs

GEOT-IDF Equations (Figura 3) é uma ferramenta baseada na linguagem de programação R que calcula a equação IDF.

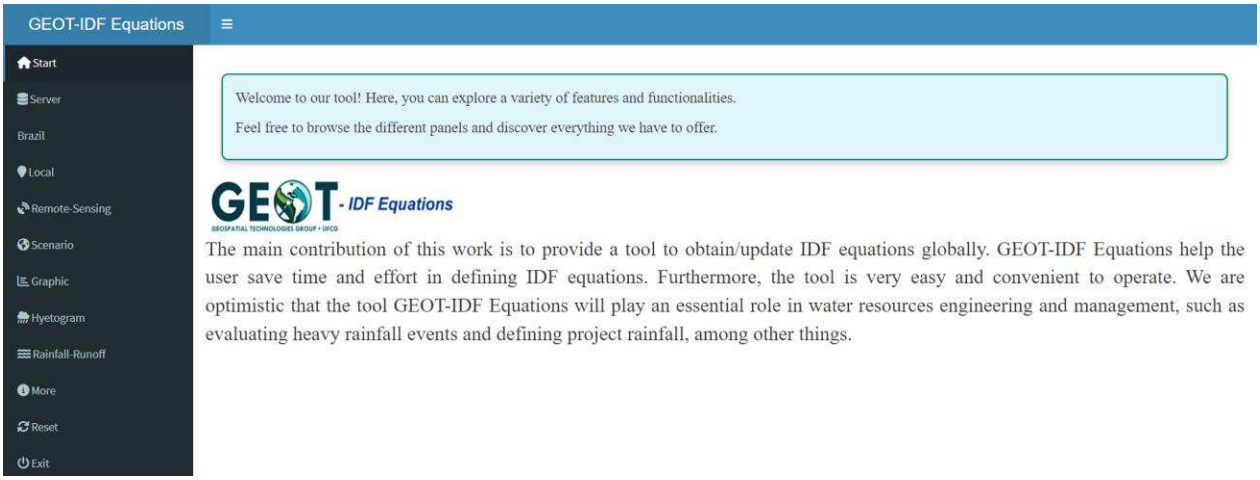

Figura 3 - Ilustração da interface principal da ferramenta GEOT-IDF Equations

Optou-se em utilizar a linguagem R, porque é uma linguagem de programação estatística e gráfica que vem se especializando na manipulação, análise e visualização de dados, sendo atualmente considerada uma das melhores ferramentas para essa finalidade.

A linguagem R ainda possui como diferencial a facilidade no aprendizado, mesmo para aqueles que nunca tiveram contato anterior com programação.

A ferramenta utiliza a metodologia de série máxima anual (CETESB, 1986). Ela é integrada com diferentes distribuições estatísticas de probabilidade mais amplamente utilizadas para determinação da relação IDF (Tabela 2), além de utilizar diferentes pacotes, a saber: tibble; optimx;

hydroGOF; fitdistrplus; e1071; smwrBase; evd; GEVcdn; PearsonDS; tidyverse; readxl, entre outros (para maiores detalhes, ver Capítulo 5).

A principal contribuição desta ferramenta foi a obtenção/atualização de equações IDF. A GEOT-IDF Equations ajuda o usuário a economizar tempo e esforço na definição de equações IDF. Além disso, a ferramenta é muito fácil e conveniente de operar.

2.3. Referências

Aha D. W., Kibler D., Albert M. K. (1991). Instance-Based Learning Algorithms. Machine Learning. https://www.researchgate.net/publication/220343419.

AESA (2021) Agency Executive Water Management of the State of Paraíba. Daily rainfall (mm), january 1994 to december 2020. Retrieved from. http://www.aesa.pb.gov.br.

Back Á. J. (2020). Alternative model of intense rainfall equation obtained from daily rainfall disaggregation. Brazilian Journal of Water Resources. https://doi.org/10.1590/2318-0331.252020190031.

Ballarin A., Sone J., Gesualdo G., Schwamback D., Reis A., Almagro A., Wendland E. (2023). CLIMBra - Climate Change Dataset for Brazil. Scientific Data. https://doi.org/10.1038/s41597-023-01956-z.

Barbero R., Fowler H. J., Lenderink G., Blenkinsop S. (2017). Is the intensification of precipitation extremes with global warming better detected at hourly than daily resolutions?. Geophysical Research Letters. http://dx.doi.org/10.1002/2016GL071917.

Basumatary V., Sil B. S. (2017). Generation of Rainfall Intensity-Duration-Frequency curves for the Barak River Basin. Meteorology Hydrology and Water Management. https://doi.org/10.26491/mhwm/79175.

Bathelemy R., Brigode P., Boisson D., Tric E. (2022). Rainfall in the Greater and Lesser Antilles: performance of five gridded datasets on a daily timescale. J. Hydrol.: Reg. Stud. https://doi.org/10.1016/j.ejrh.2022.101203.

Beck H. E., Wood E. F., Pan M., Fisher C. K., Miralles D. G., Dijk A. I. J. M. V., Mcvicar T. R., Adler R. F., 2019. MSWEP V2 Global 3-Hourly 0.1° Precipitation: Methodology and Quantitative Assessment. Bulletin of the American Meteorological Society. https://doi.org/10.1175/BAMS-D-17-0138.1.

Bibi T. S. (2023). Derivation of short-term design rainfall intensity from daily rainfall data for urban drainage design using empirical equations in robe town, Ethiopia. International Journal of Hydrology. https://doi.org/10.15406/ijh.2023.07.00340.

Brocca L., Filippucci P., Hahn S., Ciabatta L., Massari C., Camici S., Schüller L., Bojkov B., Wagner W., 2019. SM2RAIN-ASCAT (2007-2018): Global daily satellite rainfall data from ASCAT soil moisture observations. Earth System Science Data. https://doi.org/10.5194/essd-11-1583-2019.

CETESB (1986) Company Environmental Sanitation Technology of the State of São Paulo. Drainage urban: project manual, 1ª ed. São Paulo: CETESB. 466p. Retrieved from. https://repositorio.cetesb.sp.gov.br/handle/123456789/2863.

Funk C. C., Peterson P. J., Landsfeld M. F., Pedreros D. H., Verdin J. P., Rowland J. D., Romero B. E., Husak G. J., Michaelsen J. C., Verdin A. P. (2014). A quasi-global precipitation time series for drought monitoring. US Geological Survey data series. https://doi.org/10.3133/ds832.

Kendall M. G. (1975). Rank Correlation Methods, 4th edition. Charles Griffin, London, U.K.

Liu H., Yang F., Wang H. (2023). Research on Threshold Selection Method in Wave Extreme Value Analysis. Water. https://doi.org/10.3390/w15203648.

Makkonen L. (2005). Plotting Positions in Extreme Value Analysis. Journal of Applied Meteorology and Climatology. http://dx.doi.org/10.1175/JAM2349.1.

Mann H. B. (1945). Non-parametric tests Against trend. Econometrica. https://doi.org/10.2307/1907187.

Moriasi D. N., Arnold J. G., Van Liew M. W., Bingner R. L., Harmel R. D., Veith T. L. (2007). Model evaluation guidelines for systematic quantification of accuracy in watershed simulations. ASABE -Engineering a Sustainable Future. http://dx.doi.org/10.13031/2013.23153.

Naghettini M., Pinto E. J. A. (2007). Statistical hydrology. Belo Horizonte: CPRM. 600p.

Nash J. E., Sutcliffe J. V. (1970). River flow forecasting through conceptual models part I: a discussion of principles. Journal of Hydrology. http://dx.doi.org/10.1016/0022-1694(70)90255-6.

Nguyen P., Ombadi M., Gorooh V. A., Shearer E., Sadeghi M., Sorooshian S., Hsu K., Bolvin K., Ralph M. F.(2020). PERSIANN Dynamic Infrared-Rain Rate (PDIR-Now): A Near-Real-Time, Quasi-Global Satellite Precipitation Dataset. Journal of Hydrometeorology. https://doi.org/10.1175/jhm-d-20-0177.1.

Nurmi P. (2003). Recommendations on the verification of local weather forecasts (at ECWMF member states). ECMWF Operations Department. October. https://doi.org/10.21957/y1z1thg5l.

R Core Team. R: A language and environment for statistical computing. R Foundation for Statistical Computing, 2024. Available on: <https://www.R-project.org/>. Acessado em janeiro de 2024.

Rodrigues D. T., Silva C. M. S., Reis J. S., Palharini R. S. A., Júnior J. B. C., Silva H. J. F., Mutti P. R., Bezerra B. G., Gonçalves W. A. (2021). Evaluation of the Integrated Multi-Satellite Retrievals for the Global Precipitation Measurement (IMERG) Product in the São Francisco Basin (Brazil). Water. https://doi.org/10.3390/w13192714.

Santos R. A. (2015). Cálculo da chuva intensa pelo método das Isozonas para cidades do estado da Paraíba. Revista Eletrônica em Gestão, Educação e Tecnologia Ambiental. http://dx.doi.org/105902/2236117016748.

Sam M. G., Nwaogazie I. L., Ikebude C. (2021). Improving Indian meteorological department method for 24- hourly rainfall downscaling to shorter durations for IDF modelling. International Journal of Hydrology. http://dx.doi.org/10.15406/ijh.2021.05.00268.

Shamkhi M., Azeez M. K., Obeid Z. H. (2022). Deriving rainfall intensity–duration–frequency (IDF) curves and testing the best distribution using EasyFit software 5.5 for Kut city, Iraq. Open Engineering. https://doi.org/10.1515/eng-2022-0330.

Silveira A. L. L. (2000). Equation for rainfall breakdown coefficients. Brazilian Journal of Water Resources. http://dx.doi.org/10.21168/rbrh.v5n4.p143-147.

Stanski H. R., Wilson L. J., Burrows W. R. (1989). Survey of common verification methods in meteorology, World Weather Watch Tech. Rept. No.8, WMO/TD No.358. WMO, Geneva, p. 114pp. https://library.wmo.int/idurl/4/39578.

Tan M. L., Duan Z. (2017). Assessment of GPM and TRMM precipitation products over Singapore. Rem. Sens. https://doi.org/10.3390/rs9070720.

Tanaka S. (2021). Comparison of AMS and POT Analysis with Long Historical Precipitation and Future Change Analysis Using “d4PDF”. In: Hoshino, N., Mano, S., Shimura, T. (eds) Pioneering Works on Extreme Value Theory. SpringerBriefs in Statistics(). Springer, Singapore. https://doi.org/10.1007/978-981-16-0768-4_5.

Torrico J. J. T. (1974). Hydrological practices. Rio de Janeiro: Transcon, 120p.

Ziveh A. R., Bakhtar A., Shayeghi A., Kalantari Z., Bavani A. M., Ghajarnia M. (2022). Spatio-temporal performance evaluation of 14 global precipitation estimation products across river basins in southwest Iran. J. Hydrol.: Reg. Stud. https://doi.org/10.1016/j.ejrh.2022.101269.

Capítulo 3

Este capítulo refere-se ao artigo publicado na Revista AGRIAMBI[1]. O título e o resumo são apresentados inicialmente em português e, em seguida, o texto do artigo é transcrito aqui em inglês conforme foi publicado.

3. EQUAÇÕES DE INTENSIDADE-DURAÇÃO-FREQUÊNCIA (IDF) PARA O ESTADO DA PARAÍBA, BRASIL, E REGIONALIZAÇÃO DE SEUS PARÂMETROS

Resumo:

Nos dimensionamentos de estruturas hidráulicas, um parâmetro fundamental é a vazão de projeto, determinada a partir da série temporal observada ou por meio de modelos de escoamento, como o método racional, que relaciona o pico do fluxo de superfície com um evento de escoamento intenso. O evento extremo de precipitação a ser considerado no projeto, geralmente é estabelecido a partir das relações de Intensidade-Duração-Frequência (IDF) por meio de dados sub-diários observados

[1] Aragão R., Costa F. F., Rufino I. A. A., Filho R. S. R., Vajapeyam S. S., Neto J. B. T. (2024). Intensity-Duration-Frequency equations (IDF) for the state of Paraíba, Brazil, and regionalization of its parameters. Brazilian Journal of Agricultural and Environmental Engineering. http://dx.doi.org/10.1590/1807-1929/agriambi.v28n10e283679.

na série de precipitação. Na ausência ou escassez desses dados, os dados diários da rede de pluviômetros podem ser usados por meio do processo de desagregação. Assim, o objetivo deste estudo é gerar as relações IDF para o estado da Paraíba, Brasil, onde há uma extensa rede de pluviômetros (263 estações). Para isso, os dados diários de precipitação foram desagregados para várias durações entre 5 minutos e 24 horas, e a distribuição de melhor ajuste foi escolhida entre as distribuições *Gumbel*, *Weibull, Pearson, Log-Pearson* e *GEV* para as séries temporais desses dados de durações das precipitações. A partir da distribuição ajustada, a precipitação para várias durações e frequências foi obtida para gerar as curvas IDF para cada local. Não foi identificada uma única distribuição satisfatória para todos os casos, sendo *Pearson III* e *Log-Pearson III* as mais comuns. Para as curvas IDF, uma equação de quatro parâmetros foi ajustada e os valores dos parâmetros foram determinados por regressão não linear. Esses valores variaram muito dentro do estado da Paraíba e foram regionalizados para obter a equação IDF para qualquer localidade do estado. As intensidades de chuva obtidas com os parâmetros determinados neste estudo quando comparadas com as derivadas das equações IDF existentes anteriormente, apresentam grandes diferenças e indicam uma necessidade de atualização.

INTENSITY-DURATION-FREQUENCY EQUATIONS (IDF) FOR THE STATE OF PARAÍBA, BRAZIL, AND REGIONALIZATION OF ITS PARAMETERS

Abstract:

In the design of major hydraulic structures, a key element is the design discharge, determined from the time series of flow or through runoff models such as the rational method, which relates the peak surface flow with a rainstorm. The design storm is generally established from the Intensity-Duration-Frequency (IDF) relationships via recording gauges data. In the absence/scarcity of these data, daily data from the rain gauge network can be used via the disaggregation process. Thus, the objective of this study is to develop the IDFs for the state of Paraíba, Brazil, where there is an extensive network of rain gauges (263 stations). For this purpose, daily precipitation data were disaggregated for various durations between 5 min and 24 hours and the best fit distribution was chosen among the Gumbel, Weibull, Pearson, Log-Pearson and GEV distributions for the time series of these durations. From the fitted distribution, rainfall for various durations and frequencies were obtained to generate the IDF curves for each location. No single satisfactory distribution was identified for all cases, with Pearson III and Log-Pearson III being the most common. For the IDF

curves, the four-parameter equation (Eq. 1) was fitted and the parameter values were determined by non-linear regression. These varied a lot within the Paraíba state and were regionalized to obtain the IDF equation for any location in the state. The rainfall intensities obtained from the parameters determined in this study, when compared with those derived from the previously existing equations, show large differences and need updating.

Keywords:
Intense rainfall, maximum discharge, desagregation, rainfall-runoff.

3.1. Introduction

The natural disasters that have occurred in Brazil have been, over the last few decades, mostly caused by flooding (Tellman et al., 2021; Souza & Haddad, 2021). This is due to various factors including inadequate storm water drainage (Madakumbura et al., 2021). This phenomenon has been increasing over the last two decades, with losses of lives and property (Souza & Haddad, 2021; Ashizawa et al., 2022). In rural areas, heavy rains and floods remove topsoil and reduce the productivity (Souza & Haddad, 2021). Adequate planning of drainage systems requires information on design discharge associated with a return period (Machado et al., 2021; Kreibich et al., 2022). This discharge can be determined from a time series of measured flow data or from a design storm rainfall through a runoff model (Dorneles et al., 2019; Lima Neto et al., 2021; Suzuki et al., 2022).

In general, the design storm is derived from Intensity-Duration-Frequency (IDF) relationships (Dorneles et al., 2019). In the North-eastern region of Brazil, the network of recording rain gauges is sparse but, the network of conventional rain gauges is quite dense (ANA, 2021). The data from these gauges can be disaggregated into shorter-duration rainfall, to establish the IDF curves or equations (CETESB, 1979; Silveira, 2000; Aragão et al., 2013; Caldeira et al., 2015). The rise in global temperatures necessitates an updating of all the current IDF relationships in use (Wang et al., 2020; IPCC, 2022).

Thus, considering the extreme importance of IDF relationships, and the need to update the existing equations for the state of Paraíba, Brazil, the objective of the present work is to develop IDF equations for the whole State of Paraíba, by using the data from the rain gauge network.

3.2. Material and Methods

The state of Paraíba, Brazil, with an area of 56,467.242 km² (IBGE, 2021), has the states of Rio Grande do Norte to the north and Pernambuco to the south, the Atlantic Ocean to the east and the State of Ceará to the west. The average annual temperature varies between 22 and 26 ºC. Annual evaporation is very high, with potential evaporation values ranging from 1000 to 3000 mm, the latter in some locations in the Sertão and Cariri (Francisco & Santos, 2017), as shown in Figure 2. The average annual relative air humidity varies from 50 to 90% (Aragão, 2000; Francisco & Santos, 2017). The Paraíba state is divided into 223 municipalities whose total population is 4,059.905 inhabitants (IBGE, 2021).

The Paraíba state has a humid tropical climate on the coast, with well-distributed rainfall. As one moves to the interior, the climate becomes semi-arid, rainfall becomes irregular and droughts are frequent. The spatial variation of rainfall in the Paraíba state is caused by different atmospheric systems that act on the east coast of north-eastern Brazil. There is a need for determining safer design storms through updated IDFs that would lead to design discharges that offer the expected security for the hydraulic structures and reduce the risk of flooding. The state of Paraíba has a well-defined rainy season from January to July (Francisco & Santos, 2017). It occurs from January to May, in the Sertão, Alto Sertão and Cariri/Curimataú (Figure 4). In the transition zone, coastal areas and marsh it occurs from April to July. In general terms, the months of March, April, and June are the wettest months in Paraíba state, with the coast being the region where the highest total rainfall is recorded. According to the studies by Becker et al. (2011), the Paraíba state can be divided into six regions with homogeneous rainfall conditions (Figure 4) namely: Litoral, Brejo, Agreste, Cariri/Curimataú, Sertão and Alto Sertão.

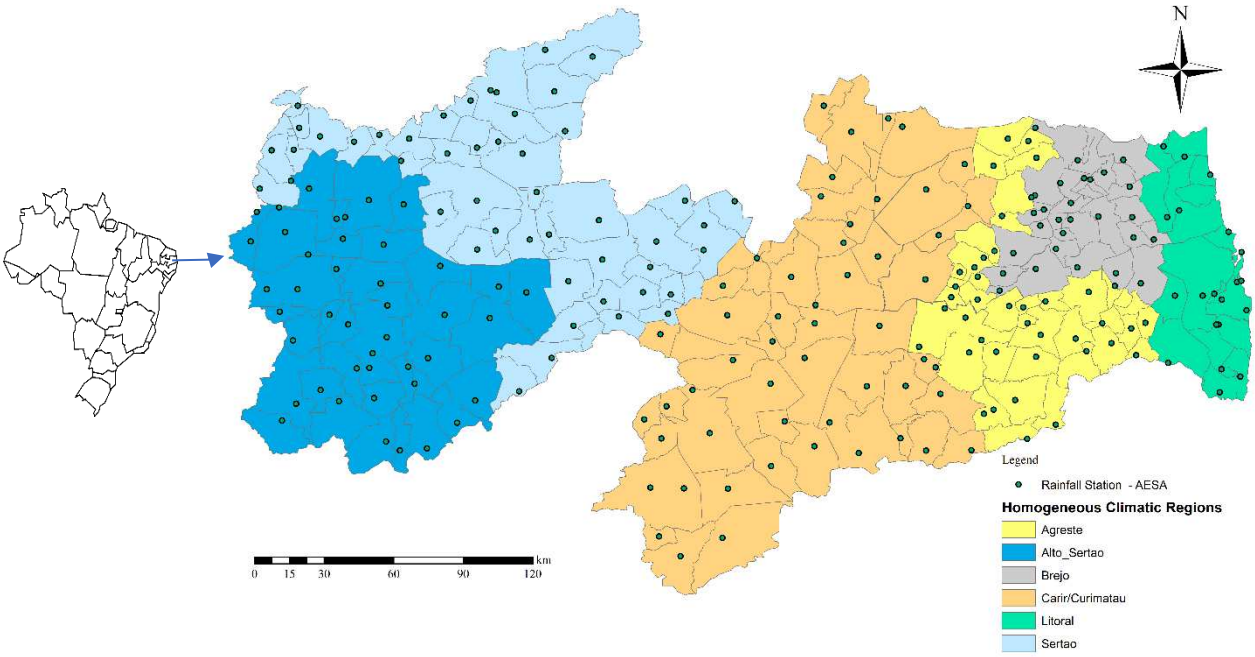

Source: adapted from Becker et al. (2011)

Figura 4 - Location of rainfall stations and homogeneous rainfall regions in the state of Paraíba, Brazil

In this study, the rainfall network of 263 stations monitored by the Executive Agency for Water Management of the state of Paraíba (AESA), with data from 1994 and 2020, has been used. Becker et al. (2011) made a statistical comparison of data from 89 stations within this network, which were previously collected by the Superintendency for the Development of North-east (SUDENE) until 1990, using monthly rainfall series. The objective of this procedure was to find out if this short time series (15 years) could represent the climatology inherent in the data from SUDENE. They concluded that the series from 1996 to 2010 monitored by AESA were statistically similar to the data series up to 1990.

From this point of view, longer the time series, the better would be the representation of the climatology of the region. In the present study, daily rainfall data from the 263 stations monitored by AESA and made available by AESA (2021) and ANA (2021), for the period of 1994-2020, were considered. From the 263 stations, data from 30 were disregarded because the time series of them were less than 27 years, with the remaining 233 gauges with consistent data series of 27 years were used for the development of IDF relationships.

The relationship between Intensity-Duration-Frequency (IDF) is generally represented by Eq. 20 (Aragão et al., 2013).

$$i = \frac{a \times Tr^{b}}{(t+c)^{d}}$$

Equação 20

where:

i - intensity (mm h^{-1});

Tr - return period (years);

t - duration of rainfall (min); and

a, b, c and d - empirical parameters of the equation.

The parameters of Eq. 20 are best determined using data collected from recording rain gauges, which record the variation of the total precipitation over time. However, these data are scarce, and processing is costly. An approach that has provided good results in many other studies (Aragão et al., 2013; Campos et al., 2017) uses daily rainfall data collected in rain gauges using a rainfall disaggregation method (CETESB, 1979). This method utilizes the daily rainfall and calculates maximum rainfall values for durations ranging from 5 to 1440 min.

From the daily rainfall series, the first step would be generating the maximum daily annual rainfall series for each gauge station. A frequency analysis of this series makes it possible to adjust a probability distribution curve for these series, from which it would be possible to determine the precipitation values that might be equalled or exceeded for the return periods of 2, 5, 10, 15, 20, 25, 50, 75 and 100 years. Naghettini & Pinto (2007), and Gandini & Queiroz (2018) indicate that the most suitable maximum event probability distributions for this type of time series are: Gumbel, Weibull, Pearson, Pearson III, Log-Pearson III, and Generalized Extreme Values (GEV). These distributions have been tested in the present study, and the distribution that fits best for each series has been used in the development of IDF Equations to determine the precipitation for any required return period.

The goodness of fit for the series of annual daily maximums to the distributions used was verified using the Kolmogorov-Smirnov (KS) test at 0.05 level of significance (Eq. 1). The KS test is non-parametric and evaluates the maximum deviation between the values predicted by the distribution under test and the values associated with the empirical distribution represented by the data sample, and is widely used in hydrological studies (Naghettini & Pinto, 2007; Silva et al., 2012; Aragão et al., 2013; Gandini & Queiroz, 2017). In this study, the frequency of occurrence of an event of order mi in a sample of n events was obtained by the Weibull method (mi/(n+1)),

(Naghettini & Pinto, 2007). From the adjusted distribution, the values of maximum daily rainfall were obtained for various return periods. After adjusting the maximum daily value for the duration of 24 hours, these values were disaggregated into shorter intervals as per the methodology of CETESB (1979).

Once the series of intensities for different return periods and durations were generated, the next step was to fit Eq. 20 for each rain gauge location. Nonlinear regression method was used to obtain the optimal values of the parameters of Eq. 20. In the optimization process to determine the parameters, it is customary to employ objective functions that seek to minimize the error between the values generated by the equation and those observed. However, as Eq. 20 is nonlinear (Aragão et al., 2013), the use of optimization may lead to non-global optimal values of the parameters. Thus, to ensure global optimization, the approach used was to use an objective function that allows identifying the local optimal values (Eq. 8) and, from these values, use another objective function (Eq. 9) to determine the global optimal values of the parameters of Eq. 20. In this sense, Eq. 8 is an objective function for minimizing the relative error (ERR), and the second one, Eq. 9, maximizes the Nash-Sutcliffe efficiency coefficient – NS (Moriasi et al., 2007). The use of Eq. 8 is an innovative approach of this study and the local optimal value is obtained when the relative error is as low as possible. The NS value can vary from -∞ to 1, with NS equal to 1, for a perfect fit to the observed data.

Once the parameters of Eq. 20 were obtained, the degree of proximity between the values calculated by Eq. 20 and the values of the generated series was verified through the coefficient of determination (R^2; Eq. 10); as well as by the adjustment coefficient (CA; Eq. 13); and by the residual mass coefficient (CMR; Eq. 14).

The CA coefficient describes the ratio between the dispersion of calculated and observed values and should tend to the value of 1 (one). The CMR coefficient tends to zero in the absence of systematic deviations between the observed and calculated values, indicating over estimation ($CMR > 0$) or underestimation ($CMR < 0$) of the values estimated by the adjusted probability distributions (Silva et al., 2012). The above four criteria were used to choose the best distribution for the series when no single distribution stood out as the best in the KS adherence test.

All processing of daily rainfall information, determination of the maximum annual daily rainfall, as well as the calculation of various statistics (mean, mode, standard deviation, median, variance), KS test, NS coefficient, coefficient of determination (R^2), coefficient of adjustment (CA), residual

mass coefficient (CMR), as well as other calculations necessary to obtain the parameters of Eq. 20, were performed through scripts developed in R 4.2.2 (R Core Team, 2022), or via the use of packages available for this language, namely: tibble; optimx; hydroGOF; fitdistrplus; e1071; smwrBase; evd; GEVcdn; PearsonDS; tidyverse; and readxl. Once the parameters of the IDF equation were determined, its regionalization was performed using the kriging method and using the R gstat package (R Core Team, 2022).

Among the methods available to transform daily rainfall into shorter intervals, the method proposed by CETESB (1979) has been used by Aragão et al. (2013), and Caldeira et al. (2015). In this method, the total measured daily rainfall is related to the 24 hour rainfall, and the maximums for lesser intervals are established as a fraction of this value. Caldeira et al. (2015) tested three different groups of disaggregation coefficients proposed by Backet al. (2012), CETESB (1979) and Damé et al. (2010), utilizing data from 15 recording rain gauge stations in Rio Grande do Sul State. The values of the parameters of the IDF equations were generated, and the results were compared with the values of the IDF generated from rainfall data. They concluded that, from the three groups of disaggregation coefficients used, the one proposed by CETESB (1979) generated results closer to those obtained with data from recording rain gauges. On the other hand, Abreu et al. (2022) analysed the equivalence and applicability of the disaggregation methods compared with sub-daily rain gauge data, concluding that in case of existence of this data the design storm must be based on these data and, in the absence of such data, the disaggregation coefficients by CETESB (1979) could give satisfactory results, which is consistent with the present approach.

For each rainfall duration, a minimum value above which rainfall can be considered as intense as indicated by CETESB (1979) was taken into account (Table 4). Silva et al. (2012) and Aragão et al. (2013) also used these minimum values.

To use this methodology through computer programs, Silveira (2000) adjusted an empirical exponential equation (Eq. 4), starting with the 24 hour rainfall and this equation is the one that was used in this study. The best fit distribution at each station was used to obtain the maximum daily rainfall for the desired return periods. These values were first transformed into 24 hours rainfall by multiplying by 1.14 (CETESB, 1979) and then disaggregated using Eq. 4.

While the rainfall fractions for different durations from 5 to 1440 min were generated using Eq. 8, the series were established for the return periods of 2, 5, 10, 15, 20, 25, 50, 75, and 100 years. Thus, intensity and duration data series for these return periods were established. The optimal

parameters of Eq. 20 were determined for each location from these series. The same procedure was used by Aragão et al. (2000) and Aragão et al. (2013) for the regionalization of such parameters for the state of Paraiba and the state of Sergipe, respectively.

3.3. Results and Discussion

Appendix A presents the results for each rain gauge station: the location, the adjustment distribution (D), the climatic region (RC), and the optimized parameters (a, b, c, d) of Eq. 20. For the 233 stations utilized, the number of the stations that best adjusted to each of the distributions used were: GEV - 46 (19.7%), Gumbel – 38(16.30%), Log-Pearson III – 56 (24.03%), Pearson – 20 (8.58%), Pearson III – 48 (20.60%) and Weibull – 25 (10.70%). Silva et al. (2012) and Aragão et al. (2013), who applied similar methodologies for the states of Pernambuco and Sergipe, respectively, observed a predominance of Gumbel or Weibull distributions. In the present study, it was observed that there was no predominance of any one distribution, being the most frequent ones, the Log-Pearson III (22.74%) and Pearson III (20.6%) distributions. These results show that, despite being widely used to adjust maximum or minimum extreme values, the Gumbel distribution is not always the one with optimal results.

In terms of the indices used to assess the fit of the data to the IDF equation (Eq. 20), it is possible to summarize the results as follows: among the 233 selected stations, the NS (Nash-Sutcliffe index) had a variation of 0.809 (Frei Martinho) to 0.996 (Salgadinho), and the R^2 value ranged from 0.783 (Frei Martinho) to 0.973 (Salgadinho). These stations where the indices present extreme values (minimum or maximum) are in the climatic region of Sertão (Frei Martinho) or Cariri/Curimataú (Salgadinho), with the Salgadinho station being in the transition region between the region of Cariri and the Sertão of Paraíba state.

The parameters a, b, c, d, of Eq. 20, varied a lot between the rain gauge stations (Appendix A), indicating the large climatic variability in the Paraíba state and the need to determine these equations for each location.

Appendix A indicates that: the parameter a ranges from 558.92 (Ingá - in the Agreste) to 1695.47 (João Pessoa-Mangabeira), the parameter b varies from 0.067 (Montadas - in the Agreste) to 0.423 (Pilar - in the Agreste), the parameter c varies from 8.19 (São José da Lagoa Tapada – in the Alto Sertão) to 15.55 (Pilar – in the Agreste), and the parameter d varies from 0.654 (São José da Lagoa Tapada – in the Alto Sertão) to 0.817 (Pilar – in the Agreste). This wide variability of the

parameters of Eq. 20 means a great variability in the occurrence of intense rains. This fact was also observed by Silva et al. (2012), and Aragão et al. (2013).

For a comparative evaluation of the results of the present study, with those of Aragão et al. (2000) and Campos et al. (2017), rainfall intensities were calculated with a return period of 10 years (for all durations in Table 7) for the stations of Campina Grande, Guarabira, São João do Rio do Peixe and Monteiro. These stations are located in different climatic regions (Figure 4) and were chosen arbitrarily.

In general, the intensity values calculated by Aragão et al. (2000) were slightly higher than the other two for Campina Grande, São João do Rio do Peixe, and Monteiro. However, the calculation of R^2 and the NS values permit a good comparative evaluation by correlating the values generated by Aragão et al. (2000), taken here as a reference, with those generated in the present work, as well as by Campos et al. (2017) for the same locations (Table 6).

Aragão et al. (2000) used the limited data from the recording rain gauges operated by SUDENE to develop the IDF equations for 16 locations in the state of Paraíba. However, given the large extension of the state, many important cities and regions of the state were not covered by this study. Campos et al. (2017) used daily rainfall data to determine the IDF equations for 90 rain gauge stations in the state of Paraíba.

Tabela 6 - R^2 and NS values obtained by correlating the results generated with the parameters of Aragão et al. (2000), taken as a reference, and those form Campos et al. (2017) and from the present work

Stations	Campos et al. (2017)		Present work	
	R^2	NS	R^2	NS
Campina Grande	0.994	0.988	0.996	0.993
Guarabira	0.997	0.526	0.998	0.915
São João do Rio do Peixe	0.994	0.912	0.995	0.983
Monteiro	0.999	0.599	0.997	0.953

The results of the present study are consistent with the trend of the previous ones and present better indices of performance. Thus, using the values of the parameters of Eq. 20, presented in this work, would be safer for calculating the design discharge. Considering a return period (Tr) of 10 years and a rainfall duration of t = 10 min, widely used in urban micro-drainage works (Souza et al., 2019), the intensities for all the stations in Table 8 were calculated and the values of maximum and minimum intensities in each climatic region of Figure 4 were identified and are presented in Table 7.

Tabela 7 - Maximum and minimum intensity values calculated for each climatic region and the stations where they were determined

	Maximum intensity (mm h^{-1})		Minimum intensity (mm h^{-1})	
Climatic Region	Station	Intensity	Station	Intensity
Litoral	João Pessoa	187.15	Gurinhém	111.15
Brejo	Capim	134.64	Areial	90.99
Agreste	Pilar	144.80	Montadas	86.88
Cariri/Curimataú	Pararí	170.82	Gado Bravo	87.16
Sertão	Cacimba de Areia	158.01	Santa Luzia	99.08
Alto Sertão	Itaporanga	173.74	Damião	101.74

These results show a great variation in rainfall intensity from the east (coast) to the west (Alto Sertão), with the lowest intensity values at stations located in the Serra da Borborema region (Agreste to Sertão transition). Araújo et al. (2016) cited that rainfall in the Sertão and Alto Sertão regions is greatly influenced by the effect of the intertropical convergence zone (ITCZ), high-level cyclonic vortices (HCV), while rainfall in the coastal region is greatly influenced by squall lines (LI), which occur from January to March and promote large volumes of rain. In addition, the same authors mention that the Borborema mountain range influences the values of intensities for the stations located in the region, a fact that is also evident in the present work.

It is observed that for Litoral, Cariri/Curimataú, and Alto Sertão, the highest values of intense rainfall as calculated, are very close, around 163.46 mm h^{-1}, differing between them by only 7%. The values of a and c parameters were also higher for these climatic regions. The wide variation of the parameter a indicates a great variability of intense rains among the climatic regions of Paraíba.

Table 8 presents the maximum and minimum values of the parameters in each climatic region of the Paraíba state. A large variation of the parameters between the regions is noticed, and the transitional Agreste region presents the widest range. This variation occurs due to the climatic condition of the transition from the coastal to the Cariri/Curimataú region.

Tabela 8 - Maximum (max) and minimum (min) values of parameters a, b, c, d, of the Intensity-Duration-Frequency (IDF) equation for the climatic regions of the state of Paraíba

Climatic Region	Stations	$a_{mín}$	a_{max}	$b_{mín}$	b_{max}	$c_{mín}$	c_{max}	$d_{mín}$	d_{max}
Litoral	21	854.47	1697.07	0.089	0.217	11.41	13.13	0.759	0.798
Brejo	25	573.87	1204.48	0.067	0.274	10.23	14.90	0.704	0.809
Agreste	36	558.92	1087.36	0.067	0.425	11.65	15.55	0.751	0.817
Cariri/Curimataú	55	581.03	1363.13	0.100	0.313	11.29	14.19	0.739	0.801
Sertão	55	749.69	1437.35	0.086	0.325	11.49	13.37	0.754	0.806
Alto Sertão	41	611.36	1403.36	0.092	0.260	8.19	13.18;	0.654	0.797

The average values of the IDF parameters were calculated for each climatic region, as well as the intensity of the 10 min rainfall for a 10 years return period, whose values are shown in Table

9. Values of the parameter a and rainfall intensity values vary a lot from the coastal region to the state's interior. The other parameters presented a very narrow range of variation. However, an interesting fact is that in the Cariri/Curimataú region, where rainfall totals are, on average, low, the intensity of heavy rainfalls is close to those of Sertão and Alto Sertão and higher than those of Agreste and Brejo.

Tabela 9 - Average parameters of the Intensity-Duration-Frequency (IDF) equation for the climatic regions

Climatic Regions	Parameters of IDF equations				Intensity (mm h^{-1})**
	a	b	c	d	
Litoral	1348.27	0.152	12.61	0.784	164.94
Agreste	813.03	0.183	12.71	0.771	110.98
Brejo	930.82	0.168	12.82	0.781	117.35
Cariri/Curimataú	906.48	0.179	12.42	0.774	121.98
Sertão	1070.70	0.161	12.79	0.786	132.37
Alto Sertão	1080.75	0.160	12.61	0.781	136.18

**Intensity for return period (Tr) = 10 years and rainfall duration (t) = 10 min

The availability of a large number of rain gauge stations (233) made it possible to trace isolines of the parameters within the Paraíba state, enabling their regionalization, as shown in Figures 5 to 8. These figures help to determine the values of the parameters of Eq. 20 for any location by interpolating the parameter values. Once the parameter values for the desired location are obtained, the rainfall intensities can be calculated by Eq. 20.

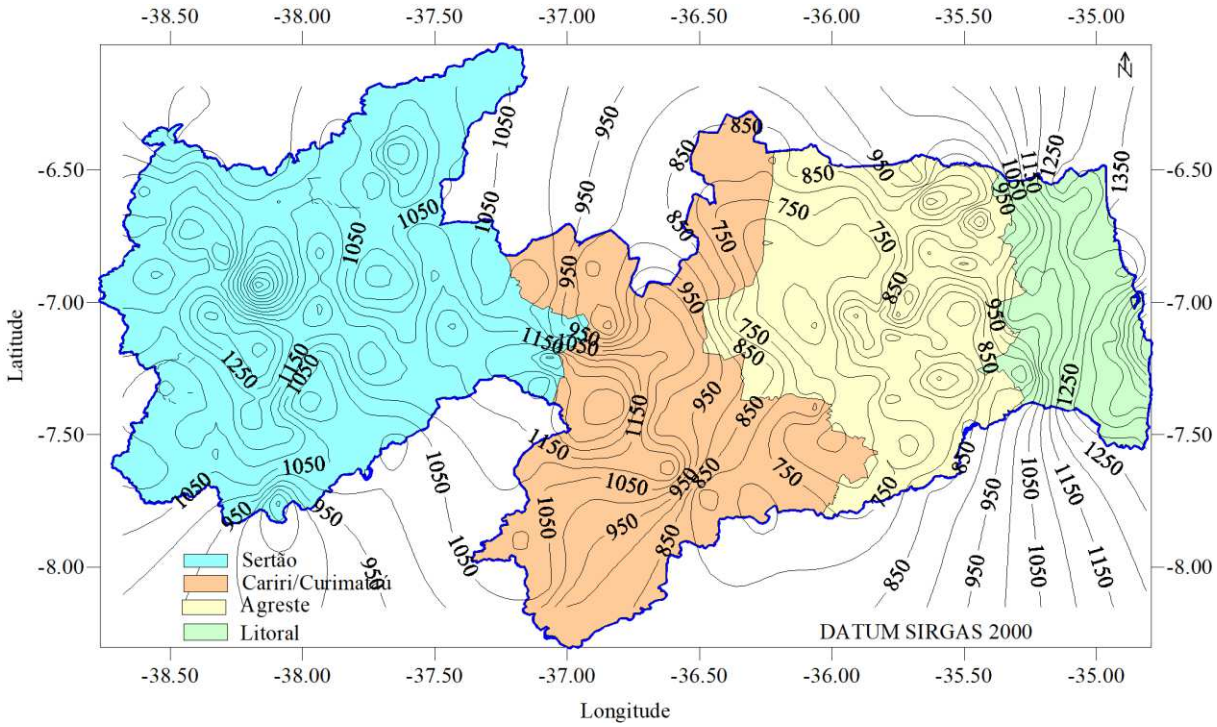

Figura 5 - Spatialization of parameter a

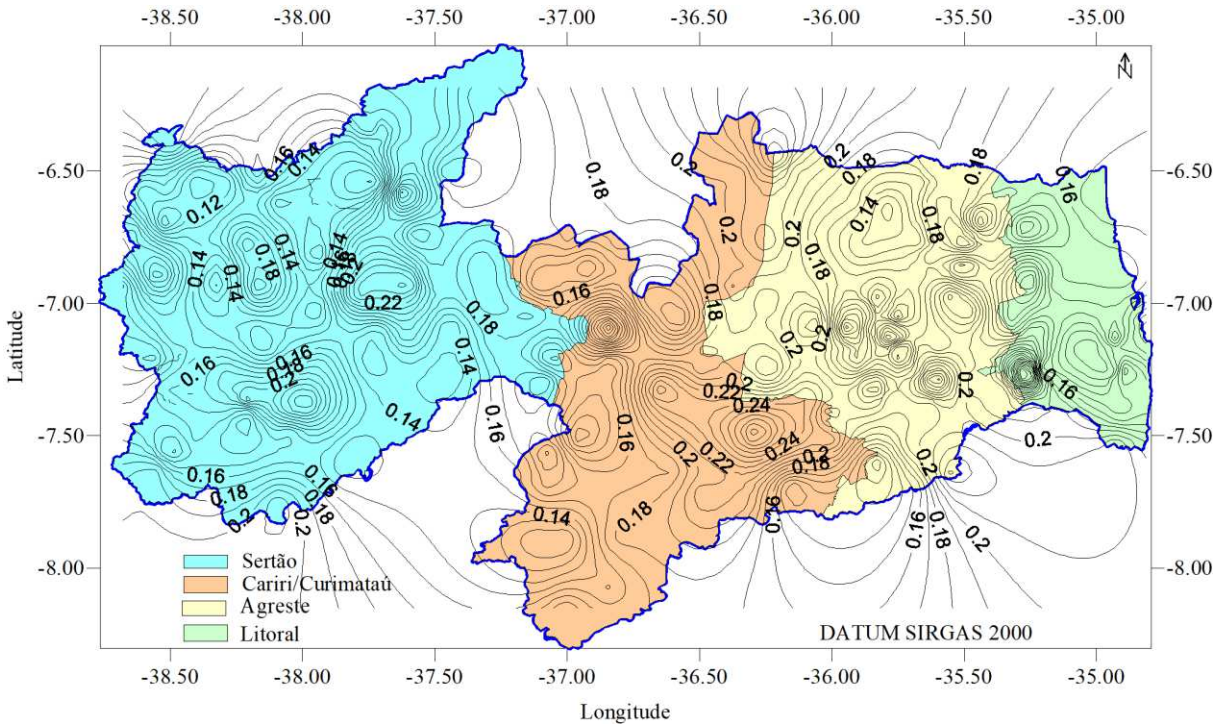

Figura 6 - Spatialization of parameter b

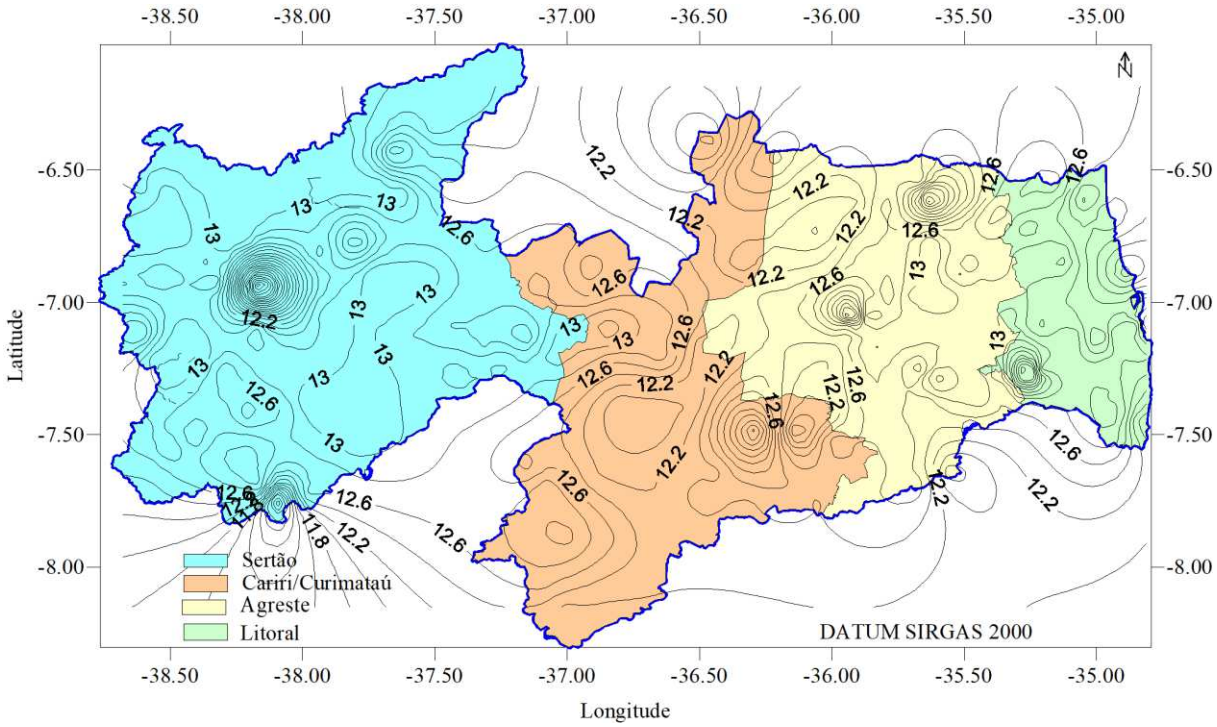

Figura 7 - Spatialization of parameter c

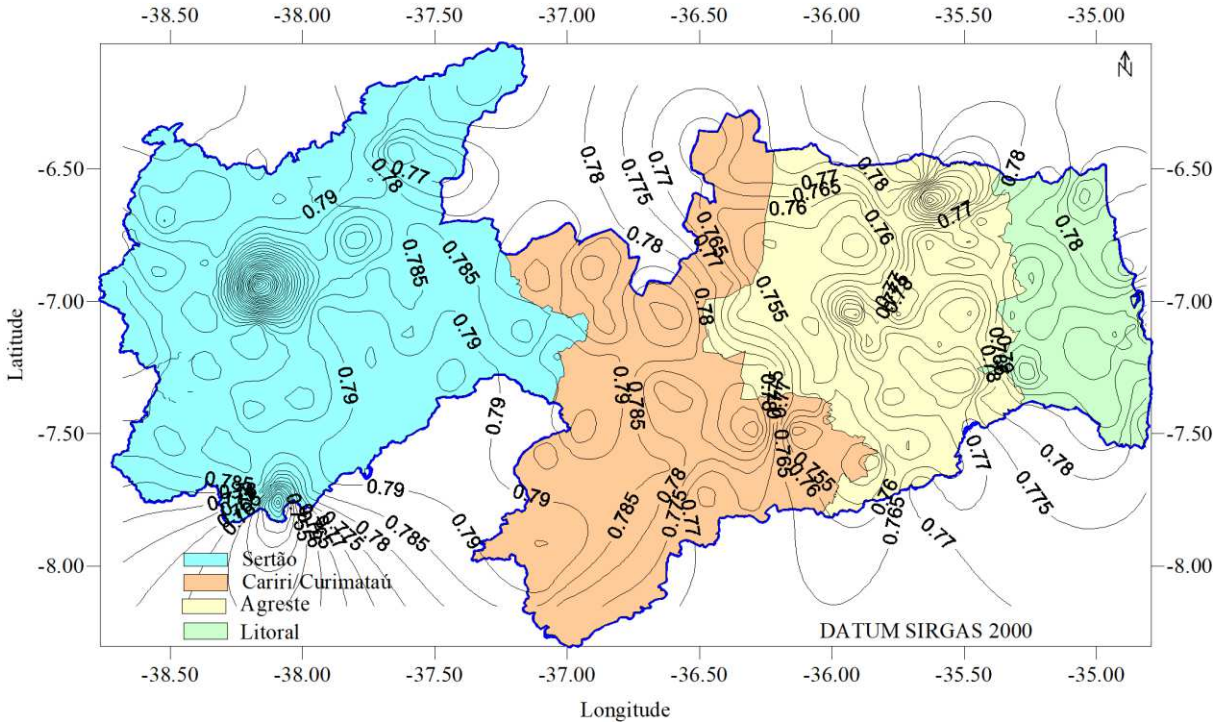

Figura 8 - Spatialization of parameter d

3.4. Conclusions

1. The availability of a large number of well-distributed rainfall stations in the state of Paraíba, Brazil, permits the determination of Intensity-Duration-Frequency (IDF) relationships in the form of Eq. 19 for any location through the regionalization of its parameters a, b, c, d.

2. The Pearson III and Log-Pearson III distributions were the most frequent, with 22.7 and 20.6% of the total, respectively.

3. The parameters a, b, c, d of the Intensity-Duration-Frequency (IDF) varied a lot from the coast to the Alto Sertão, with the lowest values found in the Agreste/Cariri/Curimataú region of the Paraíba state, Brazil, and the highest values in the Litoral and Sertão/Alto Sertão.

4. In most cases, the intensities of rainfall obtained in this study were higher compared to the earlier ones. Thus, using the results of this study would provide higher levels of safety for drainage works in the state of Paraíba, Brazil.

3.5. References

Abreu, M. C.; Cecílio, R. A.; Pruski, F. F.; Almeida, L. T.; Santos, G. R.; Zanetti, S. S.; Pereira, S. B.; Silva, D. D. Daily Rainfall disaggregation to estimate the intensity-duration-frequency relationship in Minas Gerais State, Brazil. Brazilian Archives of Biology and Technology, v.65. p.1-15. 2022. https://doi.org/10.1590/1678-4324-2022210694.

AESA - Agência Executiva de Gestão das Águas do Estado da Paraíba. Precipitação pluviométrica mensal, janeiro de 1994 a dezembro de 2020 para o estado da Paraíba. Available on:<http://www.aesa.pb.gov.br>. Accessed on: Jul. 2021.

ANA - Agência Nacional das Águas. Hidro Web: Sistemas de Informações Hidrológicas. Available on:<http://hidroweb.ana.gov.br>. Accessed on: Jul. 2021.

Aragão, R.; Figueiredo, E. E.; Srinivasan, V. S.; Gois, R. S. S. Chuvas intensas no Estado da Paraíba. In: Simpósio de Recursos Hídricos do Nordeste, 5., 2000, Natal. Anais. Natal: ABRH, 2000. p.74-85.

Aragão, R.; Santana, G.R.; Costa, C.E.F.F.; Cruz, M.A.S.; Figueiredo, E.E.; Srinivasan, V.S. Chuvas intensas para o estado de Sergipe com base em dados desagregados de chuva diária. Revista

Brasileira de Engenharia Agrícola e Ambiental, v.17, p.243-252, 2013. https://doi.org/10.1590/S1415-43662013000300001.

Araújo, A.R.; Belchior, G.P.N.; Viegas, T.E. de S. Os impactos das mudanças climáticas no Nordeste brasileiro. Fortaleza: Fundação Sintaf, 2016. 382p.

Ashizawa, T.; Sudo, N.; Yamamoto, H. How do Floods Affect the Economy? An Empirical Analysis using Japanese Flood Data. Tokyo: Bank of Japan, 2022. 40p.

Back, A. J.; Oliveira, J. L. R.; Henn, A. Relações entre precipitações intensas de diferentes durações para desagregação da chuva diária em Santa Catarina. Revista Brasileira de Engenharia Agrícola e Ambiental, v.16, p.391-398, 2012. https://doi.org/10.1590/S1415-43662012000400009.

Becker, C.T.; Melo, M.M.M.S.; Costa, M.N.de M.; Ribeiro, R.E.P. Caracterização climática das regiões pluviometricamente homogêneas do estado da Paraíba. Revista Brasileira de Geografia Física, v.4, p.286-299, 2011. https://doi.org/10.26848/rbgf.v4i2.232720.

Caldeira, T.L.; Beskow, S.; Mello, C.R. de; Vargas, M.M.; Guedes, H.A.S.; Faria, L.C. Daily rainfall disaggregation: on analysis for the Rio Grande do Sul state. Scientia Agraria, v.16, p.1-21, 2015. http://dx.doi.org/10.5380/rsa.v16i3.46320.

Campos, A.R.; Silva, J.B.L.; Santos, G.G.; Ratke, R.F.; Aquino, I.O. de. Estimate of intense rainfall equation parameters for rainfall stations of the Paraíba state, Brazil. Pesquisa Agropecuária Tropical, v.47, p.15-21, 2017.https://doi.org/10.1590/1983-40632016v4743821.

CETESB - Companhia de Tecnologia de Saneamento Ambiental. Drenagem urbana: manual de projeto. 1.ed. São Paulo: DAEE/CETESB, 1979. 466p.

Damé, R. C. F.; Teixeira, C. F. A.; Terra, V. S. S.; Rosskoff, J. L. Hidrograma de projeto em função da metodologia utilizada na obtenção da precipitação. Revista Brasileira de Engenharia Agrícola e Ambiental, v. 14, p.46-54, 2010. https://doi.org/10.1590/S1415-43662010000100007.

Dorneles, V.R.; Damé, R. de C.F.; Teixeira-Gandra, C.F.A.; Méllo, L.B.; Ramirez, M.A.A.; Manke, E.B. Intensity-duration-frequency relationships of rainfall through the technique of

disaggregation of daily rainfall. Revista Brasileira de Engenharia Agrícola e Ambiental, v.23, p.506-510, 2019. https://doi.org/10.1590/1807-1929/agriambi.v23n7p506-510.

Francisco, P.R.M.; Santos, D. Climatologia do Estado da Paraíba. 1.ed. Campina Grande: EDUFCG, 2017. 75p.

Gandini, M.L.T.; Queiroz, P.I.B. de. Analysis of probabilistic frequency models to obtain IDF equations in the city of Cunha-SP. Revista DAE, v.66, p.105-117, 2018. http://dx.doi.org/10.4322/dae.2018.017.

IBGE – Instituto Brasileiro de Geografia e Estatística. População estimada da Paraíba com data de referência 1º de julho de 2021. Available on:<https://cidades.ibge.gov.br/brasil/pb/panorama>. Accessed on: Dec.2021.

IPCC – Intergovernmental Panel on Climate Change. Climate Change 2022: Mitigation of Climate Change. 2022. Available on: https://www.ipcc.ch/report/ar6/wg3/. Accessed on: Oct., 2022.

Kreibich, H.; Van Loon, A. F.; Schröter, K.; Ward, P. J.; Mazzoleni, M.; Sairam, N.; Abeshu, G. W.; Agafonova, S.; Agha Kouchak, A.; Aksoy, H. and 71 more. The challenge of unprecedented floods and droughts in risk management. Nature, v. 608, p.80–86, 2022. https://doi.org/10.1038/s41586-022-04917-5.

Lima Neto, V.S.; Tavares, P.R.L.; Batista, T.L. Ajuste e validação de equações IDF a partir de dados pluviométricos para cidades do estado de Pernambuco, Brasil. Revista Brasileira de Meteorologia, v.36, p.713-721, 2021. https://doi.org/10.1590/0102-7786360031.

Machado, C. B.; Campos, T. L. O. B.; Rafee, S. A. A.; Martins, J. A.; Grimm, A. M.; Freitas, E. D. Extreme rainfall events in the macro metropolis of São Paulo: Trends and connection with climate oscillations. Journal of Applied Meteorology and Climatology,v.60, p.661-675,2021. https://doi.org/10.1175/JAMC-D-20-0173.1.

Madakumbura, G.D., Thackeray, C.W., Norris, J., Goldenson, N., Hall, A. Anthropogenic influence on extreme precipitation over global land areas seen in multiple observational datasets. Nature Communication, v.12, p.1-9, 2021. https://doi.org/10.1038/s41467-021-24262-x.

Moriasi, D.; Arnold, J.; Van Liew, M.; Bingner, R.; Harmel, R.D.; Veith, T. Model Evaluation guidelines for systematic quantification of accuracy in watershed simulations. Transactions of the ASABE, v.50, p.885-900, 2007. https://doi.org/10.13031/2013.23153.

Naghettini, M.; Pinto, E.J.A. Hidrologia estatística. Belo Horizonte: CPRM, 2007. 600p.

R Core Team. R: A language and environment for statistical computing. R Foundation for Statistical Computing, 2022. Available on: <https://www.R-project.org/>. Accessed on Jun. 2022.

Silva, B.M.; Montenegro, S.M.G.L.; Silva, F.B.; Araújo Filho, P.F. Chuvas intensas em localidades do Estado de Pernambuco. Revista Brasileira de Recursos Hídricos. v. 17, p.135-147. 2012. https://doi.org/10.21168/rbrh.v17n3.p135-147.

Silveira, A.L.L. Equação para os coeficientes de desagregação de chuva. Revista Brasileira de Recursos Hídricos. v.5, p.143-147, 2000. http://dx.doi.org/10.21168/rbrh.v5n4.p143-147.

Souza, B.; Haddad, E. Climate change in Brazil: dealing with uncertainty in agricultural productivity models and the implications for economy-wide impacts, Spatial Economic Analysis, v.17, p.83-10, 2021. http://dx.doi.org/10.1080/17421772.2021.1934524.

Souza, G. R. de; Bello, I. P.; Oliveira, L. F. C. de; Corrêa, F.V. Heavy rainfall maps in Brazil to 5 years return period. Revista Ambiente & Água, v.14, p.1-10, 2019. https://doi.org/10.4136/ambi-agua.2403.

Suzuki, Y.; Nakamura, K.; Hama, T. Peak discharge mitigation effects in different rainfall patterns at a paddy plot with a runoff control plate, Journal of Hydrology: Regional Studies, v.42, p.1-19, 2022. https://doi.org/10.1016/j.ejrh.2022.101165.

Tellman, B.; Sullivan, J.A.; Kuhn, C.; Kettner, A. J.; Doyle, C. S.; Brakenridge, G. R.; Erickson, T. A.; Satyback, D. A. Satellite imaging reveals increased proportion of population exposed to floods. Nature, v.596, p.80–86 2021. https://doi.org/10.1038/s41586-021-03695-w.

Wang, W.; Wang, L.; Miao, Y.; Cheng, C.; Chen, S. A survey on the influence of intense rainfall induced by climate warming on operation safety and service life of urban asphalt pavement. Journal

of Infrastructure Preservation and Resilience, v.1, p.1-14, 2020. https://doi.org/10.1186/s43065-020-00003-0.

Capítulo

4

Este capítulo refere-se ao artigo publicado na Revista Remote Sensing Applications: Society and Environment[2]. O título e o resumo são apresentados inicialmente em português e, em seguida, o texto do artigo é transcrito aqui em inglês conforme foi publicado**.**

4. AVALIAÇÃO DO DESEMPENHO DE QUATRO PRODUTOS DE SENSORIAMENTO REMOTO A PARTIR DA ESTIMATIVA DE PRECIPITAÇÃO NO ESTADO DA PARAÍBA, NORDESTE DO BRASIL

Resumo:

Considerando a importância das séries temporais de precipitação para o planejamento e a gestão de recursos hídricos, a variabilidade espacial da precipitação torna o registro de pluviômetros

[2] Costa F. F., Rufino I. A. A., Aragão R., Filho R. S. R. (2024). Performance evaluation of four remote-sensing products throughout precipitation estimation in the State of Paraíba, Northeast Brazil. Remote Sensing Applications: Society and Environment. https://doi.org/10.1016/j.rsase.2024.101256.

economicamente inviável para descrever sua distribuição para todo o Brasil devido a sua extensa área territorial. Nesse contexto, analisamos as estimativas de precipitação de quatro produtos de sensoriamento remoto para o Estado da Paraíba, Brasil, em diferentes resoluções espaciais e temporais, considerando um conjunto de dados de 149 pluviômetros. Foram usadas métricas contínuas e categóricas para avaliar a precisão dos produtos de precipitação em comparação com os pluviômetros. Entre os produtos de precipitação por satélite avaliados (CHIRPS, MSWEP, PDIR-now e SMRRAIN), a estimativa dos produtos de precipitação CHIRPS e MSWEP é geralmente satisfatória em comparação com o PDIR-Now e o SM2RAIN, com uma tendência de diminuição da precisão quando os dados analisados são da região costeira (região da Zona da Mata). Como um estudo de avaliação de desempenho de diferentes produtos de estimativa de precipitação por sensoriamento remoto em escala local, este trabalho pode fornecer uma referência para pesquisas futuras na área estudada.

PERFORMANCE EVALUATION OF FOUR REMOTE-SENSING PRODUCTS THROUGHOUT PRECIPITATION ESTIMATION IN STATE OF THE PARAÍBA, NORTHEAST BRAZIL

Abstract:

Considering the importance of rainfall time series for planning and managing water resources, the spatial variability of precipitation makes the record of rain gauges economically unfeasible to describe its distribution in Brazil due to its extensive territorial area. In this context, we analyse the precipitation estimates from four remote-sensing products for Paraíba, State, Brazil, on different spatial and temporal resolutions considering a dataset from 149 rain gauges. Continuous and Categorical metrics were used to evaluate the precipitation products's accuracy compared with rain gauges. Among the satellite precipitation products being evaluated (CHIRPS, MSWEP, PDIR-now and SMRRAIN), the estimation of precipitation products CHIRPS and MSWEP are generally satisfactory compared to PDIR-Now and SM2RAIN, with a tendency for decreasing of precision when the data analysed are from the coastal region (Mata region). As a performance evaluation study of different remote-sensing precipitation estimation products on a local scale, this work may provide a reference for future research in the area currently studied.

Keywords:
Precipitation, rain gauges, remote-sensing, accuracy.

4.1.Introduction

Considered the main input component of the water balance, total rainfall is a significant hydrological variable to understand the behaviour of other variables, such as evapotranspiration, soil moisture and runoff. However, as in other regions on planet Earth, Northeast Brazil (NEB) severely lacks *in-situ* precipitation records (FREITAS et al., 2020), either due to the absence of rainfall time series, failures in forms, or even unreliable data.

In recent years, precipitation estimation from remote-sensing (RS) has been a significant contributor (LLAUCA et al., 2021), mainly due to the extensive spatial coverage and refined space-time resolution (MIN et al., 2020). Currently, many *Satellite Precipitation Products* (SPPs) and merged (terrestrial datasets, satellite and reanalysis) are available for several applications (FUNK et al., 2015, BECK et al., 2019, BROCCA et al., 2019, HUFFMAN et al., 2019, MASSARI et al., 2020, NGUYEN et al., 2020), containing valuable information distributed across the globe.

Satellite precipitation products (SPPs) have gained considerable notoriety in recent years because they are not limited by complex terrain and provide broader spatial and temporal coverage compared to gauge-based data (ARYAL et al., 2023). Many studies have confirmed IMERG's ability to detect extreme rainfall (DA SILVA et al., 2021, RAMADHAN et al., 2022). There is also the Climate Hazards Group InfraRed Precipitation with Station data (CHIRPS), which is a near-global dataset from the US Geological Survey (USGS), generated in collaboration with the Climate Hazards Group at the University of California, Santa Barbara (FUNK et al., 2015). In recent years, this product has been widely applied for monitoring droughts, mainly in northeastern Brazil (PAREDES-TREJO et al., 2017), western Africa (AGUTU et al., 2017) and southern China (ZHONG et al., 2019). Precipitation Estimation from Remotely Sensed Information using Artificial Neural Networks–Dynamic Infrared Rain Rate near-real-time (PDIR-Now) is one of the latest PERSIANN products developed by the Center for Hydrometeorology and Remote Sensing (CHRS) at the University of California, Irvine (UCI). Its sampling of high-frequency infrared images allows precipitation to be accurately estimated shortly after the event's start (ALHARBI et al., 2024). Another SPP widely used is Multi-Source Weighted-Ensemble Precipitation (MSWEP). This global dataset uses satellite infrared and microwave precipitation estimates, rain gauge

observations, and reanalysis products (BECK et al., 2017a). In a recent evaluation of 22 SPPs, MSWEP was shown to be one of the best performers (BECK et al., 2017b). Last, we have the Soil Moisture to Rain - Advanced SCATterometer (SM2RAIN-ASCAT), which is a global product that incorporates soil moisture conditions collected by the European Meteorological Satellite Organization (EUMETSAT) MetOp satellite and uses the SM2RAIN algorithm through a bottom-up approach, to obtain precipitation estimates (BROCCA et al., 2019).

Considering the broad applicability of these products, such as water resource management (DUBE et al., 2023), hazard and disaster monitoring (GETIRANA et al., 2020) and hydrological modelings (JUNQUEIRA et al., 2022), their accuracy should be evaluated and compared with *in-situ* datasets, reducing uncertainties and allowing their practical use (LÓPEZ-BERMEO et al., 2022, NAWAZ et al., 2021). Moreover, selecting the region's most representative for a given SPP product is crucial for its right use. With this in mind, different studies have been conducted over the world (RINCÓN-AVALOS et al., 2022, SHEARER et al., 2022, ZHOU et al., 2022). Even so, few works analysed the accuracy of precipitation products estimated by remote-sensing versus *in-situ* data at a local scale in Brazil (ANDRADE et al., 2022, DUARTE et al., 2022, SANTOS et al., 2022).

In Brazil, there is a current regulatory framework for basic sanitation (BRASIL, 2022) on a local scale. Still, it depends on regional and national management policies and an increased need for data for modelling the present and future scenarios. In this context, climate change models use a non-stationary component in the rainfall time series (AGILAN et al., 2016) and the lack of *in-situ* data has contributed to the use of remote-sensing products in the calibration and validation of hydrological models (BENNOUR et al., 2022).

Considering the scarcity of studies in the NEB on the assessment of SPP accuracy at a regional scale using *in-situ* data, as far as we know, the present work evaluates four precipitation products at different spatial and temporal scales at the local level in this region; the main goal is to analyse other remote-sensing estimation products of precipitation in the state of Paraíba, a small state located in the NEB. This state comprises 223 municipalities, suffering almost every year from water shortage and is covered with a network of 266 rain gauges, suitable for studies related to comparison between *in-situ* rainfall data and SPP. Although Soares et al. (2016) had a similar study, they analysed the TRMM (i.e., *Tropical Rainfall Measuring Mission*) product for Paraíba. However, this product was discontinued. Additionally, this study analyses the feasibility of

combining data from the SPPs to use in studies of water resources. Therefore, the present study becomes unique in the region since the following questions will be analysed: (a) Which remote-sensing product best represents the total precipitation *in-situ*? (b) Do the rainfall estimated by remote-sensing products have similar performance on a local scale compared to the application of the observed one? Moreover, (c) Does the quality of these products vary in different time and space scales?

4.1.1. Study area

The state of Paraíba (Fig. 9) is around 56,467.242 km² in area, comprising 223 municipalities. João Pessoa is this state's capital and the total population is approximately 3,974.495 inhabitants (IBGE, 2022). A large percentual of the state area has a semiarid climate and the rainy season is sectorized as follows: from January to April in the region of the state called "Sertão"; from April to July, in the region called "Zona da Mata" (highest precipitation values). The months between March and July are the rainiest in Paraíba. Its rectangular shape influences different factors that interfere with the circulation of winds and the climate of the region; standing out among these factors is the proximity to the Atlantic Ocean, the existence of plateaus, the mountain range and depressions (BRASIL NETO et al., 2021). More details about the characterization of Paraíba State can be found in Brasil Neto et al. (2020), Santos et al. (2019a) and Santos et al. (2019b).

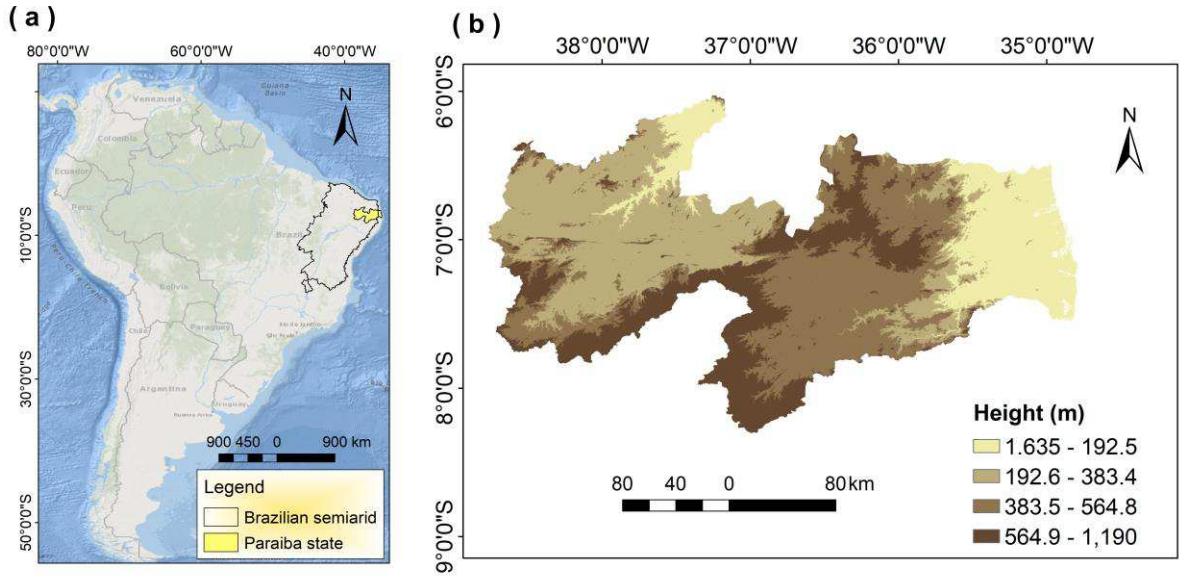

Figura 9 - Space location of the study area (a) and topography map (b)

Knowing that different factors influence precipitation behaviour over a given region, it is understood that precipitation patterns are not uniform in space or time over the state. In addition to these factors, the precipitation regime of regions located close to the equator, as is the case of the study area, is strongly influenced by atmospheric systems such as Cold Fronts, Intertropical Convergence Zone (ITCZ) and Cyclonic Vortices of High Level (VCAS) (ASSIS et al., 2015), favoring distinct climate behaviour, in terms of total precipitation, among the state's mesoregions. Therefore, this study becomes relevant to better planning and managing water resources in the state.

4.2. Data and methodology

4.2.1. Sensing-remote precipitation

Four remote-sensing estimation precipitation products were evaluated in this study (Table 1). They are the product of the Climate Hazards Center (CHC) technique version 2.0 (CHIRPSv2.0, hereafter CHIRPS) on a daily scale as the latest climate reanalysis product, Multi-Source Weighted-Ensemble Precipitation version 2 (MSWEPv2, hereafter MSWEP) and precipitation estimation from remote-sensing information using artificial neural networks Climate Data Recording (PEDIR-Now, hereafter PERSIANN) on a daily scale, also as the data set of the SM2RAIN method applied to the ASCAT soil moisture product (SM2RAIN-ASCAT, hereafter SM2RAIN).

These four products are classified into two main categories: (1) satellite-based products (CHIRPS, PDIR-now and SM2RAIN-ASCAT) and (2) merged products (MSWEP). Satellite-based products are on satellite data, while merged products combine measurement, satellite and reanalysis datasets. Satellite-based products are first based on satellite data and then corrected by measured datasets. This study used twenty years of data from 2000 to 2020 of these four products. Specific information about these products is summarized in Table 1.

The CHIRPS infrared precipitation data is a near-global ensemble (50°S–50°N, 180°E–180°W) that combines satellite observations of sea surface temperatures with data from ground stations. The algorithm employs spatial interpolation and statistical modeling techniques to estimate precipitation in areas without direct observations. With a spatial resolution of 0.05º x 0.05º and available with daily, pentadal, and monthly temporal frequencies, it produces an estimated information product with a latency of around 2 days and a final product with an average latency of

around 3 weeks. This publicly accessible dataset stores gridded rainfall time series information since 1981, mainly for trend analysis and seasonal drought monitoring, and is provided in formats NetCDF, GeoTiff e Esri BIL (FUNK et al., 2014, 2015).

The MSWEP is a merged global dataset with 0.1° × 0.1° spatial resolution data available from 1979 to the present. This product is the only one that combines measurement, satellite and reanalysis data to obtain the highest quality precipitation estimates at each location. It incorporates daily measurement observations and considers measurement reporting times to reduce temporal mismatches between satellite reanalysis estimates and measurement observations. Version 2 of this dataset features new data sources, improved weight maps, precipitation estimates with fewer peaks, a longer record, near real-time estimates, and compatibility with multisource weather (BECK et al., 2019).

The PDIR-Now (Dynamic Infrared-Rain Rate) product was produced considering remote-sensing information using near real-time artificial neural networks. It is a real-time, high-resolution (0.04° x 0.04°) global (60°N to 60°S) satellite precipitation product developed by the University of California's Center for Hydrometeorology and Remote-Sensing (CHRS), Irvine (UCI). The main advantage of PDIR-Now, compared to other near-real-time precipitation datasets, is its reliance on the high-frequency sampled IR imagery; consequently, the latency of PDIR-Now from the time of rainfall occurrence is very short (15-60 min). Additionally, PDIR-Now accounts for the errors and uncertainties that result from the use of IR imagery by adopting a variety of techniques most notable is the dynamic shifting of (Tb-R) curves using rainfall climatology. The short latency of PDIR-Now renders the dataset well-suited for near-real-time hydrologic applications such as flood forecasting and developing flood inundation maps (NGUYEN et al., 2020).

The SM2RAIN-ASCAT uses soil moisture data obtained from the Advanced Scatterometer (ASCAT) satellite through the application of the SM2RAIN (Soil Moisture to Rain) algorithm to estimate precipitation on a near-global scale (terrestrial only) on a regular grid with a sampling of 0.1º (12.5 km) from 2007 to 2022 (continues with updates). The rainfall dataset (mm/day) is provided in NetCDF format. In addition to the daily accumulated precipitation value, precipitation noise (mm/day) for each day is also provided. A monthly version with 0.25º and 0.5º degree resolution is also provided. The estimation has some limitations, such as underestimating extreme precipitation events and spurious precipitation events due to high-frequency fluctuations in soil

moisture. These deficits may be corrected in the future using more advanced bias correction techniques (BROCCA et al., 2019).

4.2.2. Gauged precipitation

To evaluate the accuracy of the four precipitation products mentioned above, these datasets were compared with precipitation observations at rain gauges (stations), which provide relatively accurate local information. Therefore, daily precipitation observations from 149 rain gauges (Fig. 10) over the study area from January 1, 2000, to December 31, 2020 were provided by the Executive Agency of Water Management for the State of Paraíba (AESA, 2021). The selection criterion was a time series with low data gaps. That is, not exceeding 10% of missing data, condition imposed by several researches reported by Rodrigues et al. (2021).

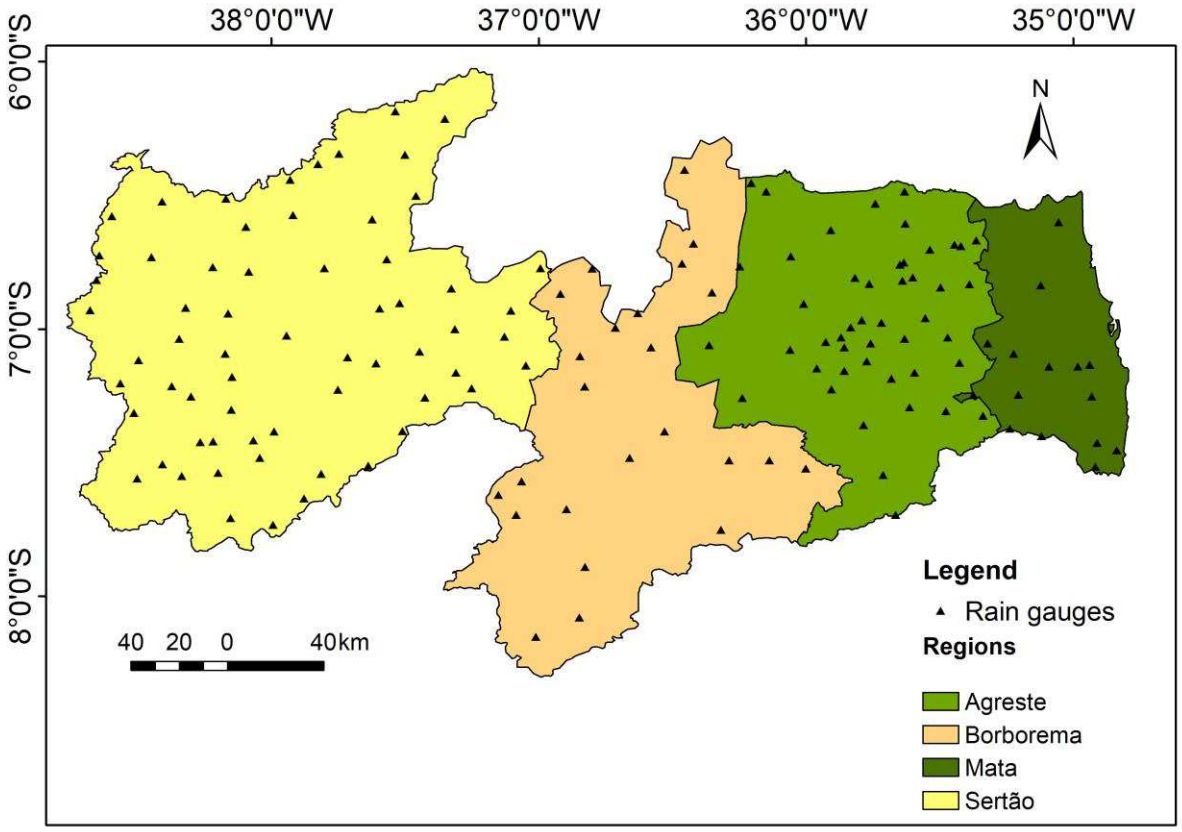

Figura 10 - Space location of rain gauges used of this study

4.2.3. Evaluation method

To evaluate rainfall data, a mismatch in the spatial scales of products is always a critical issue and needs to be carefully considered (TAN and DUAN, 2017). A common way to solve this issue

is to interpolate the data. However, interpolation may cause some uncertainties (HUANG et al., 2019). Thus, only the pixels containing at least one rainfall station were considered for evaluating the precipitation products, that is, a point-pixel analysis (BATHELEMY et al., 2022). For each point, the time series recorded by a rain gauge is directly compared with satellite observations of the area referred to the grid pixel where the rain gauge is located.

In this study, the value of each precipitation product at its spatially corresponding station was extracted to provide a direct comparison with the rain gauges. To evaluate the accuracy of these products, this study adopted five continuous metrics such as: the root mean square error ($RMSE$; Eq. 11), the standard deviation (SD; Eq. 15), the mean absolute error (MAE; Eq. 12), the Kling-Gupta efficiency index (KGE; Eq. 16) proposed by Gupta et al. (2009), modified by Kling et al. (2012).

In addition to continuous metrics that measure the accurateness of SPPs, it is essential to investigate their capability of precipitation occurrence detection. Therefore, in order to detect the precipitation forecast capacity of the products, the following categorical metrics are used: Probability of Detection (POD; Eq. 17), False Alarm Rate (FAR; Eq. 18) and Success Rate (TS; Eq. 19), were used (STANSKI et al., 1989, NURMI, 2003). These metrics were applied to total daily rainfall, considering a 1 mm/day threshold (TAN and DUAN, 2017, ZIVEH et al., 2022). Initially, the precipitation data derived from RS products and rainfall stations were converted to binary data (0 and 1), which means zero (0), is no event above the threshold and one (1) is an event above the threshold. For application and statistical metrics, the study developed a contingency table (NURMI, 2003).

Such metrics are used in several studies to assess the performance of satellite products (TANG et al., 2016, CHEN et al., 2019, FANG et al., 2019, FILHO et al., 2022). The technical route of this study is shown in Fig. 11.

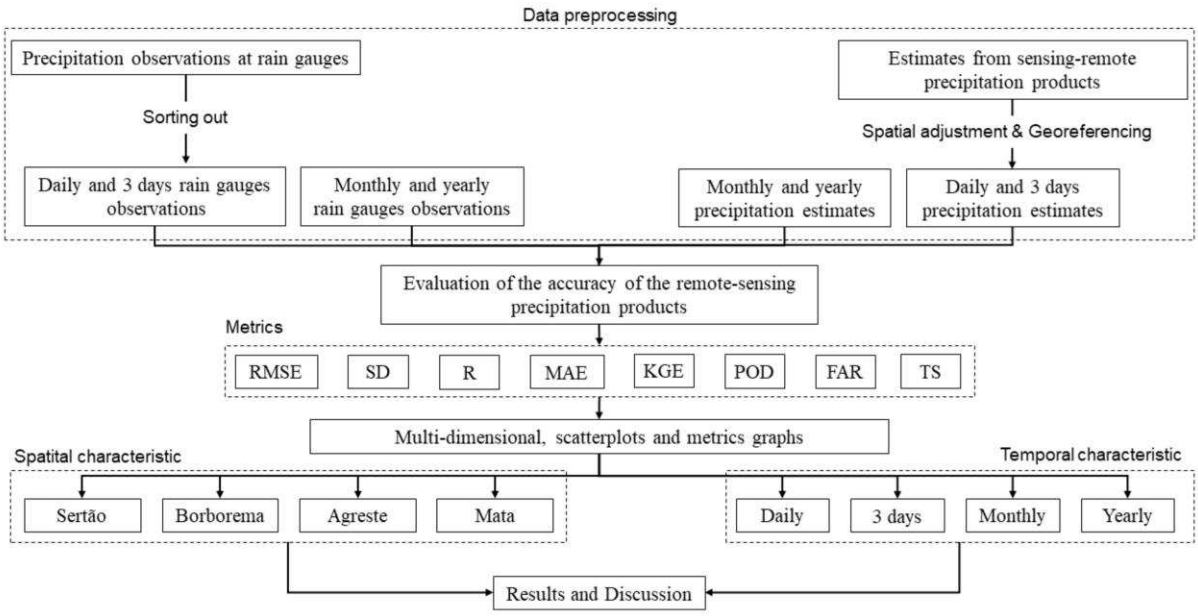

Figura 11 - Processing workflow for the precipitation observations at rain gauges and estimates from sensing-remote precipitation products of this study

4.3. Results

As stated earlier, the comparisons and validation steps were carried out on different time scales using daily, monthly, and yearly observations, the results of which are presented in the following subsections.

4.3.1. Accuracy evaluation at a daily time scale

This section compared corresponding daily precipitation values from SPPs and rain gauges. These precipitation values were compared daily for the whole study period and with data accumulated over three days. Continuous (KGE, R, RMSE, and MAE) and categorical metrics (POD, FAR, and TS) were employed in this section.

In terms of daily basis, statistically, all SPPs performed poorly in all regions of the study area, with values of KGE below 0.48 (Table 10). In contrast, the KGE efficiency value improved considerably when moving from the daily scale to the accumulated three-day values (Table 14). The best results were observed when using the time series from MSWEP (from 0.48 to 0.64 for KGE), following CHIRPS (from 0.42 to 0.60 for KGE). Even though these products have shown elevated results, the KGE values are still classified as weak, with the worst results presented by PDIR-Now. Similar to the KGE metric, the SPPs also showed poor performance for R in all regions

of the study area, with values below 0.51 and a slight improvement considering the 3-day accumulation and the KGE. Considering the RMSE metric, SM2RAIN obtained, on average, the lowest value (7.63 mm), and the second most accurate SPP was MSWEP, with an RMSE value of 7.91 mm, on average. PDIR-Now and CHIRPS, on the other hand, were less accurate when acquiring, on average, RMSE values of 10.97 mm and 10.11 mm, respectively. Finally, in terms of the MAE metric, the RM2RAIN and MSWEP achieved the first and second lowest MAE values of 2.73 mm and 2.85 mm, on average, while other SPPs with overestimation characteristics, obtained higher MAE values, with the highest value (5.20 mm) for CHIRPS in the region MATA. All this statistical behavior can be better visualized in Fig. 12. It is noted that the SPPs present, on average, better KGE (Fig. 12-a) and R (Fig. 12-b) statistics in the Sertão region mainly, as well as in the forest region. On the other hand, in the most central region of the state, represented by the Agreste and Borborema regions, the SPPs present slight difficulty in simulating precipitation.

Tabela 10 - Summary of the continuous metrics average used in this study to evaluate the estimate of SPPs precipitation

Region	**Product**	**Daily totals**				**3 days**			
		Metrics				Metrics			
		KGE	R	RMSE	MAE	KGE	R	RMSE	MAE
Sertão	CHIRPS	0.42	0.48	8.12	2.66	0.60	0.65	13.83	5.94
	MSWEP	0.48	0.50	8.23	2.50	0.64	0.66	14.12	5.47
	PDIR-Now	0.37	0.41	9.45	2.94	0.52	0.56	16.83	6.83
	SM2RAIN	0.20	0.44	8.02	2.51	0.42	0.62	14.19	5.64
Borborema	CHIRPS	0.23	0.34	7.07	2.11	0.42	0.53	12.08	4.86
	MSWEP	0.29	0.36	6.94	1.93	0.52	0.57	11.64	4.27
	PDIR-Now	0.11	0.28	9.01	2.52	0.27	0.47	15.94	5.98
	SM2RAIN	0.06	0.36	6.32	1.83	0.28	0.56	11.19	4.25
Agreste	CHIRPS	0.19	0.29	10.09	3.35	0.38	0.48	16.80	7.63
	MSWEP	0.29	0.39	6.98	2.82	0.48	0.59	11.82	6.03
	PDIR-Now	0.05	0.24	9.80	3.06	0.17	0.41	17.55	7.39
	SM2RAIN	0.07	0.38	6.48	2.59	0.26	0.57	11.68	5.81
Mata	CHIRPS	0.24	0.38	15.16	5.20	0.45	0.56	24.94	11.78
	MSWEP	0.42	0.51	9.47	4.14	0.58	0.67	16.29	8.78
	PDIR-Now	0.01	0.38	15.62	4.88	0.10	0.52	28.66	11.78
	SM2RAIN	0.14	0.45	9.72	3.97	0.31	0.62	18.22	8.89

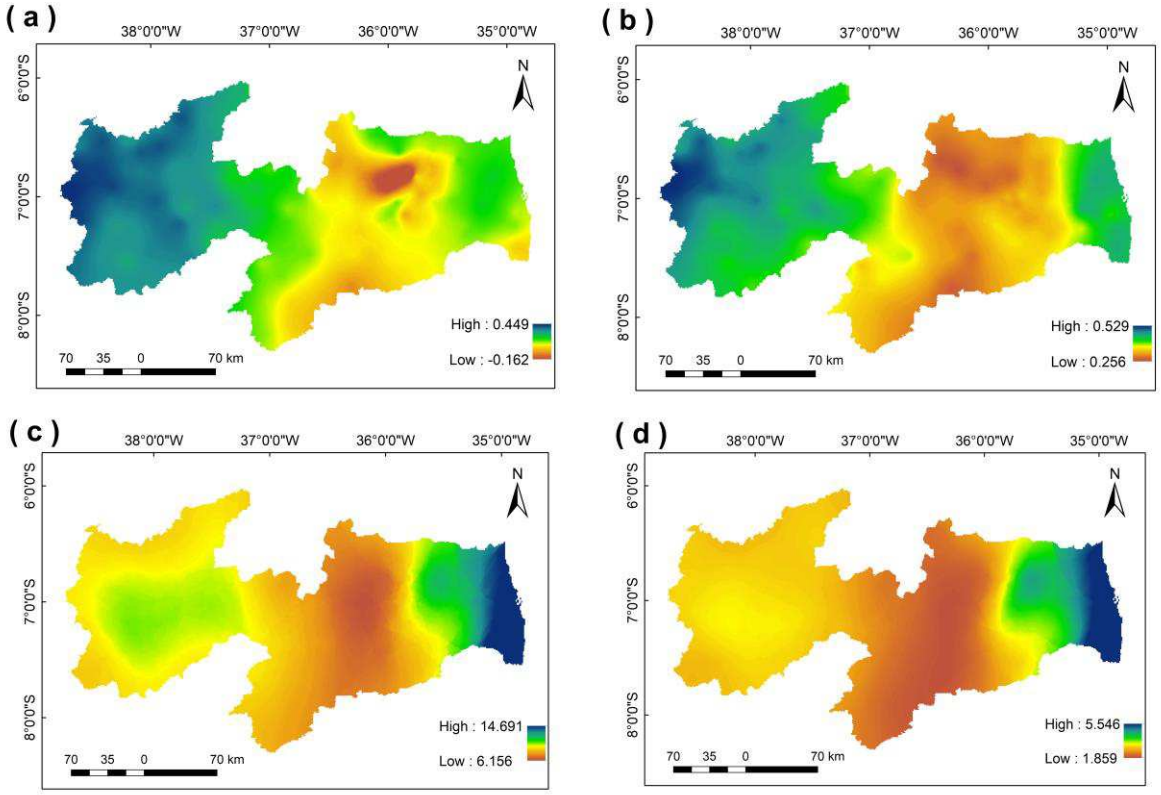

Figura 12 - Variability space averaged continuous metrics including (a) KGE, (b) R, (c) RMSE, and (d) MAE

Analyzing spatially the data quality of all SPPs evaluated in this study (Fig. 13), we find a slight decrease in the accuracy of the SPPs (Fig. 13-a); when the elevation decreases, what was reported in the results illustrated in Table 2 discussed previously. The RMSE (Fig. 13-b) and MAE (Fig. 13-c) are relatively stable, with a peak in regions of low elevation, where precipitation totals are higher.

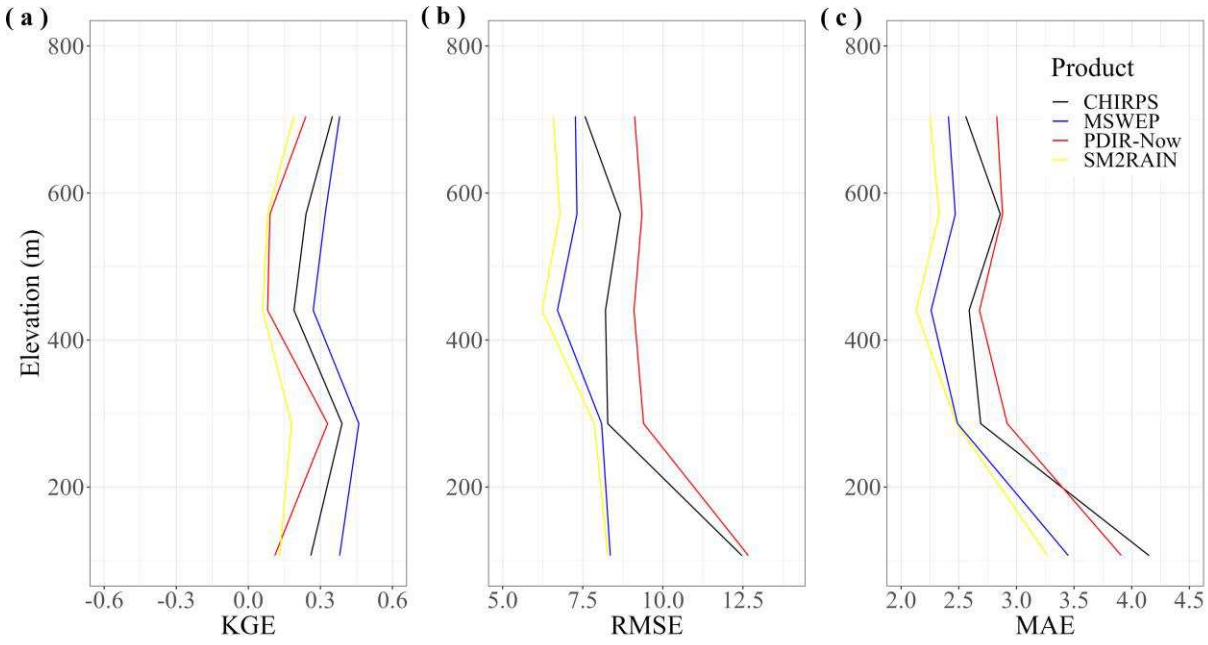

Figura 13 - Distribution curves of averaged daily continuous metrics including (a) KGE, (b) RMSE and (c) MAE along the topography of the study area

The Performance Diagram (ROEBBER, 2009) focuses on precipitation occurrence assessment metrics, i.e, POD, success rate (1 - FAR), TS, and biases, to compare the performance of SPPs, and related results are presented in Fig. 14. In these diagrams, the points (i.e., representing the target precipitation for SPPs) closer to the upper right corner had better detectability of precipitation occurrence. In other words, the points closest to the upper right corner showed high POD and TS values and low FAR and bias values. According to Fig. 14, on average, the RS precipitation estimation products presented poor results that support the perceptions drawn from Table 2. For example, the POD is around 0.40, with a significant predominance of values above 0.40 in the Mata region. The Borborema region had slightly lower detection accuracies with POD values below 0.40. On the other hand, in terms of TS, no products were satisfactorily performed, with TS values below 0.40, presenting small fluctuations between MSWEP and SM2RAIN. Taking all Performance Diagram metrics into account, data from MSWEP remained the most accurate SPP and SM2RAIN came in second, followed by CHIRPS and PDIR-Now.

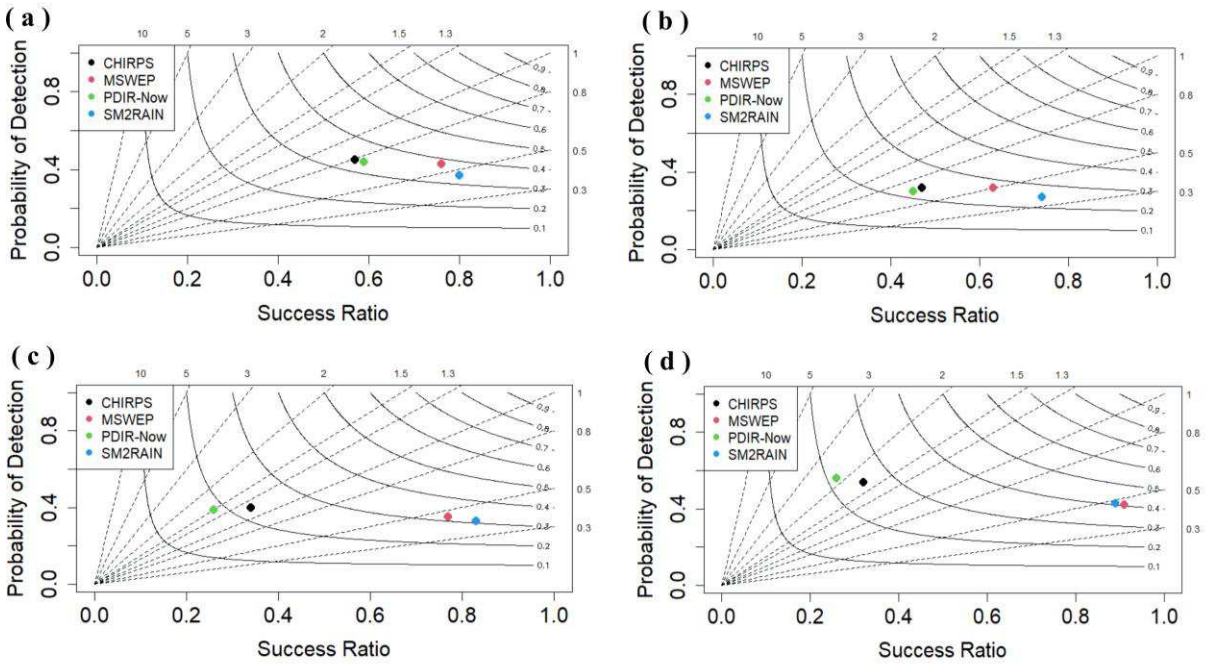

Figura 14 - Performance diagram of the categorical metrics for the regions of (a) Sertão, (b) Borborema, (c) Agreste and (d) Mata

4.3.2. Accuracy evaluation at an monthly time scale

This section compared corresponding monthly precipitation values from SPPs and rain gauges. These precipitation values were compared for the whole study period on a monthly basis. Continuous metrics were employed in this section.

To gain better insights into the accuracy of these four products at a monthly scale, RMSE (Green dashed lines), SD (Blue dashed lines), and R (Black dashed lines) were calculated and presented in Taylor diagrams (Fig. 15). Taylor diagrams (TAYLOR, 2001) can concisely and appropriately summarize the degree of correspondence between the estimates from the precipitation products and observations at stations by considering the three statistical indices mentioned above, with the points closer to the observation point on the X-axis showing better accuracy. In other words, closer points to the X-axis had lower RMSE values, higher R values, and similar SD values to the reference precipitations. In general, Fig. 15 illustrates that the SPPs are relatively closer to the X-axis point, indicating their best performances, mainly from Jan to Jun, when the amount of precipitation is large, compared to the other months of the year when the amount of precipitation seems to be smaller (Fig. 16). This was because, the obtained RMSE and SD values in these SPPs were closer to the ones obtained from rain gauges, with an improvement in CHIRPS as you move from the Sertão to the zone Mata. The SPPs, namely CHIRPS, MSWEP, PDIR-Now, and SM2RAIN, had

comparable performances since, in the regions of Sertão and Borborema, MSWEP and SM2RAIN performed better, PDIR-Now in the Sertão, Agreste and Mata regions, and CHIRPS in the regions Borborema, Agreste and Mata. Broadly speaking, MSWEP presents the best overall statistical results.

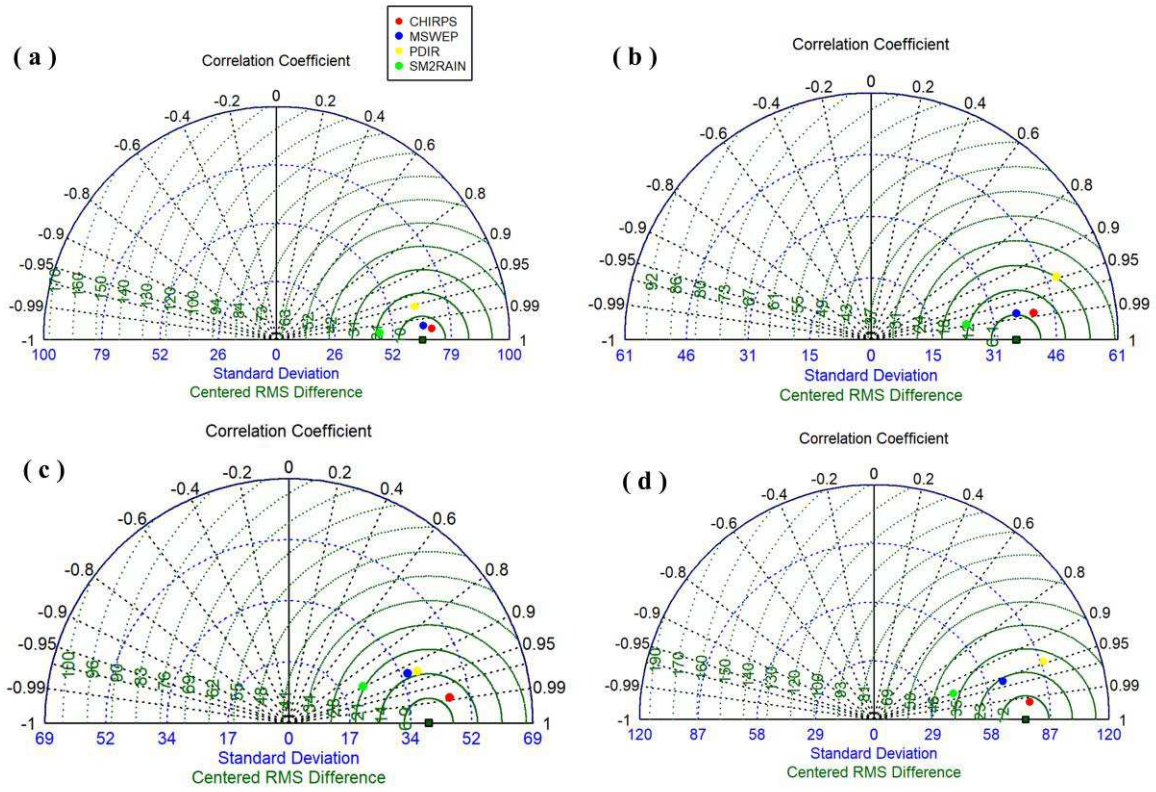

Figura 15 - Taylor diagrams of monthly precipitation estimates from each SPPs in comparison with observations at stations over the (a) Sertão, (b) Borborema, (c) Agreste and (d) Mata

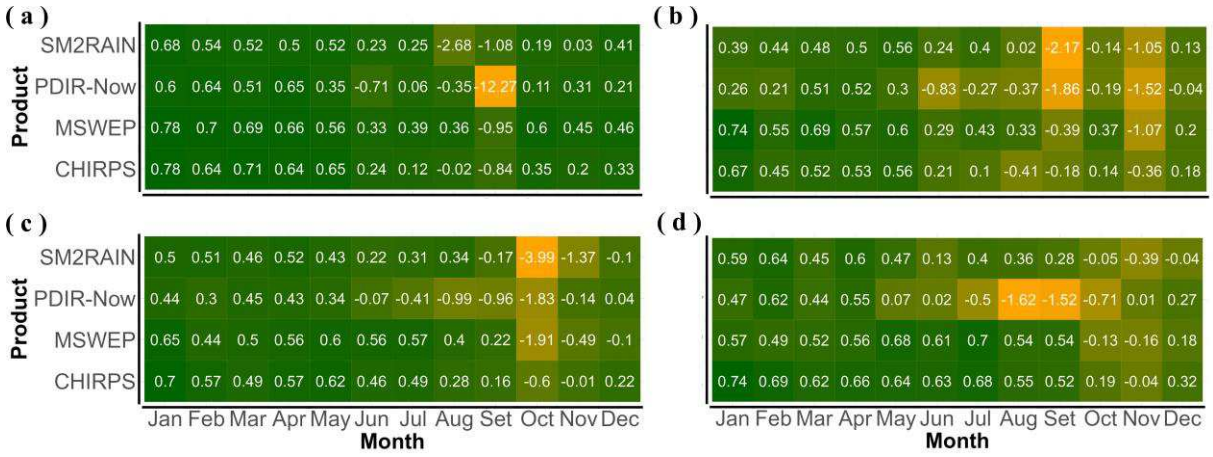

Figura 16 - Heat maps of average monthly efficiency KGE of the SPPs for the regions of (a) Sertão, (b) Borborema, (c) Agreste, and (d) Mata. Darker tones have better KGE values, and lighter tones have the worst

4.3.3. Accuracy evaluation at a yearly time scale

This section compared corresponding yearly precipitation values from SPPs and rain gauges. These precipitation values were compared on a yearly basis for the whole study period. Continuous metrics were employed in this section. This analysis may support a better understanding of the temporal characteristics of the selected SSP, revealing whether they had stable performances from 2000 to 2020.

In general, it is observed that MSWEP presents the best results (R=0.91, RMSE=114.68 and MAE=88.73) and CHIRPS also presents a relatively good performance (R=0.91, RMSE=136.12 and MAE =95.56), as shown in Fig. 17 and in Fig. 18. As can be seen, the CHIRPS and MSWEP products showed a high frequency of values above 0.70 of the KGE efficiency in the four regions of the study area, with greater frequency for the Sertão regions (Fig. 18-a), Borborema (Fig. 18-b) and Mata (Fig. 18-d).

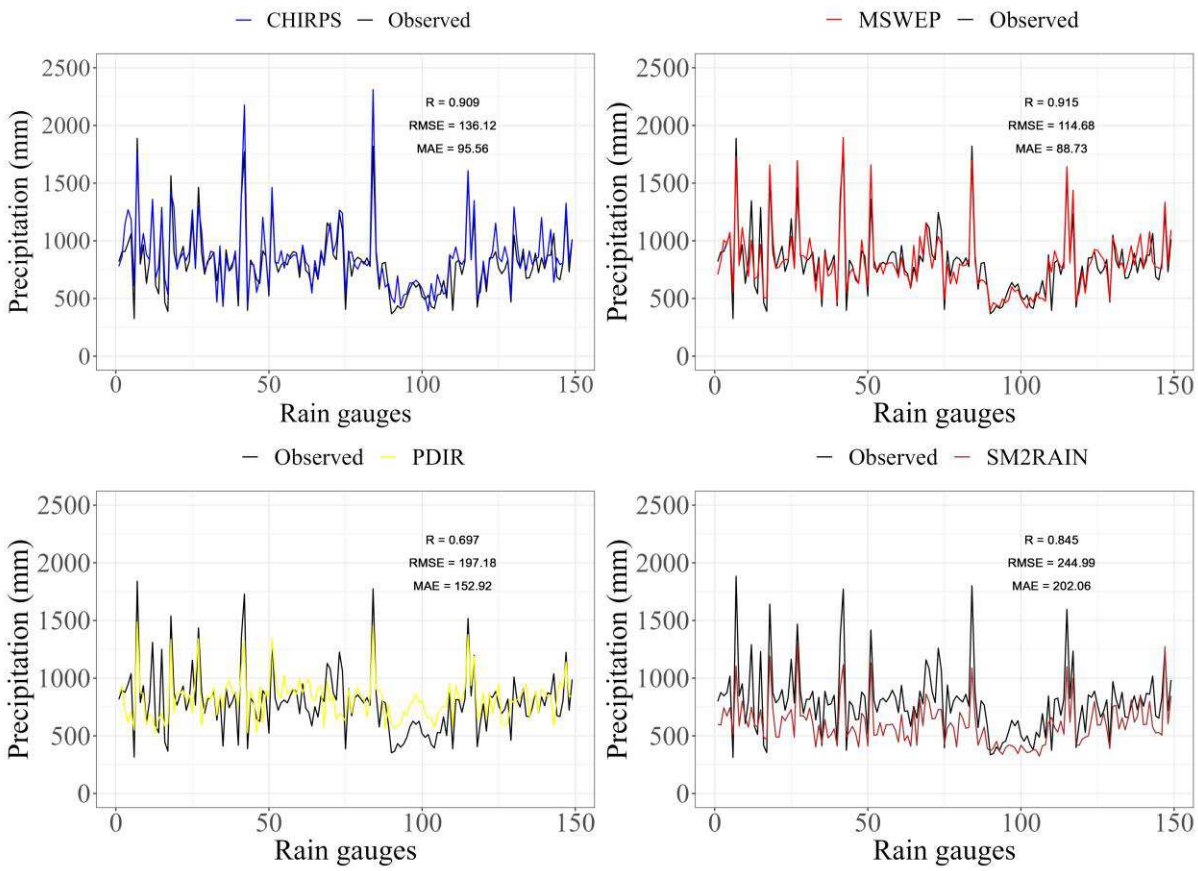

Figura 17 - Variability of time series of yearly averaged precipitation of the each SPPs in relations to the rain gauges

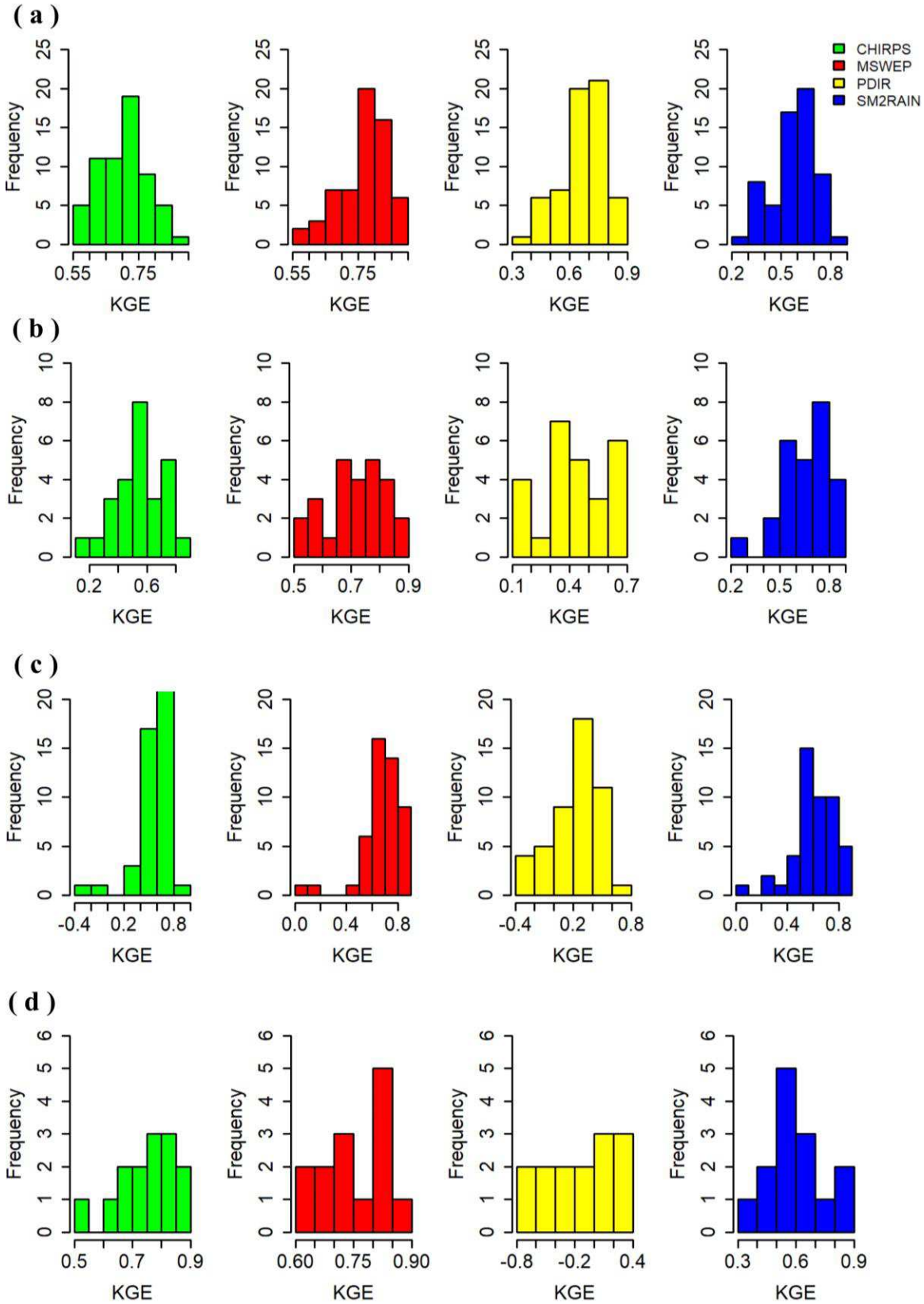

Figura 18 - Frequency distribution the efficiency KGE of SPPs for the regions of (a) Sertão, (b) Borborema, (c) Agreste and (d) Mata

4.4. Discussion

4.4.1. General remarks

The increasing availability of SPP has attracted the interest of many researchers from different areas worldwide (GETIRANA et al., 2020; JUNQUEIRA et al., 2022; DUBE et al., 2023). However, reliability in SPPs is a warning that must be cautiously treated (NAWAZ et al., 2021, LÓPEZ-BERMEO et al., 2022). Any error in precipitation estimates, such as magnitude errors, will propagate in the models and, consequently, in the final results (ALEMU et al., 2020, CHEN et al., 2020, GUMINDOGA et al., 2021, GAVAHI et al., 2022, KAZEMZADEH et al., 2022). For example, Kou et al. (2024) reported different bias and error characteristics of precipitation data from different sources. In these circumstances, an alternative is to evaluate the SPPs to quantify the magnitudes of the errors and adequately identify the characteristics of the errors; however, significant efforts are still needed to understand and address this challenge entirely.

It is essential to incorporate different metrics to evaluate the performance of SPPs. In this sense, continuous and categorical metrics focused on estimating precipitation totals can be used. However, a critical reason underlying multiple metrics is that no single metric addresses all aspects of interest (OMAR et al., 2023). In other words, the metric's definition is based on the analysis type. For this reason, it is crucial to consider various performance metrics to understand the information they can provide.

4.4.2. Discussing and comparing the results

This article evaluated four SPPs using observations from rainfall stations across Paraíba State, Brazil. Both continuous and categorical metrics were considered in the validation process. The results generally suggested discrepant performance of all SPPs, which was expected since each SPP was generated using multiple sources, different approaches, and algorithm principles to combine the different databases.

Analyzing the main points in terms of daily scale, Table 2 shows that the indices used to evaluate the performance of SSPs improved considerably when moving from the daily scale to three-day accumulated values. This corroborates the study by Soares et al. (2016), who showed that the longer the precipitation accumulation period, the better the correlations between data observed in rain gauges and those estimated by remote sensing products. According to the authors, this happens

because the increase in the temporal scale makes it possible to compensate for temporal errors. Still, based on Table 2, the best results were observed when using the MSWEP time series, followed by CHIRPS dataset. Bathelemy et al. (2022) also reported satisfactory results when using CHIRPS and MSWEP. According to the authors, these products are recommended due to their ability to estimate intense rainfall percentiles. Still, for them, MSWEP is recommended for most hydrometeorological applications. However, as was evident, the MSWEP and CHIRPS products, for example, performed well in the regions Sertão but not very well in the Borborema and Agreste regions (Table 2). This highlights the need to consider the product that best represents the region for carrying out studies and hydraulic works, for example, and not consider one product as being the best for the entire study area, as generally happens, because this can favor underestimation or overestimation of the work, directly impacting the final budget.

Moving toward monthly observations, the efficiency of KGE values improved, presenting satisfactory results in the first half of the year, which corroborates the study by Campos and Andrade (2021), who mention that the rain season in NEB reaches its peak in March, April and May when the Intertropical Convergence Zone (ITCZ) is further south. Medeiros et al. (2019) also observed this same behaviour, that is, that the highest rainfall is concentrated in the first half of the year when they carried out a study on the spatial variability of precipitation in the state of Paraíba. Reis et al. (2017) also reported that remote-sensing products reproduced monthly precipitation more accurately than daily products.

Finally, moving towards annual observations, in general, a certain agreement was observed in the data simulated by the SPPs in comparison to the rain gauge records (Fig. 17), except for the PDIR-Now and SM2RAIN products which had a tendency to underestimate, as was reported on daily and monthly scales. In general terms, the values of the continuous metrics (KGE, R, RMSE and MAE) reflect this agreement (Figs. 17 and 18). However, due to the complex topography and the particular climate system of the study area, affected by the proximity of the coastal region and the Borborema plateau, the SPPs have difficulty in estimating the total precipitation, which can be proven by the low values of the categorical metrics (Fig 15) as it approaches the coastal region. Similar results were reported by Ziveh et al. (2022).

Generally, the Borborema plateau's precipitation estimate tends to be underestimated towards the coast. On the opposite side, after the sudden elevation change, it tends to overestimate precipitation. Corroborating these results, Nascimento et al. (2021) also observed trends of

underestimation of precipitation by the IMERG product in high-elevation regions and overestimation in coastal regions in southern Brazil, possibly due to the spatial resolution and correction of ground clutter made by the satellite (DUAN et al., 2015, RODRIGUES et al., 2021). Furthermore, in high altitude regions, precipitation is extremely variable and there are changes in the distribution of rainfall (NAVARRO et al., 2019), which can result in lower precision (NASCIMENTO et al., 2021), in addition to other possible reasons (DINKU et al., 2008, KARASEVA et al., 2012, GUO et al., 2016). This corroborates that studies in different regions, purposes and scales favour safer and more effective applicability at local and regional scales.

4.4.3. Sources of uncertainties

In this paper, the point-pixel analysis (BATHELEMY et al., 2022) comparison method was implemented to assess the performance of the SPPs throughout study area. For each point, the time series recorded by a rain gauge is directly compared with satellite observations of the area referred to the grid pixel where the rain gauge is located. Accordingly, the results may undervalue the accuracy of the SPPs due to mismatches between point measurements (i.e., rain gauges) and pixel measurements (i.e., SPPs). This issue may also be a source of uncertainty as the spatial resolution of SPPs differs (Table 1), and the limited representativeness of point observations could affect the results. For instance, the temporal inconsistency between the Coordinated Universal Time (UTC) and local time of record *in-situ*, which differs around the world, could probably introduce some uncertainties in the validations (YANG et al., 2019). Furthermore, the inherent spatial mismatch between in situ data and SPPs, as well as the precipitation under-catch of in situ instruments due to the relief and wind effect, are other sources of uncertainties (LIU et al., 2022), in addition to the low density of rain gauges, or even their poor distribution (Fig. 10). The region presents variations in relief (Fig. 9), with the presence of the Borborema plateau which acts as a natural barrier (CACCAMO et al., 2017), preventing or even hindering the passage of humid masses from the Atlantic Ocean and is pushed towards the interior of the NEB, favoring orographic rains (also called relief), as it is located in a region of high altitudes, with variable intensity and longer durations, characteristic of these types of rain (LUIZ-SILVA et al., 2021). However, it is recommended that other types of analysis be carried out for future studies, such as those carried out by Zhu et al. (2020). Although, the current state of SPPs requires further modifications and enhancement to provide more accurate datasets.

4.4.4. Criteria beyond accuracy

In addition to the discussed criteria for measuring the accuracy of SPPs, some other criteria might be considered simultaneously to select the most appropriate SPP. For instance, the spatial resolution of SPPs might be a constraint in some applications (ZHU et al., 2023). Among the SPPs, PDIR-Now provides precipitation estimates with the highest spatial resolution ($0.04° \times 0.04°$) and, thus, could be useful for the application needing more data for a particular region. Additionally, some other applications require sub-daily datasets also limit the choices considering the original SPPs. However, to overcome this situation, it's possible to apply downscaling approaches to have the SPP with higher spatial-temporal resolutions (ZHU et al., 2023). Moreover, the necessity of having precipitation data for a more extended period, i.e., before 2000, could also introduce another factor that limits the choices SPPs, except for CHIRPS and MSWEP. However, it is not recommended that any of these products, even the most reliable ones (CHIRPS and MSWEP), can be used for calibration/validation of a hydrological model at daily and monthly time intervals.

4.4.5. Current state and future perspectives

The climate of the state of Paraíba, is dominated by a semi-arid climate characterized by low precipitation and high evapotranspiration rates. The state faces many climate hazards, such as droughts and floods. Therefore, it is a paramount need to have access to high-quality data, such as accurate precipitation estimates.

In particular, reliable and long-term precipitation data allow for better monitoring of water resource conditions and, consequently, adopting strategies to mitigate the water crisis (droughts and floods).

Considering that more accurate SPPs allow for more concise monitoring of relevant phenomena, such as drought and floods, improving the accuracy of these SPPs for the entire study area becomes relevant. The most common practice is to apply bias corrections, as happens in other regions (LIU et al., 2023). Another possibility would be to generate a precipitation dataset that combines different data sources (SPPs and *in-situ* data) and generate a unified and accurate SPP for the entire study area. This precipitation dataset could provide more precise precipitation to help scholars conduct research and public managers make decisions regarding monitoring and managing water resources.

4.5. Conclusions

The evaluation of different data sources of precipitation estimation products was important for understanding the spatiotemporal distribution of precipitation totals in the state of Paraíba. This highlighted the need to consider the SPPs that best estimate the precipitation totals in the region where they are intended to be used, for carrying out studies, hydraulic projects, applications in hydrological models, etc.

Based on statistical metrics, we found that the unsatisfactory performance of SPPs should be attributed mainly to high elevation regions (precipitation is extremely variable and there are changes in rainfall distribution) and coastal regions (sudden elevation change), where SPPs were unable to perform well compared to rain gauge observations, especially on the daily scale.

Finally, we hope the results presented in this study can serve as a reference for be used in hydrological studies, although the current state of SPPs requires further improvements to provide more accurate estimates of precipitation in the study area.

4.6. References

AESA (2021) Agency Executive Water Management of the State of Paraíba. Daily rainfall (mm), january 1994 to december 2020. Retrieved from. http://www.aesa.pb.gov.br.

Agilan, V., Umamahesh, N.V., 2016. Is the covariate-based non-stationary rainfall IDF curve capable of encompassing future rainfall changes? Journal of Hydrology. https://doi.org/10.1016/j.jhydrol.2016.08.052.

Agutu, N.O., Awange, J.L., Zerihun, A., Ndehedehe, C.E., Kuhn, M., Fukuda, Y., 2017. Assessing multi-satellite remote sensing, reanalysis, and land surface models' products in characterizing agricultural drought in East Africa. Remote sensing of environment. https://doi.org/10.1016/j.rse.2017.03.041.

Andrade, J.M., Neto, A.R., Bezerra, U.A., Moraes, A.C.C., Montenegro, S.M.G.L., 2022. A comprehensive assessment of precipitation products: Temporal and spatial analyses over terrestrial biomes in Northeastern Brazil. Remote-sensing Applications: Society and Environment. https://doi.org/10.1016/j.rsase.2022.100842.

Alemu, M.L., Worqlul, A.W., Zimale, F.A., Tilahun, S.A., Steenhuis, T.S., 2020. Water Balance for a Tropical Lake in the Volcanic Highlands: Lake Tana, Ethiopia. Water. https://doi.org/10.3390/w12102737.

Alharbi, R.S., Dao, V., Jimenez Arellano, C., Nguyen, P., 2024. Comprehensive Evaluation of Near-Real-Time Satellite-Based Precipitation: PDIR-Now over Saudi Arabia. Remote Sensing. https://doi.org/10.3390/rs16040703.

Aryal, A., Tran, T.N.D., Kumar, B., Lakshmi, V., 2023. Evaluation of Satellite-Derived Precipitation Products for Streamflow Simulation of a Mountainous Himalayan Watershed: A Study of Myagdi Khola in Kali Gandaki Basin, Nepal. Remote Sensing. https://doi.org/10.3390/rs15194762.

Bathelemy, R., Brigode, P., Boisson, D., Tric, E., 2022. Rainfall in the Greater and Lesser Antilles: Performance of five gridded datasets on a daily timescale. Journal of Hydrology: Regional Studies. https://doi.org/10.1016/j.ejrh.2022.101203.

Beck, H.E., Wood, E.F., Pan, M., Fisher, C.K., Miralles, D.G., Dijk, A.I.J.M.V., Mcvicar, T.R., Adler, R.F., 2019. MSWEP V2 Global 3-Hourly 0.1° Precipitation: Methodology and Quantitative Assessment. Bulletin of the American Meteorological Society. https://doi.org/10.1175/BAMS-D-17-0138.1.

Beck, H.E., Dijk, A.V., Levizzani, V., Schellekens, J., Miralles, D.G., 2017a. MSWEP: 3-hourly 0.25◦ global gridded precipitation (1979–2015) by merging gauge, satellite, and reanalysis data. Hydrology and Earth System Sciences. https://doi.org/10.5194/hess-21-589-2017.

Beck, H.E., Vergopolan, N., Pan, M., Levizzani, V., Van Dijk, A.I., Weedon, G.P., ... & Wood, E.F., 2017b. Global-scale evaluation of 22 precipitation datasets using gauge observations and hydrological modeling. Hydrology and Earth System Sciences. https://doi.org/10.5194/hess-21-6201-2017.

Bennour, A., Jia, L., Menenti, M., Zheng, C., Zeng, Y., Barnieh, B.A., Jiang, M., 2022. Calibration and Validation of SWAT Model by Using Hydrological Remote-sensing Observables in the Lake Chad Basin. Remote-sensing. https://doi.org/10.3390/rs14061511.

BRASIL (2022) Law nº 14,026, july 15, 2020. Updates the basic sanitation legal framework. Retrieved from. http://www.planalto.gov.br/ccivil_03/_ato2019-2022/2020/lei/l14026.htm.

Brasil Neto, R.M., Santos, C.A.G., Silva, R.M., Santos, C.A.C., Liu, Z., Quinn, N.W., 2021. Geospatial cluster analysis of the state, duration and severity of drought over Paraíba State, northeastern Brazil. Science of The Total Environment. https://doi.org/10.1016/j.scitotenv.2021.149492.

Brasil Neto, R.M., Santos, C.A.G., Nascimento, T.V.M., Silva, R.M., Santos, C.A.C., 2020. Evaluation of the TRMM product for monitoring drought over Paraíba state, northeastern Brazil: a statistical analysis. Remote-sensing. https://doi.org/10.3390/rs12142184.

Brocca, L., Filippucci, P., Hahn, S., Ciabatta, L., Massari, C., Camici, S., Schüller, L., Bojkov, B., Wagner, W., 2019. SM2RAIN-ASCAT (2007-2018): Global daily satellite rainfall data from ASCAT soil moisture observations. Earth System Science Data. https://doi.org/10.5194/essd-11-1583-2019.

Caccamo, M.T., Castorina, G., Colombo, F., Insinga, V., Maiorana, E., Magazù, S., 2017. Weather forecast performances for complex orographic areas: impact of different grid resolutions and of geographic data on heavy rainfall event simulations in sicily. Atmospheric Research. https://doi.org/10.1016/j.atmosres.2017.07.028.

Campos, D.A., Andrade, E.M., 2021. Seasonal trend of climate variables in an area of the Caatinga phytogeographic domain. Water. http://dx.doi.org/10.18227/1982-8470ragro.v15i0.6833.

Chen, F., Yuan, H., Sun, R., Yang, C., 2020. Streamflow Simulations Using Error Correction Ensembles of Satellite Rainfall Products over the Huaihe River Basin. Journal of Hydrology. https://doi.org/10.1016/j.jhydrol.2020.125179.

Chen, C., Chen, Q., Duan, Z., Zhang, J., Mo, K., Li, Z., Tang, G., 2018. Multiscale Comparative Evaluation of the GPM IMERG v5 and TRMM 3B42 v7 Precipitation Products from 2015 to 2017 over a Climate Transition Area of China. Remote Sensing. https://doi.org/10.3390/rs10060944.

Da Silva, N.A., Webber, B.G., Matthews, A.J., Feist, M.M., Stein, T.H., Holloway, C.E., Abdullah, M.F., 2021. Validation of GPM IMERG extreme precipitation in the Maritime Continent by station and radar data. Earth and Space Science. https://doi.org/10.1029/2021EA001738.

Dinku, T., Chidzambwa, S., Ceccato, P., Connor, S.J., Ropelewski, C.F., 2008. Validation of high-resolution satellite rainfall products over complex terrain. International Journal of Remote Sensing. https://doi.org/10.1080/01431160701772526.

Duarte, L.V., Formiga, K.T.M., Costa, V.A.F., 2022. Analysis of the IMERG-GPM Precipitation Product Analysis in Brazilian Midwestern Basins Considering Different Time and Spatial Scales. Water. https://doi.org/10.3390/w14162472.

Dube, T., Seaton, D., Shoko, C., Mbow, C., 2023. Advancements in earth observation for water resources monitoring and management in Africa: A comprehensive review. Journal of Hydrology. https://doi.org/10.1016/j.jhydrol.2023.129738.

Duan, Y., Wilson, A.M., Barros, A.P., 2015. Scoping a field experiment: error diagnostics of TRMM precipitation radar estimates in complex terrain as a basis for IPHEx2014. Hydrology and Earth System Sciences. https://doi.org/10.5194/hess-19-1501-2015.

Fang, J., Yang, W., Luan, Y., Du, J., 2019. Evaluation of the TRMM 3B42 and GPM IMERG products for extreme precipitation analysis over China. Atmospheric Research. https://doi.org/10.1016/j.atmosres.2019.03.001.

Filho, G.M.R., Coelho, V.H.R., Freitas, E.S.F., Xuan, Y., Brocca, L., Almeida, C.N., 2022. Regional-scale evaluation of 14 satellite-based precipitation products in characterising extreme events and delineating rainfall thresholds for flood hazards. Atmospheric Research. http://dx.doi.org/10.1016/j.atmosres.2022.106259.

Freitas, E.S., Coelho, V.H.R., Xuan, Y., Melo, D.C.D., Gadelha, A.N., Santos, E.A., Galvão, C.O., Filho, G.M.R., Barbosa, L.R., Huffman, G.J., Petersen, W.A., Almeida, C.N., 2020. The performance of the IMERG satellite-based product in identifying sub-daily rainfall events and their properties. Journal of Hydrology. http://dx.doi.org/10.1016/j.jhydrol.2020.125128.

Funk, C., Peterson, P., Landsfeld, M., Pedreros, D., Verdin, J., Shukla, S., Husak, G., Rowland, J., Harrison, L., Hoell, A., Michaelsen, J., 2015. The climate hazards infrared precipitation with stations - a new environmental record for monitoring extremes. Scientific Data. https://doi.org/10.1038/sdata.2015.66.

Funk, C.C., Peterson, P.J., Landsfeld, M.F., Pedreros, D.H., Verdin, J.P., Rowland, J.D., Romero, B.E., Husak, G.J., Michaelsen, J.C., Verdin, A.P., 2014. A quasi-global precipitation time series for drought monitoring. US Geological Survey data series. https://doi.org/10.3133/ds832.

Gavahi, K., Abbaszadeh, P., Moradkhani, H., 2022. How Does Precipitation Data Influence the Land Surface Data Assimilation for Drought Monitoring? Science of The Total Environment. https://doi.org/10.1016/j.scitotenv.2022.154916.

Getirana, A., Kirschbaum, D., Mandarino, F., Ottoni, M., Khan, S., Arsenault, K., 2020. Potential of GPM IMERG Precipitation Estimates to Monitor Natural Disaster Triggers in Urban Areas: The Case of Rio de Janeiro, Brazil. Remote-sensing. https://doi.org/10.3390/rs12244095.

Gumindoga, W., Rientjes, T.H.M., Haile, A.T., Reggiani, P., Makurira, H., 2021. Propagation of CMORPH Rainfall Errors to REW Streamflow Simulation Mismatch in the Upper Zambezi Basin. Journal of Hydrology: Regional Studies. https://doi.org/10.1016/j.ejrh.2021.100966.

Guo, H., Chen, S., Bao, A., Behrangi, A., Hong, Y., Ndayisaba, F., Hu, J., Stepanian, P.M., 2016. Early assessment of Integrated Multi-satellite Retrievals for Global Precipitation Measurement over China. Atmospheric Research. https://doi.org/10.1016/j.atmosres.2016.02.020.

Gupta, H.V., Kling, H., Yilmaz, K.K., Martinez, G.F., 2009. Decomposition of the mean squared error and NSE performance criteria: Implications for improving hydrological modelling. Journal of Hydrology. https://doi.org/10.1016/j.jhydrol.2009.08.003.

Huang, J., Jing, C., Fu, J., Huang, Z., 2019. Uncertainty Analysis of Rainfall Spatial Interpolation in Urban Small Area. In: Gao H, Yin Y, Yang X, Miao H (2019) (eds) Testbeds and Research Infrastructures for the Development of Networks and Communities. TridentCom 2018. Lecture Notes of the Institute for Computer Sciences. Social Informatics and Telecommunications Engineering. https://doi.org/10.1007/978-3-030-12971-2_5.

Huffman, G. J., Bolvin, D. T., Nelkin, E. J., & Tan, J. (2019). Integrated Multi-satellite Retrievals for GPM (IMERG) technical documentation (technical documentation) (p. 71). NASA. Retrieved from. https://pmm.nasa.gov/data-access/downloads/gpm.

IBGE (2022) Institute Brazilian of Geographic and Statistics. Retrieved from. https://cidades.ibge.gov.br/brasil/pb/panorama.

Junqueira, R., Viola, M.R., Amorim, J.S., Camargos, C., Mello, C.R., 2022. Hydrological modeling using remote-sensing precipitation data in a Brazilian savanna basin. Journal of South American Earth Sciences. https://doi.org/10.1016/j.jsames.2022.103773.

Karaseva, M.O., Prakash, S., Gairola, R.M., 2012. Validation of high-resolution TRMM-3B43 precipitation product using rain gauge measurements over Kyrgyzstan. Theoretical and Applied Climatology. https://doi.org/10.1007/s00704-011-0509-6.

Kazemzadeh, M., Noori, Z., Alipour, H., Jamali, S., Akbari, J., Ghorbanian, A., Duan, Z., 2022. Detecting Drought Events over Iran during 1983–2017 Using Satellite and Ground-Based Precipitation Observations. Atmospheric Research. https://doi.org/10.1016/j.atmosres.2022.106052.

Kling, H., Fuchs, M., Paulin, M., 2012. Runoff conditions in the upper Danube basin under an ensemble of climate change scenarios. Journal of Hydrology. https://doi.org/10.1016/j.jhydrol.2012.01.011.

Kou, L., Mao, Y., Lin, Z., Gao, H., Chu, Z., Chen, A., 2024. Error modeling and hierarchical Bayesian fusion for spaceborne and ground radar rainfall data. Journal of Hydrology. https://doi.org/10.1016/j.jhydrol.2023.130599.

Liu, X., Yong, Z., Liu, L., Chen, T., Zhou, L., Li, J., 2023. Improving Hydrological Simulation Accuracy through a Three-Step Bias Correction Method for Satellite Precipitation Products with Limited Gauge Data. Water. https://doi.org/10.3390/w15203615.

Liu, Z., Yang, Q., Shao, J., Wang, G., Liu, H., Tang, X., Xue, Y., Bai, L., 2022. Improving daily precipitation estimation in the data scarce area by merging rain gauge and TRMM data with a transfer learning framework. Journal of Hydrology. https://doi.org/10.1016/j.jhydrol.2022.128455.

Luiz-Silva, W., Oscar-Júnior, A.C., Cavalcanti, I.F.A., Treistman, F., 2021. An overview of precipitation climatology in Brazil: space-time variability of frequency and intensity associated with atmospheric systems. Hydrological Sciences Journal. http://dx.doi.org/10.1080/02626667.2020.1863969.

Llauca, H., Lavado-Casimiro, W., León, K., Jimenez, J., Traverso, K., Rau, P., 2021. Assessing Near Real-Time Satellite Precipitation Products for Flood Simulations at Sub-Daily Scales in a

Sparsely Gauged Watershed in Peruvian Andes. Remote-sensing. http://dx.doi.org/10.3390/rs13040826.

López-Bermeo, C., Montoya, R.D., Caro-Lopera, F.J., Díaz-García, J.A., 2022. Validation of the Accuracy of the CHIRPS Precipitation Dataset at Representing Climate Variability in a Tropical Mountainous Region of South America. Physics and Chemistry of the Earth, Parts A/B/C. https://doi.org/10.1016/j.pce.2022.103184.

Massari, C., Brocca, L., Pellarin, T., Abramowitz, G., Filippucci, P., Ciabatta, L., Maggioni, V., Kerr, Y., Prieto, D.F., 2020. A daily 25km short-latency rainfall product for data-scarce regions based on the integration of the Global Precipitation Measurement mission rainfall and multiple-satellite soil moisture products. Hydrology and Earth System Sciences. https://doi.org/10.5194/hess-24-2687-2020.

Medeiros, E.S., Lima, R.R., Olinda, R.A., Santos, C.A.C., 2019. Modeling Spatiotemporal Rainfall Variability in Paraíba, Brazil. Water. http://dx.doi.org/10.3390/w11091843.

Min, X., Yang, C., Dong, N., 2020. Merging Satellite and Gauge Rainfalls for Flood Forecasting of Two Catchments Under Different Climate Conditions. Water. http://dx.doi.org/10.3390/w12030802.

Nascimento, J.G., Althoff, D., Bazame, H.C., Neale, C.M.U., Duarte, S.N., Ruhoff, A.L., Gonçalves, I.Z., 2021. Evaluating the Latest IMERG Products in a Subtropical Climate: The Case of Paraná State, Brazil. Remote Sensing. https://doi.org/10.3390/rs13050906.

Nawaz, M., Iqbal, M.F., Mahmood, I., 2021. Validation of CHIRPS Satellite-Based Precipitation Dataset over Pakistan. Atmospheric Research. https://doi.org/10.1016/j.atmosres.2020.105289.

Navarro, A., García-Ortega, E., Merino, A., Sánchez, J.L., Kummerow, C., Tapiador, F.J., 2019. Assessment of IMERG Precipitation Estimates over Europe. Remote Sensing. https://doi.org/10.3390/rs11212470.

Nguyen, P., Ombadi, M., Gorooh, V.A., Shearer, E., Sadeghi, M., Sorooshian, S., Hsu, K., Bolvin, K., Ralph, M.F., 2020. PERSIANN Dynamic Infrared-Rain Rate (PDIR-NOW-NOW-NOW-Now): A Near-Real-Time, Quasi-Global Satellite Precipitation Dataset. Journal of Hydrometeorology. https://doi.org/10.1175/jhm-d-20-0177.1.

Nurmi, P., 2003. Recommendations on the verification of local weather forecasts (at ECWMF member states). ECMWF Operations Department. October. https://doi.org/10.21957/y1z1thg5l.

Omar, G.M., Paturel, J.E., Salles, C., Mahé, G., Jalludin, M., Satgé, F., Nour, M.I., 2023. Evaluation of Rainfall Products in Semi-Arid Areas: Application to the Southeast of the Republic of Djibouti and a Focus on the Ambouli Catchment. Water. https://doi.org/10.3390/w15122168.

Paredes-Trejo, F.J., Barbosa, H.A., & Kumar, T.L., 2017. Validating CHIRPS-based satellite precipitation estimates in Northeast Brazil. Journal of arid environments. https://doi.org/10.1016/j.jaridenv.2016.12.009.

Ramadhan, R., Yusnaini, H., Marzuki, M., Muharsyah, R., Suryanto, W., Sholihun, S., ... & Tokay, A., 2022. Evaluation of GPM IMERG performance using gauge data over Indonesian maritime continent at different time scales. Remote Sensing. https://doi.org/10.3390/rs14051172.

Reis, J.B.C., Rennó, C.D., Lopes, E.S.S., 2017. Validation of Satellite Rainfall Products over a Mountainous Watershed in a Humid Subtropical Climate Region of Brazil. Remote-sensing. https://doi.org/10.3390/rs9121240.

Rincón-Avalos, P., Khouakhi, A., Mendoza-Cano, O., López-De, L.A.C.J., Paredes-Bonilla, K.M., 2022. Evaluation of satellite precipitation products over Mexico using Google Earth Engine. Journal of Hydroinformatics. https://doi.org/10.2166/hydro.2022.122.

Roebber, P.J., 2009. Visualizing Multiple Measures of Forecast Quality. Weather Forecast. https://doi.org/10.1175/2008WAF2222159.1.

Rodrigues, D.T., Silva, C.M.S., Reis, J.S., Palharini, R.S.A., Júnior, J.B.C., Silva, H.J.F., Mutti, P.R., Bezerra, B.G., Gonçalves, W.A., 2021. Evaluation of the Integrated Multi-Satellite Retrievals for the Global Precipitation Measurement (IMERG) Product in the São Francisco Basin (Brazil). Water. https://doi.org/10.3390/w13192714.

Santos, A.L.M., Gonçalves, W.A., Rodrigues, D.T., Andrade, L.M.B., Silva, C.M.S., 2022. Evaluation of Extreme Precipitation Indices in Brazil's Semiarid Region from Satellite Data. Atmosphere. https://doi.org/10.3390/atmos13101598.

Santos, C.A.G., Brasil Neto, R.M., Silva, R.M., Costa, S.G.F., 2019a. Cluster analysis applied to spatiotemporal variability of monthly precipitation over Paraíba state using tropical rainfall measuring Mission (TRMM) data. Remote-sensing. https://doi.org/10.3390/rs11060637.

Santos, C.A.G., Brasil Neto, R.M., Silva, R.M., Santos, D.C., 2019b. Innovative approach for geospatial drought severity classification: a case study of Paraíba state, Brazil. Stoch Environ Res Risk Assess. https://doi.org/10.1007/s00477-018-1619-9.

Shearer, E.J., Gorooh, V.A., Nguyen, P., Kuo-Lin, H., Sorooshian, S., 2022. Unveiling four decades of intensifying precipitation from tropical cyclones using satellite measurements. Scientific Reports. https://doi.org/10.1038/s41598-022-17640-y.

Soares, A.S.D., Paz, A.R., Piccili, D.G.A., 2016. Assessment of rainfall estimates of TRMM satellite on Paraíba state. Journal Brazilian of Water Resources. https://doi.org/10.21168/rbrh.v21n2.p288-299.

Stanski, H.R., Wilson, L.J., Burrows, W.R., 1989. Survey of common verification methods in meteorology. World Weather Watch Tech. Rept. No.8, WMO/TD No.358, WMO, Geneva, 114pp. https://library.wmo.int/idurl/4/39578.

Tan, M.L., Duan, Z., 2017. Assessment of GPM and TRMM Precipitation Products over Singapore. Remote-sensing. https://doi.org/10.3390/rs9070720.

Tang, G., Ma, Y., Long, D., Zhong, L., Hong, Y., 2016. Evaluation of GPM Day-1 IMERG and TMPA Version-7 legacy products over Mainland China at multiple spatiotemporal scales. Journal of Hydrology. https://doi.org/10.1016/j.jhydrol.2015.12.008.

Taylor, K.E., 2001. Summarizing multiple aspects of model performance in a single diagram. Journal of Geophysical Research. http://dx.doi.org/10.1029/2000JD900719.

Wang, Y., Zhao, N., 2022. Evaluation of Eight High-Resolution Gridded Precipitation Products in the Heihe River Basin, Northwest China. https://doi.org/10.3390/rs14061458.

Yang, S., Jones, P.D., Jiang, H., Zhou, Z., 2019. Development of a near-real-time global in situ daily precipitation dataset for 0000–0000 UTC. https://doi.org/10.1002/joc.6367.

Zhu, H., Liu, H., Zhou, Q., Cui, A., 2023. Towards an Accurate and Reliable Downscaling Scheme for High-Spatial-Resolution Precipitation Data. Remote Sensing. https://doi.org/10.3390/rs15102640.

Zhu, S., Shen, Y., Ma, Z., 2020. A New Perspective for Charactering the Spatio-temporal Patterns of the Error in GPM IMERG Over Mainland China. Earth and Space Science. https://doi.org/10.1029/2020EA001232.

Zhong, R., Chen, X., Lai, C., Wang, Z., Lian, Y., Yu, H., Wu, X., 2019. Drought monitoring utility of satellite-based precipitation products across mainland China. Journal of hydrology. https://doi.org/10.1016/j.jhydrol.2018.10.072.

Zhou, B., Hu, S., He, Y., Wang, S., Li, D., Feng, G., 2022. Quantitative evaluations of subtropical westerly jet simulations over East Asia based on multiple CMIP5 and CMIP6 GCMs. Atmospheric Research. https://doi.org/10.1016/j.atmosres.2022.106257.

Ziveh, A.R., Bakhtar, A., Shayeghi, A., Kalantari, Z., Bavani, A.M., Ghajarnia, M., 2022. Spatio-temporal performance evaluation of 14 global precipitation estimation products across river basins in southwest Iran. Journal of Hydrology: Regional Studies. https://doi.org/10.1016/j.ejrh.2022.101269.

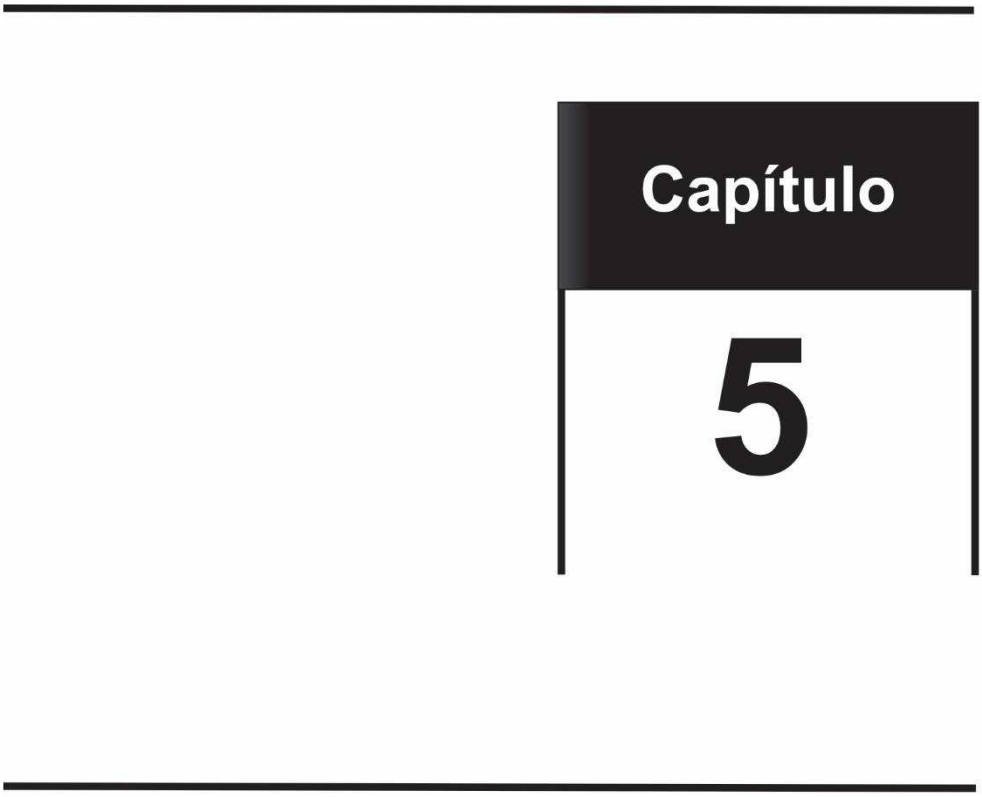

Este capítulo refere-se ao artigo publicado na Revista Earth Science Informatics[3]. O título e o resumo são apresentados inicialmente em português e, em seguida, o texto do artigo é transcrito aqui em inglês conforme foi publicado.

5. GEOT-IDF EQUATIONS: UMA FERRAMENTA BASEADA EM R PARA ESTUDOS DE CHUVAS INTENSAS

Resumo:

O GEOT-IDF Equations é uma ferramenta para determinar relações Intensidade-Duração-Frequência (IDF) e suas respectivas equações. Foi especialmente desenvolvido para facilitar o ajuste de diferentes modelos probabilísticos na análise de frequência de séries temporais de precipitação e o modelo de curva IDF sem exigir conhecimento prévio sobre os parâmetros do

[3] Costa F. F., Rufino I. A. A., Aragão R., Castro M. A. H., Filho R. S. R. (2024). GEOT-IDF Equations: An R-based tool for intense rainfall studies in Brazil. Earth Science Informatics (**Submetido**).

modelo pelo usuário. A ferramenta integra as sete distribuições estatísticas mais utilizadas para estimar valores máximos de precipitação de 1 dia para diferentes períodos de retorno (Tr) e três metodologias para desagregar a precipitação em intervalos subdiários. Os parâmetros empíricos (a, b, c, d, e e f) de cinco equações IDF são calibrados usando duas funções objetivo (FO1 e FO2). A ferramenta GEOT-IDF Equations é conectada a dois servidores de banco de dados de precipitação (ANA, NOAA e CLIMBra). Ela também fornece equações IDF de produtos de precipitação de sensoriamento remoto. Os resultados mostram que, em comparação com trabalhos anteriores, as equações IDF geradas pelo GEOT-IDF Equations apresentaram erros relativos em torno de 10% (mais ou menos) para valores baixos de Tr (< 25 anos) e duração - t (< 60 minutos), indicando que a ferramenta é confiável na aplicação de sistemas de drenagem urbana de projeto, foco principal da ferramenta. Espera-se que esta ferramenta seja útil para projetistas, pesquisadores e especialistas que estudam chuvas intensas.

GEOT-IDF EQUATIONS: AN R-BASED TOOL FOR INTENSE RAINFALL STUDIES

Abstract:

The GEOT-IDF Equations is a tool for determining Intensity-Duration-Frequency (IDF) relations and their respective equations. It was specially developed to facilitate the adjustment of different probabilistic models in the frequency analysis of rainfall time series and the IDF curve model without requiring prior knowledge about the model parameters by the user. The tool integrates the seven most used statistical distributions to estimate maximum 1-day precipitation values for different return periods (Tr) and three methodologies for disaggregating precipitation into sub-daily intervals. The empirical parameters (a, b, c, d, e, and f) of five IDF equations are calibrated using two objective functions (FO1 and FO2). The GEOT-IDF Equations tool is connected to two precipitation database servers (ANA and CLIMBra). It also provides IDF equations from remote-sensing precipitation products. The results show that, compared to previous works, the IDF equations generated by GEOT-IDF Equations presented relative errors of around 10% (more or less) for low Tr (< 25 years) and duration - t (< 60 minutes) values, indicating that the tool is reliable in the application of design urban drainage systems, the main focus of the tool. This tool is expected to be useful for designers, researchers, and specialists studying intense rainfall.

Keywords
Heavy rain, floods, IDF equations. R language

5.1. Introduction

Natural hazards triggered by extreme events (floods and heavy rainfall) generate profound socioeconomic impacts on local communities (Li et al. 2021; Li et al. 2022). Over time and as a result of climate change and other factors (Carpio et al. 2020; Chang et al. 2021; Filho et al. 2022; IPCC 2023), more extreme events are occurring, and more negative consequences are being registered, such as deaths and significant economic losses (Dinis et al. 2021). As Tabari (2020) discusses, there is a tendency for these problems to increase in the future. To mitigate these effects, a viable way to deal with the problem of flooding is using Intensity-Duration-Frequency (IDF) relationships (Shabankareh and Abedini 2023).

According to data from Donatti et al. (2024), 89,462 people died between 2000 and 2022 worldwide due to these catastrophes. Central America, the Caribbean, East Africa, including Madagascar, and South and East Asia were the regions that suffered the most. For the same period, Brazil is in the second most critical category as one of the countries that suffered the most from floods. The range of events varies from 58 to 108 (EM-DAT/CRED 2023). In 2024, for example, the country faced a substantial hydrological disaster that affected almost the entire state of Rio Grande do Sul (478 of 497 municipalities). Currently, it has already registered 175 deaths and 38 missing, and many other injuries, loss, and sad consequences (G1 RS 2024).

It is known that the design and maintenance of hydraulic structures, especially those designed to deal with flooding, require reliable data and information. Generally, such an estimate can be made through statistical analysis of historical controlled flow data. However, most locations do not have flow measurement stations (Shabankareh and Abedini 2023). Therefore, a viable way to deal with the problem of flood is to analyze design storm (Shabankareh and Abedini 2023), which, in turn, is defined based on Intensity-Duration-Frequency (IDF) relations for the application of methodologies that can convert rainfall into flow, such as Unitary Hydrograph (UH), Curve Number (CN), Rational Method and Gradex Method, among others.

The IDF relations, or their respective equations, were initially proposed by Sherman (1931) and have since been widely used worldwide (Ogbozige 2022; Hussein et al. 2023). However, due to the little availability of record rain gauge time series, in recent decades, IDF equations have been developed based on techniques for disaggregating daily rainfall from rain-gauges (conventional or automatic), such as the methodology proposed by the Environmental Agency of the state of São Paulo (CETESB 1986), which is still widely used today in Brazil and the proposed by the Indian

Meteorological Department - IMD (Basumatary and Sil 2017; Sam et al. 2021; Shamkhi et al. 2022; Bibi 2023), between others (Torrico 1974; Back 2020).

By the year 2020, for example, Brazil had catalogued around 3,096 intense rainfall equations, published in 118 articles, including 10 academic articles, theses and dissertations, 61 articles published in scientific journals, 27 articles in scientific events and 20 articles classified as books and technical reports (Back and Cadorin 2021). This number of studies shows the importance of such information for a suitable design of hydraulic works. However, the available studies can be considered old, reinforcing the need for updated with recent information on IDF equations, such as several studies have argued that IDF equations must be updated (Pérez-Zanón et al. 2016; Hosseinzadehtalaei et al. 2019; Ren et al. 2019; Fowler et al. 2021a; Kourtis et al. 2021; Kourtis and Tsihrintzis 2021), to ensure accuracy, relevance, development of management plans and crucially, the reduction of losses (Ghebreyesus and Sharif, 2021; Alsumaiti et al. 2023; Shabankareh and Abedini 2023).

Another challenge is that there still needs to be a tool capable of generating IDF equations globally. Most publications are on a local scale or outdated equations (Simonovic et al. 2015; Rodrigues et al. 2023; Vargas et al. 2023; GPRH 2024). A tool connected to a precipitation database server is highly relevant, especially nowadays. Since the rainfall pattern worldwide is changing, these equations must to express those new patterns.

Specific contributions of this article include the following:

- Connect to the National Agency of Water and Basic Sanitation (ANA) server to obtain/update IDF equations for municipality in Brazil almost in real-time;
- Insert the product CLIMBra to obtain IDF equations considering the principle of non-stationarity for municipality in Brazil, currently considered an interest for water resources researchers and
- Enable the generation of IDF equations from remote-sensing daily precipitation estimation products.

5.2. Design and Implementation

5.2.1. Database

The GEOT-IDF Equations tool is connected directly with the National Agency of Water and Basic Sanitation of Brazil (ANA), Brazil's official water management agency. The tool currently provides approximately 5,634 rain-gauge stations with precipitation records.

The tool considers a minimum time series of 30 years, as recommended by the World Meteorological Organization (WMO), to define the IDF equations by applying the annual maximum series (AMS) methodology, a type of block maxima - BM (Tanaka 2021). When the time series is less than 30 years, the tool works with the peak over threshold (POT) method (Liu et al. 2023). Finally, the algorithm removes any outliers and checks whether the series has a climate trend using the Mann-Kendall test (Mann 1945; Kendall 1975) at a significance level of 5% (Barbero et al. 2017).

The selection criterion is that the time series must have low data gaps (no more than 10% of missing data), a condition imposed by several studies reported by Rodrigues et al. (2021). When the data gap exceeds 10%, the tool applies the K-*Nearest Neighbors* (Aha et al. 1991) regression method, a machine learning technique used to predict continuous values based on data similarity. The basic idea is to predict the value of a new observation, the K neighboring (neighboring rain-gauge stations) fills in the gaps in the time series.

Although it is not the focus of the tool, it also provides the option of using daily precipitation estimation product CLIMBra bias-corrected and scale reduction (Ballarin et al. 2023) and remote-sensing daily precipitation estimation products, such as MSWEP that already comes with bias-corrected (Beck et al. 2019), to define IDF equations. However, these meteorological datasets are based on in-situ data interpolation, which introduces an embedded error. Therefore, a performance analysis should be conducted to verify whether these datasets can simulate in-situ data for which IDF equations are intended to be developed.

5.2.2. Frequency analysis

Different probability distributions (Table 2) were considered to obtain the maximum daily precipitation that could be Equaled every 5, 10, 15, 20, 25, 50, and 100 years (Naghettini and Pinto 2007).

After calculating the parameters of the distributions, the algorithm defines the best distribution based on the Kolmogorov-Smirnov—KS (Eq. 1) statistics and likelihood ratio (Eq. 2). This distribution is considered the most efficient for large samples because it presents less variance in the estimators (Naghettini and Pinto 2007). It also considers a Chi-Square (Eq. 3) test to choose between candidate distributions.

The present algorithm uses the Weibull method (Makkonen 2005), plus the non-parametric Kolmogorov-Smirnov test (Eq. 1), at a significance level of 5%, to define the best distribution, taking into account the lowest value of KS. In situations of ties, the likelihood ratio criterion (Eq. 2) is applied, in conjunction with the Chi-Square test (Eq. 3), at a significance level of 5% to define the best distribution.

5.2.3. Downscaling of rainfall

After identifying the proper probability distribution for the rainfall time series, the maximum precipitation values were obtained for the following return periods (Tr): 5, 10, 15, 20, 25, 50, and 100 years. Then, these values were first transformed into 24 hours rainfall (CETESB 1986) and then disaggregated for the durations listed in Table 4 using the exponential equation (Eq. 4) proposed by Silveira (2000). It is also possible to disaggregate daily rainfall into intervals through the Isozone method (Torrico 1974) (Eq. 5, Table 3 and Fig. 2) and the one proposed by Back (2020) (Eq. 6). For each rainfall duration, the algorithm considers a minimum value (Table 4) above which the precipitation can be considered as intense, as indicated by CETESB (1986). The algorithm further incorporates the precipitation disaggregation method (Eq. 7) proposed by the Indian Meteorological Department - IMD (Basumatary and Sil 2017; Sam et al. 2021; Shamkhi et al. 2022; Bibi 2023).

5.2.4. Determination of the suitable IDF equations and its parameters

From the disaggregated precipitations for different Tr (5, 10, 15, 20, 25, 50, and 100 years), the intensity for durations of 6, 10, 15, 20, 30, 60, 360, 480, 600, 720 and 1440 min are calculated for different types of IDF equations (Table 5).

In order to calibrate the empirical parameters (Table 5), two objective functions (FO) were applied: FO1, a minimization function (Relative error), and the second (FO2), a maximization function (Nash-Sutcliffe efficiency; NS). The NS (Nash and Sutcliffe 1970) value can range from

-∞ to 1, and if the NS equals 1, there is a perfect fit to the observed data (Moriasi et al. 2007). Therefore, the approach used was to apply F01 (Eq. 8) to identify the local optimal values and, from the findings, use F02 (Eq. 9) to calculate the parameters' global optimal values for the previously selected IDF equation.

5.2.5. Statistical analyses

This study used different statistics to compare the intensities calculated from the observed data with those generated by the IDF equations calculated by the tool GEOT-IDF Equations. The statistics used were coefficient of determination—R^2 (Eq. 10), root mean square error—RMSE (Eq. 11), and mean absolute error—MAE (Eq. 12).

5.2.6. Tool installation

To use the tool GEOT-IDF Equations, simply follow the setup shown in Figure 19. The tool requires a Windows operating system.

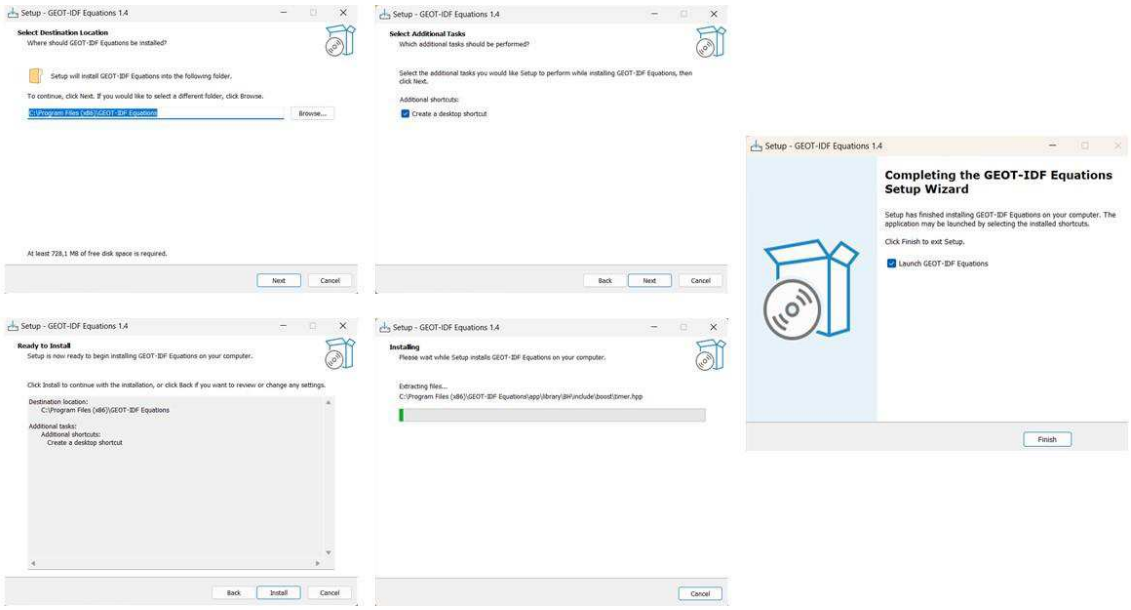

Figura 19 - Illustration of the installation setup of the tool GEOT-IDF Equations

After completing the steps described in Figure 19, the user will have access to the main interface (Figure 3) of the tool GEOT-IDF Equations. The tool can generate IDF equations for Brazil, estimate design hyetogram, and simulate rainfall-runoff.

5.2.7. Output data

The GEOT-IDF Equations tool generates a table containing descriptive information related to the station code, latitude, longitude, and the values of the coefficients of the IDF equation, among other things (Fig. 20).

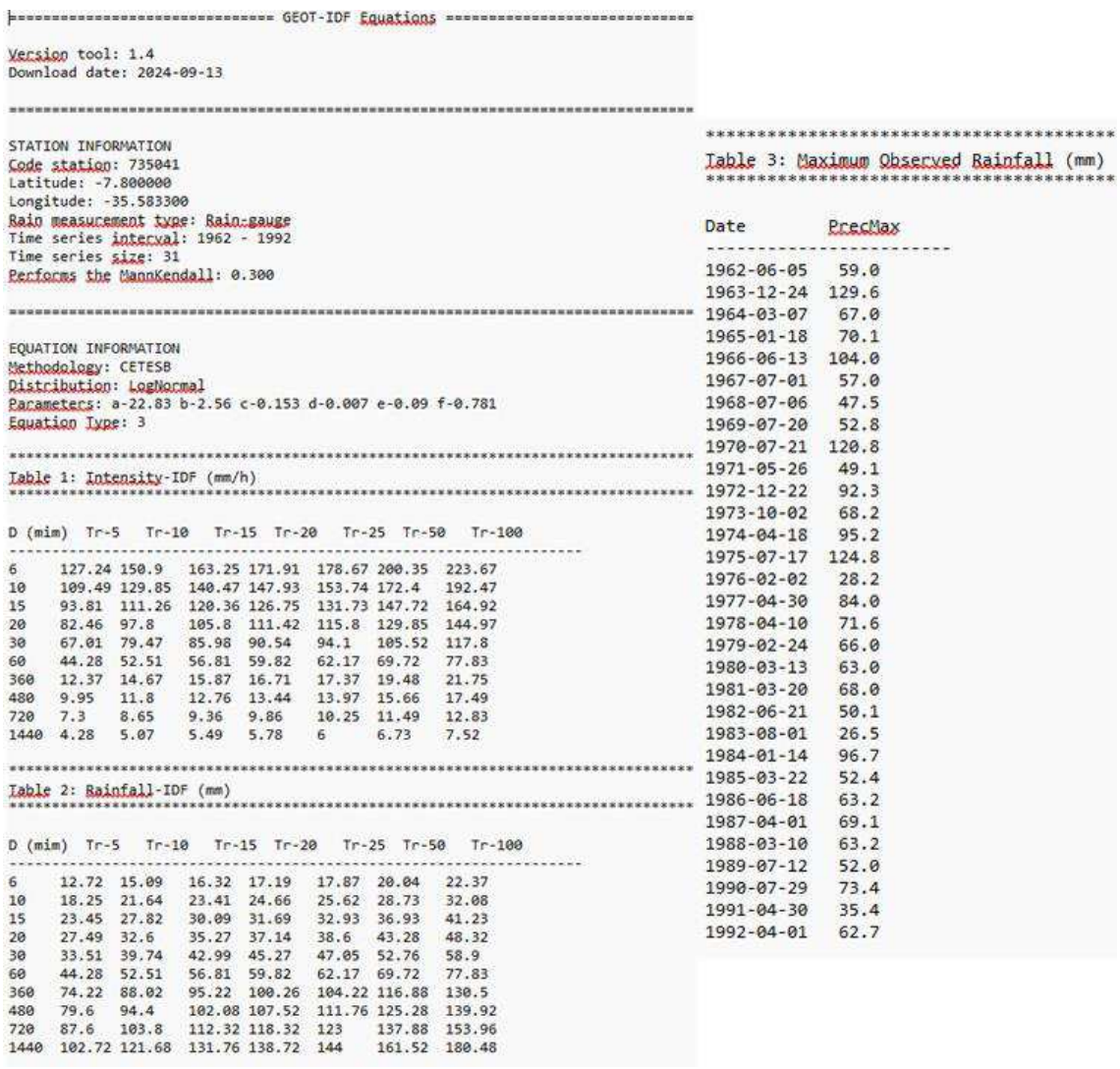

```
========== GEOT-IDF Equations ==========

Version tool: 1.4
Download date: 2024-09-13

================================================================================

STATION INFORMATION
Code station: 735041
Latitude: -7.800000
Longitude: -35.583300
Rain measurement type: Rain-gauge
Time series interval: 1962 - 1992
Time series size: 31
Performs the MannKendall: 0.300

================================================================================

EQUATION INFORMATION
Methodology: CETESB
Distribution: LogNormal
Parameters: a-22.83 b-2.56 c-0.153 d-0.007 e-0.09 f-0.781
Equation Type: 3

================================================================================
Table 1: Intensity-IDF (mm/h)
================================================================================

D (mim)  Tr-5   Tr-10   Tr-15  Tr-20   Tr-25  Tr-50   Tr-100
--------------------------------------------------------------
6     127.24 150.9   163.25 171.91  178.67 200.35  223.67
10    109.49 129.85  140.47 147.93  153.74 172.4   192.47
15    93.81  111.26  120.36 126.75  131.73 147.72  164.92
20    82.46  97.8    105.8  111.42  115.8  129.85  144.97
30    67.01  79.47   85.98  90.54   94.1   105.52  117.8
60    44.28  52.51   56.81  59.82   62.17  69.72   77.83
360   12.37  14.67   15.87  16.71   17.37  19.48   21.75
480   9.95   11.8    12.76  13.44   13.97  15.66   17.49
720   7.3    8.65    9.36   9.86    10.25  11.49   12.83
1440  4.28   5.07    5.49   5.78    6      6.73    7.52

================================================================================
Table 2: Rainfall-IDF (mm)
================================================================================

D (mim)  Tr-5   Tr-10   Tr-15  Tr-20   Tr-25  Tr-50   Tr-100
--------------------------------------------------------------
6     12.72  15.09   16.32  17.19   17.87  20.04   22.37
10    18.25  21.64   23.41  24.66   25.62  28.73   32.08
15    23.45  27.82   30.09  31.69   32.93  36.93   41.23
20    27.49  32.6    35.27  37.14   38.6   43.28   48.32
30    33.51  39.74   42.99  45.27   47.05  52.76   58.9
60    44.28  52.51   56.81  59.82   62.17  69.72   77.83
360   74.22  88.02   95.22  100.26  104.22 116.88  130.5
480   79.6   94.4    102.08 107.52  111.76 125.28  139.92
720   87.6   103.8   112.32 118.32  123    137.88  153.96
1440  102.72 121.68  131.76 138.72  144    161.52  180.48
```

```
======================================
Table 3: Maximum Observed Rainfall (mm)
======================================

Date        PrecMax
------------------------
1962-06-05   59.0
1963-12-24  129.6
1964-03-07   67.0
1965-01-18   70.1
1966-06-13  104.0
1967-07-01   57.0
1968-07-06   47.5
1969-07-20   52.8
1970-07-21  120.8
1971-05-26   49.1
1972-12-22   92.3
1973-10-02   68.2
1974-04-18   95.2
1975-07-17  124.8
1976-02-02   28.2
1977-04-30   84.0
1978-04-10   71.6
1979-02-24   66.0
1980-03-13   63.0
1981-03-20   68.0
1982-06-21   50.1
1983-08-01   26.5
1984-01-14   96.7
1985-03-22   52.4
1986-06-18   63.2
1987-04-01   69.1
1988-03-10   63.2
1989-07-12   52.0
1990-07-29   73.4
1991-04-30   35.4
1992-04-01   62.7
```

Figura 20 - Example illustration of output file from tool GEOT-IDF Equations

5.3. Application

As a case study, the IDF equations generated by the GEOT-IDF Equations tool were compared with IDF equations available in the literature in different regions of Brazil according to the following equation:

$$\Delta = \frac{value(in\ this\ study) - value(literature)}{value(literature)}$$

Equação 21

In order to analyze the quality of the IDF equations generated by the GEOT-IDF Equations tool, IDF equations developed by other studies were considered (Table 11). The intensity calculation for Tr = 10 years and t = 10 minutes was considered, which is common in hydraulic works design. Table 5 shows that using the IDF equation generated by the GEOT-IDF Equations tool led to a slight overestimation of the intensity of approximately 5 (%) for station 2246013.

Tabela 11 - Comparison between the intensity values obtained considering the coefficients determined in this study and with other studies in Brazil

Code	Region	Source	i (mm/h)	Error Δ (%)
338001	Nordeste	1*	186.81	0.64
		2*	185.63	
967000	Norte	1*	140.68	0.93
		3*	139.38	
1649013	Centro-Oeste	1*	127.39	2.31
		4*	124.51	
2246013	Sudeste	1*	134.54	5.00
		5*	128.13	
2649018	Sul	1*	133.63	4.46
		6*	127.93	

1* GEOT-IDF Equations, 2* Farias and Pinto 2015, 3* Back and Candorin 2020, 4* Pickbrenner et al. 2018, 5* Capozzoli et al. 2021 and 6* Back 2020

Tables 12 to 16 also show that the maximum relative differences between the observed data (literature) and the values calculated using the IDF equation generated in this study were more significant than 19% (for less) in the cases highlighted in bold, reaching a maximum error of 23% (Table 13), for Tr = 100 years and t = 1440 minutes, when compared with the IDF equation proposed by Back and Candorin (2020). On the other hand, when analyzing the IDF equations for durations less than 60 minutes and Tr less than 50 years, the percentage, on average, drops to less than 15%, reaching exact values on some occasions. In other words, using GEOT-IDF Equations

to design structures whose contribution area has a small concentration time leads to good results, including terraces with uneven surfaces and various urban drainage works, such as urban drainage systems, which are the tool's primary focus.

Tabela 12 - Comparison between the relative errors of the rainfall intensities values calculated for different Tr and t obtained in this study with that of Farias and Pinto 2015

Tr	**t (min)**									
(years)	6	10	15	20	30	60	360	480	720	1440
5	-0.09	-0.03	-0.01	-0.01	-0.03	-0.09	-0.18	**-0.19**	**-0.19**	-0.18
10	-0.05	0.01	0.01	0.00	-0.03	-0.09	**-0.19**	**-0.20**	**-0.20**	**-0.20**
15	-0.02	0.02	0.02	0.01	-0.03	-0.09	**-0.20**	**-0.21**	**-0.21**	**-0.21**
20	-0.01	0.03	0.03	0.01	-0.02	-0.09	**-0.20**	**-0.21**	**-0.21**	**-0.21**
25	0.01	0.04	0.03	0.02	-0.02	-0.09	**-0.20**	**-0.21**	**-0.21**	**-0.21**
50	0.05	0.07	0.06	0.04	0.00	-0.08	**-0.20**	**-0.21**	**-0.21**	**-0.21**
100	0.10	0.11	0.09	0.07	0.02	-0.06	-0.18	**-0.19**	**-0.20**	**-0.19**

Tabela 13 - Comparison between the relative errors of the rainfall intensities values calculated for different Tr and t obtained in this study with that of Back and Candorin 2020

Tr	**t (min)**									
(years)	6	10	15	20	30	60	360	480	720	1440
5	-0.01	0.00	0.01	0.01	0.01	0.00	-0.09	-0.11	-0.14	-0.18
10	0.00	0.01	0.02	0.02	0.02	0.00	-0.09	-0.11	-0.13	-0.17
15	-0.01	0.00	0.01	0.01	0.01	0.00	-0.10	-0.11	-0.14	-0.18
20	-0.02	-0.01	0.00	0.00	0.00	-0.01	-0.10	-0.12	-0.15	**-0.19**
25	-0.03	-0.01	-0.01	0.00	-0.01	-0.02	-0.11	-0.13	-0.15	**-0.19**
50	-0.05	-0.04	-0.03	-0.03	-0.03	-0.04	-0.13	-0.15	-0.17	**-0.21**
100	-0.08	-0.06	-0.06	-0.05	-0.06	-0.07	-0.16	-0.17	**-0.19**	**-0.23**

Tabela 14 - Comparison between the relative errors of the rainfall intensities values calculated for different Tr (years) and t (min) obtained in this study with that of Pickbrenner et al. 2018

Tr	**t (min)**									
(years)	6	10	15	20	30	60	360	480	720	1440
5	0.00	0.03	0.06	0.08	0.11	0.14	0.18	0.17	0.17	0.16
10	-0.01	0.02	0.05	0.07	0.10	0.13	0.16	0.16	0.16	0.15
15	-0.02	0.01	0.04	0.05	0.08	0.12	0.15	0.15	0.14	0.14
20	-0.03	0.00	0.02	0.04	0.07	0.10	0.14	0.13	0.13	0.13
25	-0.04	-0.01	0.01	0.03	0.06	0.09	0.13	0.12	0.12	0.11
50	-0.07	-0.04	-0.02	0.00	0.03	0.06	0.09	0.09	0.09	0.08
100	-0.10	-0.07	-0.05	-0.03	-0.01	0.03	0.05	0.05	0.05	0.04

Tabela 15 - Comparison between the relative errors of the rainfall intensities values calculated for different Tr and t obtained in this study with that of Capozzoli et al. 2021

Tr	**t (min)**									
(years)	6	10	15	20	30	60	360	480	720	1440
5	0.06	0.04	0.01	0.00	-0.02	-0.04	-0.02	-0.01	0.00	0.02
10	0.08	0.05	0.03	0.01	0.00	-0.02	-0.01	0.00	0.01	0.03
15	0.07	0.04	0.02	0.01	-0.01	-0.03	-0.02	-0.01	0.00	0.03
20	0.06	0.03	0.01	0.00	-0.02	-0.04	-0.02	-0.02	0.00	0.02
25	0.05	0.03	0.00	-0.01	-0.03	-0.04	-0.03	-0.02	-0.01	0.01
50	0.02	0.00	-0.02	-0.04	-0.05	-0.07	-0.06	-0.05	-0.04	-0.02
100	-0.01	-0.03	-0.05	-0.07	-0.08	-0.10	-0.09	-0.08	-0.07	-0.05

Tabela 16 - Comparison between the relative errors of the rainfall intensities values calculated for different Tr and t obtained in this study with that of Back 2020

Tr	t (min)									
(years)	6	10	15	20	30	60	360	480	720	1440
5	0.01	0.00	-0.01	-0.02	-0.04	-0.08	-0.14	-0.14	-0.14	-0.15
10	0.05	0.04	0.03	0.02	0.00	-0.04	-0.10	-0.10	-0.11	-0.11
15	0.06	0.06	0.04	0.03	0.01	-0.03	-0.09	-0.09	-0.10	-0.10
20	0.07	0.06	0.05	0.03	0.01	-0.02	-0.08	-0.09	-0.09	-0.10
25	0.08	0.07	0.05	0.04	0.02	-0.02	-0.08	-0.08	-0.09	-0.09
50	0.09	0.08	0.07	0.06	0.03	0.00	-0.07	-0.07	-0.07	-0.08
100	0.12	0.11	0.09	0.08	0.05	0.02	-0.05	-0.05	-0.06	-0.06

5.4. Impact

The main contribution of this work is to provide a tool to obtain/update IDF equations for any location in Brazil. GEOT-IDF Equations tool helps the user to save time and effort in defining IDF equations. Furthermore, the tool is straightforward and convenient to operate. We are optimistic that the GEOT-IDF Equations tool will be essential in water resources engineering and management, such as defining project rainfall.

5.5. Conclusion

IDF equations are essential in water resource engineering and management, such as evaluating heavy rainfall events and defining design rainfall.

In this context, the GEOT-IDF Equations tool accelerates obtaining/updating IDF equations. Furthermore, it is verified that the relative error values are very close to zero, especially for small Tr (< 25 years) and t (< 60 minutes), indicating low underestimation or overestimation, not generating high implementation costs or posing risks to the safety of microdrainage works.

Another key feature of the algorithm is its connection to two precipitation datasets (ANA and CLIMBra), as well as the ability to incorporate precipitation estimation remote-sensing products. This enables a range of integrated analyses on intense rainfall. However, it's crucial to conduct statistical analyses of the CLIMBra product to ensure its accuracy before generating the IDF equation for the desired location.

5.6. References

Aha D. W., Kibler D., Albert M. K. (1991). Instance-Based Learning Algorithms. Machine Learning. https://www.researchgate.net/publication/220343419.

Alsumaiti T. S., Hussein K. A., Ghebreyesus D. T., Petchprayoon P., Sharif H. O., Abdalati W. (2023). Development of Intensity–Duration–Frequency (IDF) Curves over the United Arab Emirates (UAE) Using CHIRPS Satellite-Based Precipitation Products. Remote Sensing. http://dx.doi.org/10.3390/rs16010027.

Back Á. J. (2020). Alternative model of intense rainfall equation obtained from daily rainfall disaggregation. Brazilian Journal of Water Resources. https://doi.org/10.1590/2318-0331.252020190031.

Back Á. J. S., Cadorin S. B. (2020). Extreme rainfall and Intensity-Duration-Frequency equations for the state of Acre, Brazil. Brazilian Journal of Environmental Sciences. https://doi.org/10.5327/Z2176-947820200597.

Back Á. J. S., Cadorin S. B. (2021). Heavy rain equations for Brazil. International Journal of Development Research. https://doi.org/10.37118/ijdr.20850.01.2021.

Basso R. E., Allasia D. G., Tassi R., Pickbrenner K. (2016). Review of the high intensity rainfall zones of Brazil. https://doi.org/10.1590/S1413-41522016133691.

Basumatary V., Sil B. S. (2017). Generation of Rainfall Intensity-Duration-Frequency curves for the Barak River Basin. Meteorology Hydrology and Water Management. https://doi.org/10.26491/mhwm/79175.

Barbero R., Fowler H. J., Lenderink G., Blenkinsop S. (2017). Is the intensification of precipitation extremes with global warming better detected at hourly than daily resolutions?. Geophysical Research Letters. http://dx.doi.org/10.1002/2016GL071917.

Ballarin A., Sone J., Gesualdo G., Schwamback D., Reis A., Almagro A., Wendland E. (2023). CLIMBra - Climate Change Dataset for Brazil. Scientific Data. https://doi.org/10.1038/s41597-023-01956-z.

Beck H. E., Wood E. F., Pan M., Fisher C. K., Miralles D. G., Dijk A. I. J. M. V., Mcvicar T. R., Adler R. F. (2019). MSWEP V2 global 3-hourly 0.1° precipitation: methodology and quantitative assessment. Bull. Am. Meteorol. Soc. https://doi.org/10.1175/BAMS-D-17-0138.1.

Bibi T. S. (2023). Derivation of short-term design rainfall intensity from daily rainfall data for urban drainage design using empirical equations in robe town, Ethiopia. International Journal of Hydrology. https://doi.org/10.15406/ijh.2023.07.00340.

Capozzoli C. R., Pickbrenner K. P., Pinto E. J. A. (2021). Rainfall Atlas of Brazil: Intensity-Duration-Frequency Equations (Disaggregation of Daily Precipitation): rain-gauge station: Itapira, codes: 02246013 (ANA) e D3-015 (DAEE), município: Itapira/SP. CPRM. https://rigeo.sgb.gov.br/handle/doc/22421.

Carpio M., González Á., González M., Verichev K. (2020). Influence of pavements on the urban heat island phenomenon: A scientific evolution analysis. Energy and Buildings. http://dx.doi.org/10.1016/j.enbuild.2020.110379.

Chang H., Pallathadka A., Sauer J., Grimm N., Zimmerman R., Cheng C., Iwaniec D. M., Kim Y., Lloyd R., Mcphearson T., Rosenzweig B., Troxler T., Welty C., Brenner R., Herreros-Cantis P. (2021). Assessment of Urban Flood Vulnerability Using the Social-Ecological-Technological Systems Framework in Six US cities. Sustainable Cities and Society. https://doi.org/10.1016/j.scs.2021.102786.

CETESB (1986) Company Environmental Sanitation Technology of the State of São Paulo. Drainage urban: project manual, 1ª ed. São Paulo: CETESB. 466p. Retrieved from. https://repositorio.cetesb.sp.gov.br/handle/123456789/2863.

Donatti C. I., Nicholas K., Fedele G., Delforge D., Speybroeck N., Moraga P., Blatter J., Below R., Zvoleff A. (2024). Global hotspots of climate-related disasters. International Journal of Disaster Risk Reduction. http://dx.doi.org/10.1016/j.ijdrr.2024.104488.

Dinis P. A., Huvi J., Pinto M. C., Carvalho J. (2021). Disastrous Flash Floods Triggered by Moderate to Minor Rainfall Events. Recent Cases in Coastal Benguela (Angola). Hydrology. http://dx.doi.org/10.3390/hydrology8020073.

EM-DAT/CRED (2023). Centre for Research on the Epidemiology of Disasters. Bruxelas, Bélgica. Retrieved from. www.emdat.be.

Farias J. A. M., Pinto E. J. A. (2015). Rainfall Atlas of Brazil: Intensity-Duration-Frequency Equations (Disaggregation of Daily Precipitation): rain-gauge station: Pici, code: 338001 (ANA), município: Fortaleza/CE. CPRM. https://rigeo.sgb.gov.br/handle/doc/23644.

Filho G. M. R., Coelho V. H. R., Freitas E. S. F., Xuan Y., Brocca L., Almeida C. N. (2022). Regional-scale evaluation of 14 satellite-based precipitation products in characterising extreme events and delineating rainfall thresholds for flood hazards. Atmospheric Research. http://dx.doi.org/10.1016/j.atmosres.2022.106259.

Fowler H. J., Lenderink G., Prein A. F., Westra S., Allan R. P., Ban N., Barbero R., Berg P., Blenkinsop S., Do H. X., Guerreiro S., Haerter J. O., Kendon E. J., Lewis E., Schaer C., Sharma A., Villarini G., Wasko C., Zhang X. (2021a). Anthropogenic intensification of short-duration rainfall extremes. Nature Reviews Earth & Environment. https://doi.org/10.1038/s43017-020-00128-6.

G1 RS - Globo news portal of Rio Grande do Sul (2024). A month of floods in RS: see the chronology of the disaster that hit 471 cities, killed more than 170 people and forced 600 thousand from their homes. Retrieved from. https://g1.globo.com/rs/rio-grande-do-sul/noticia/2024/05/29/um-mes-de-enchentes-no-rs-veja-cronologia-do-desastre.ghtml.

Ghebreyesus D. T., Sharif H. O. (2021). Development and assessment of high-resolution radar-based precipitation intensity-duration-curve (IDF) curves for the state of Texas. Remote Sensing. https://doi.org/10.3390/rs13152890.

GPRH. Water Resources Research Group – Federal University of Viçosa. Retrieved from. https://www.gprh.ufv.br/?area=softwares.

Hosseinzadehtalaei P., Tabari H., Willems P. (2019). Regionalization of anthropogenically forced changes in 3 hourly extreme rainfall over Europe. Environmental Research Letters. https://doi.org/10.1088/1748-9326/ab5638.

Hussein D. N, Al-Zakar S. H. D., Yonis A. M. (2023). Estimating the Intensity Equations for Rain Intensity Frequency Curves (Mosul /Iraq). Tikrit Journal of Engineering Sciences. http://doi.org/10.25130/tjes.30.3.5.

IPCC (2023) Climate Change: The Physical Science Basis. Retrieved from. https://www.gov.br/mcti/pt-br/acompanhe-o-mcti/sirene/publicacoes/relatorios-do-ipcc/arquivos/pdf/copy_of_IPCC_Longer_Report_2023_Portugues.pdf.

Kendall M. G. (1975). Rank Correlation Methods, 4th edition. Charles Griffin, London, U.K.

Kourtis I. M., Bellos V., Kopsiaftis G., Psiloglou B., Tsihrintzis V. A. (2021). Methodology for holistic assessment of grey-green flood mitigation measures for climate change adaptation in urban basins. Journal of Hydrology. https://doi.org/10.1016/J.JHYDROL.2021.126885.

Kourtis I. M., Tsihrintzis V. A. (2021). Adaptation of urban drainage networks to climate change: a review. Science of the Total Environment. https://doi.org/10.1016/j.scitotenv.2021.145431.

Liu H., Yang F., Wang H. (2023). Research on Threshold Selection Method in Wave Extreme Value Analysis. Water. https://doi.org/10.3390/w15203648.

Li Z., Tang G., Kirstetter P., Gao S., Li J.-L.F., Wen Y., Hong Y. (2022). Evaluation of GPM IMERG and its constellations in extreme events over the conterminous united states. Journal of Hydrology. http://dx.doi.org/10.1016/j.jhydrol.2021.127357.

Li Z., Tang G., Hong Z., Chen M., Gao S., Kirstetter P., Gourley J. J., Wen Y., Yami T., Nabih S. (2021). Two-decades of GPM IMERG early and final run products intercomparison: similarity and difference in climatology, rates, and extremes. Journal of Hydrology. http://dx.doi.org/10.1016/j.jhydrol.2021.125975.

Makkonen L. (2005). Plotting Positions in Extreme Value Analysis. Journal of Applied Meteorology and Climatology. http://dx.doi.org/10.1175/JAM2349.1.

Mann H. B. (1945). Non-parametric tests Against trend. Econometrica. https://doi.org/10.2307/1907187.

Moriasi D. N., Arnold J. G., Van Liew M. W., Bingner R. L., Harmel R. D., Veith T. L. (2007). Model evaluation guidelines for systematic quantification of accuracy in watershed simulations. ASABE -Engineering a Sustainable Future. http://dx.doi.org/10.13031/2013.23153.

Naghettini M., Pinto E. J. A. (2007). Statistical hydrology. Belo Horizonte: CPRM. 600p.

Nash J. E., Sutcliffe J. V. (1970). River flow forecasting through conceptual models part I: a discussion of principles. Journal of Hydrology. http://dx.doi.org/10.1016/0022-1694(70)90255-6.

Ogbozige F. J. (2022). Development of Intensity-Duration-Frequency (IDF) Models for Manually Operated Rain Gauge Catchment: A Case Study of Port Harcourt Metropolis Using 50years Rainfall Data). Engineering and Technology Journal. http://doi.org/10.30684/etj.2021.131839.1064.

Pérez-Zanón N., Casas-Castillo M. C., Rodríguez-Solà R., Peña J. C., Rius A., Solé J. G., Redaño Á. (2016). Analysis of extreme rainfall in the Ebre Observatory (Spain). Theoretical and Applied Climatology. http://dx.doi.org/10.1007/s00704-015-1476-0.

Pickbrenner K. P., Pinto E. J. A. (2018). Rainfall Atlas of Brazil: Intensity-Duration-Frequency Equations (Disaggregation of Daily Precipitation): rain-gauge station: Goiânia, code: 01649013 (ANA). CPRM. https://rigeo.sgb.gov.br/handle/doc/20802.

Ren H., Hou Z. J., Wigmosta M., Liu Y., Leung L. R. (2019). Impacts of spatial heterogeneity and temporal non-stationarity on intensity-duration-frequency estimates-A case study in a mountainous California-Nevada watershed. Water. https://doi.org/10.3390/w11061296.

Rodrigues D. T., Silva C. M. S., Reis J. S., Palharini R. S. A., Júnior J. B. C., Silva H. J. F., Mutti P. R., Bezerra B. G., Gonçalves W. A. (2021). Evaluation of the Integrated Multi-Satellite

Retrievals for the Global Precipitation Measurement (IMERG) Product in the São Francisco Basin (Brazil). Water. https://doi.org/10.3390/w13192714.

Rodrigues et al., organizers (2023). IDFGeo: web tool for acquiring IDF equations and project rainfall for monitored and non-monitored locations in the state of Rio Grande do Sul, Brazil: technical manual. [electronic resource]. Pelotas: POU. 36p.

Sam M. G., Nwaogazie I. L., Ikebude C. (2021). Improving Indian meteorological department method for 24- hourly rainfall downscaling to shorter durations for IDF modelling. International Journal of Hydrology. http://dx.doi.org/10.15406/ijh.2021.05.00268.

Shabankareh R. N. T., Abedini M. J. (2023). Implementation of a probability matching method in developing intensity–duration–frequency relationships for sub-daily durations using IMERG satellite-based data. Hydrological Sciences Journal. http://dx.doi.org/10.1080/02626667.2023.2229817.

Shamkhi M., Azeez M. K., Obeid Z. H. (2022). Deriving rainfall intensity–duration–frequency (IDF) curves and testing the best distribution using EasyFit software 5.5 for Kut city, Iraq. Open Engineering. https://doi.org/10.1515/eng-2022-0330.

Sherman, C.W. (1931). Frequency and Intensity of Excessive Rainfall at Boston, Mass. Trans. Am. Soc. Civil Eng. 95, 951–960.

Simonovic S. P., Schardong A., Sandink D., Srivastav R. (2015). A web-based tool for the development of Intensity Duration Frequency curves under changing climate. Environmental Modelling & Software. https://doi.org/10.1016/j.envsoft.2016.03.016.

Silveira A. L. L. (2000). Equation for rainfall breakdown coefficients. Brazilian Journal of Water Resources. http://dx.doi.org/10.21168/rbrh.v5n4.p143-147.

Tabari H. (2020). Climate change impact on flood and extreme precipitation increases with water availability. Scientific Reports. http://dx.doi.org/10.1038/s41598-020-70816-2.

Tanaka S. (2021). Comparison of AMS and POT Analysis with Long Historical Precipitation and Future Change Analysis Using “d4PDF”. In: Hoshino, N., Mano, S., Shimura, T. (eds) Pioneering Works on Extreme Value Theory. SpringerBriefs in Statistics(). Springer, Singapore. https://doi.org/10.1007/978-981-16-0768-4_5.

Torrico J. J. T. (1974). Hydrological practices. Rio de Janeiro: Transcon, 120p.

Vargas M. M., Beskow S., Moura M.M., Cunha Z. A., Beskow T. L. C., Silveira J. P. M. (2023). GAM-IDF: a web tool for fitting IDF equations from daily rainfall data. International Journal of Hydrology Science and Technology. https://doi.org/10.1504/IJHST.2023.131882.

Capítulo

6

6. CONSIDERAÇÕES FINAIS

6.1. Conclusões

Esta Tese teve como objetivo apresentar uma abordagem metodológica para a definição de equações IDF, de forma a contribuir com os estudos de chuvas intensas no Brasil. O foco foi promover a atualização das equações IDF para os municípios do Brasil, levando em consideração a lacuna do setor de drenagem, principalmente quanto ao déficit de informações. As equações IDF necessárias em muitas regiões são inexistentes ou estão desatualizadas. Sabe-se que ter dados atualizados é de grande importância para os sistemas de alerta de eventos de cheias e na avaliação da gravidade e extensão dos danos potenciais causados por esses eventos.

Os estudos desenvolvidos ao longo desta pesquisa demonstraram que as equações de chuva intensas, também conhecidas como equações IDF, para os municípios brasileiros apresentam grande heterogeneidade das relações IDF, não sendo, portanto, recomendado a utilização de equações que foram concebidas para uma localidade diferente de onde está sendo executado o projeto.

Também foi possível extrair desta pesquisa, através da avaliação de diferentes fontes de dados de produtos de estimativa de precipitação (dados oriundos de sensoriamento remoto), que o desempenho insatisfatório dos produtos de sensoriamento remotos deve ser atribuído principalmente a regiões de alta elevação (a precipitação é extremamente variável e há mudanças na distribuição de chuvas) e regiões costeiras (mudança repentina de elevação), onde esses produtos não conseguiram ter um bom desempenho em comparação com as observações dos pluviômetros, especialmente na escala diária. Isso acaba limitando, para a realização de estudos, projetos hidráulicos, aplicações em modelos hidrológicos, entre outras aplicações, a utilização desses produtos nessas localidades.

Em relação a utilização de bases de dados, ferramentas e procedimentos analíticos, a ferramenta de apoio à gestão das águas pluviais, denominada GEOT-IDF Equations, apresentou resultados promissores. Isso foi possível devido ao seu algoritmo, que é composto por um conjunto de distribuições de probabilidade e equações IDF. Outro ponto positivo da ferramenta é que ela trabalha com diferentes conjuntos de dados de precipitação (por exemplo, dados de sensoriamento remoto), permitindo que o usuário faça uma série de análises integradas sobre chuvas intensas. Além disso, a ferramenta possibilita a obtenção/atualização das equações IDF para todo um estado do Brasil, agilizando o estudo de chuvas intensas no estado.

6.2. Limitações

De forma geral, os resultados desta Tese são fundamentais para a formulação de estratégias de gestão das águas pluviais no Brasil, como na definição de projetos de mitigação de cheias. Apesar disso, existem melhorias e aprimoramentos que podem ser desenvolvidos em trabalhos futuros.

No âmbito do emprego de modelos climáticos globais na definição de equações IDF para o futuro, o produto CLIMBra baseia-se no conjunto de dados meteorológicos interpolados com dados de campo, o que traz um erro embutido. Por isso, há dificuldade destes modelos reproduzirem as particularidades de regiões como o semiárido com chuvas intensas de curta duração, o que numa escala sub-diária precisa ser bem representado. Portanto, uma análise de desempenho deve ser conduzida para averiguar se esses conjuntos de dados são capazes de simular dados *in-situ* para a qual se pretende desenvolver equações IDF para o futuro.

Outro detalhe importante é que a ferramenta gera as equações IDF independentemente se a o teste Mann-Kendall relatar tendência ou não na série temporal de precipitação, cabendo ao usuário considerar ou não a equação IDF gerada.

Por fim, outro aspecto que merece atenção e pode ser trabalhado futuramente diz respeito aos coeficientes de desagregação da precipitação diária, tendo em vista que, nesta Tese, foram considerados coeficientes que podem não refletir a realidade em virtude das mudanças nos padrões de precipitação observados nos últimos anos, apesar desses coeficientes serem bastante difundido no Brasil. Sendo assim, há uma oportunidade de avançar nesta área para que os coeficientes de desagregação sejam mais representativos da realidade atual, com suas mudanças de clima e de usos e ocupação que tem causados as alterações do regime pluviométrico e da intensidade das chuvas, principalmente, no que tange a eventos extremos.

6.3. Recomendações

Como recomendações para trabalhos futuros, seria de todo pertinente realizar uma análise de resíduos entre os dados interpolados com o valor obtido com os dados *in-situ* do artigo apresentado no Capítulo 3, além de detalhar os procedimentos metodológicos empregados no método de interpolação (modelo, ajustes etc).

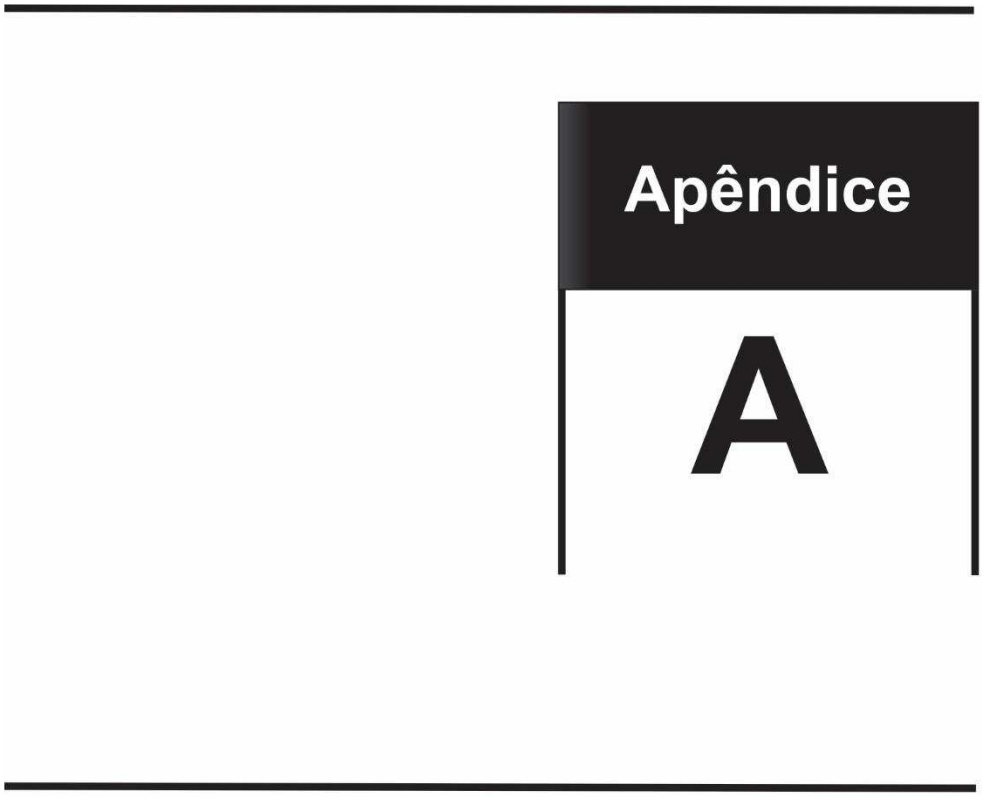

APÊNDICE A - EQUAÇÕES IDF PARA TODO O TERRITÓRIO DO ESTADO DA PARAÍBA

Estação	a	b	c	d
Água Branca	979,66	0,149	13,02	0,793
Aguiar	1286,33	0,116	13,07	0,794
Alagoa Grande	783,20	0,184	13,00	0,771
Alagoa Nova	1024,52	0,121	12,75	0,793
Alagoinha	791,38	0,238	13,10	0,774
Alcantil	758,20	0,137	12,38	0,761
Algodão de Jandaira	687,83	0,177	12,44	0,755
Alhandra	1433,09	0,144	13,07	0,793
Amparo	1110,16	0,209	12,52	0,782
Aparecida	991,75	0,155	12,40	0,775
Araçagí	917,01	0,180	12,60	0,782
Arara	727,15	0,150	12,59	0,759
Araruna	998,82	0,154	12,43	0,789
Areia	1051,81	0,152	13,00	0,791
Areial	945,16	0,113	14,90	0,809
Aroeiras	651,93	0,195	12,71	0,752
Baia da Traição	1365,25	0,146	12,67	0,781
Bananeiras	953,91	0,166	13,15	0,789
Barra de Santa Rosa	740,05	0,167	11,75	0,755
Barra de Santana	634,20	0,231	12,74	0,756
Barra de São Miguel	828,30	0,204	12,37	0,772
Bayeux	1337,43	0,181	12,98	0,787
Belém	882,72	0,211	12,56	0,780
Belém de Brejo do Cruz	1010,21	0,197	12,72	0,784
Boa Ventura	1277,56	0,116	12,22	0,776
Boa Vista	879,60	0,152	12,57	0,782
Bom Jesus	1146,93	0,188	12,76	0,785
Bom Sucesso	1051,22	0,129	13,12	0,792
Bonito de Santa Fé	1032,25	0,162	13,04	0,787
Boqueirão-Açude	647,86	0,248	11,29	0,739
Borborema	969,43	0,176	13,08	0,789
Brejo do Cruz	1010,21	0,197	12,72	0,784
Brejo Santos	1106,93	0,130	13,10	0,792
Caaporã	1290,41	0,217	12,87	0,787
Cabaceiras	798,96	0,313	14,19	0,801
Cabedelo-Cagepa	1494,08	0,145	12,60	0,794
Cabedelo-Emater	1624,73	0,117	12,90	0,796
Cachoeira dos Índios	1111,75	0,118	13,03	0,796
Cacimba de Areia	1170,35	0,175	12,19	0,776
Cacimba de Dentro	874,03	0,111	12,76	0,779
Cacimbas	1437,75	0,115	13,12	0,797
Caiçara	728,77	0,174	12,18	0,755
Cajazeiras	1019,81	0,237	13,18	0,777
Cajazeiras-Engenheiro	1177,76	0,155	12,91	0,789

Estação	a	b	c	d
Cajazeiras-Lagoa	1137,00	0,191	12,71	0,784
Cajazeirinhas	981,80	0,249	12,93	0,782
Caldas Brandao	1033,44	0,136	13,06	0,794
Camalaú	941,17	0,183	12,62	0,785
Campina Grande-Açude de Dentro	706,03	0,240	11,96	0,754
Campina Grande-Embrapa	765,95	0,137	12,74	0,765
Campina Grande-Massapé	641,66	0,263	12,82	0,759
Campina Grande-São José	695,46	0,169	12,21	0,753
Capim	1110,29	0,155	12,70	0,790
Caraúbas	715,80	0,220	12,53	0,762
Carrapateira	1403,36	0,129	12,81	0,795
Casserengue-Salgado	659,21	0,128	12,62	0,739
Catingueira	1058,99	0,181	12,80	0,783
Catolé do Rocha	974,85	0,187	12,70	0,784
Catolé do Rocha-Técnica	1095,72	0,134	12,90	0,794
Caturité	668,02	0,189	11,81	0,747
Caturité-Fazenda	866,40	0,233	12,02	0,771
Conceição	1072,71	0,108	13,01	0,793
Condado	961,43	0,260	13,15	0,779
Conde	1321,46	0,194	12,63	0,782
Conde-Gramame	1388,93	0,104	13,09	0,796
Congo	917,14	0,185	12,20	0,780
Coremas	1287,72	0,108	12,79	0,792
Coxixola	1205,77	0,168	12,24	0,786
Cruz do Espirito Santo	1198,41	0,111	13,08	0,798
Cubatí	745,54	0,196	11,86	0,758
Cuité	888,64	0,217	12,50	0,779
Cuité-Mamanguape	1204,48	0,067	12,82	0,803
Cuitegí	925,80	0,146	12,51	0,784
Curral de Cima	953,03	0,231	12,42	0,784
Curral Velho	1163,43	0,134	13,03	0,789
Damião	711,39	0,164	11,94	0,752
Desterro	1101,60	0,204	12,80	0,785
Diamante	1108,75	0,150	12,68	0,790
Dona Inés	573,87	0,190	10,23	0,704
Duas Estradas	975,37	0,120	13,04	0,788
Emas	1174,09	0,129	13,00	0,795
Esperança	849,27	0,122	12,31	0,773
Esperança - São Miguel	681,14	0,217	12,90	0,760
Fagundes	831,02	0,194	12,68	0,775
Frei Martinho	827,54	0,217	11,29	0,759
Gado Bravo	768,63	0,129	12,71	0,765
Gado Bravo-Fazenda	689,15	0,100	12,41	0,739
Guarabira	1117,01	0,114	13,04	0,798

Estação	a	b	c	d
Gurinhém	854,47	0,174	12,80	0,779
Gurjão	1017,51	0,180	12,07	0,785
Ibiara	1149,03	0,155	12,36	0,787
Igaracy	1379,13	0,112	13,01	0,791
Imaculada	1128,95	0,130	12,84	0,794
Ingá	558,92	0,318	13,41	0,758
Itabaiana	910,31	0,181	12,59	0,783
Itaporanga	1306,73	0,189	12,82	0,785
Itaporanga-faz,	1173,18	0,219	12,46	0,781
Itapororoca	1116,68	0,121	13,02	0,796
Itatuba	785,46	0,189	12,46	0,768
Jacaraú	1051,58	0,159	13,03	0,786
Jerico	1000,09	0,093	13,10	0,788
Joao Pessoa-DFAARA	1629,70	0,089	11,69	0,770
Joao Pessoa-Mangabeira	1695,47	0,121	12,88	0,795
Joao Pessoa-Mares	1500,77	0,123	12,98	0,798
Joca Claudino	1010,30	0,154	13,03	0,791
Juarez Távora	836,27	0,177	12,80	0,777
Juazeirinho	1058,51	0,104	12,77	0,798
Junco do Seridó	1068,60	0,125	12,83	0,795
Juripiranga	989,47	0,189	12,83	0,786
Juru	1026,55	0,129	13,09	0,792
Lagoa	1098,22	0,116	13,09	0,794
Lagoa de Dentro	922,81	0,158	13,09	0,789
Lagoa Seca	903,99	0,154	13,06	0,786
Lastro	949,90	0,193	13,07	0,788
Lucena	1220,54	0,168	11,41	0,766
Mãe D´água	1139,26	0,119	13,10	0,797
Malta	1164,61	0,171	13,13	0,789
Mamanguape	1198,00	0,166	13,13	0,790
Mamanguape-Asplan	1361,13	0,164	13,12	0,789
Manaíra	1043,27	0,186	13,02	0,788
Mari	1142,73	0,112	13,10	0,796
Marizópolis	1106,03	0,128	12,65	0,782
Massaranduba	785,69	0,097	12,79	0,764
Mataraca	1192,53	0,147	11,83	0,759
Matinhas	688,27	0,274	13,04	0,765
Mato Grosso	1120,99	0,087	13,10	0,792
Mogeiro	660,23	0,179	12,88	0,751
Montadas	786,32	0,067	12,32	0,759
Monte Horebe	1121,15	0,103	13,10	0,797
Monteiro-Açude Porção	980,50	0,109	13,07	0,795
Monteiro-Embrapa	1102,05	0,112	12,95	0,795
Mulungu	694,87	0,230	12,93	0,762

Estação	a	b	c	d
Natuba	826,95	0,243	11,65	0,762
Nazarezinho	1162,73	0,092	13,14	0,786
Nova Floresta	790,82	0,291	12,94	0,775
Nova Olinda	1177,81	0,149	12,80	0,790
Nova Palmeira	727,13	0,197	12,12	0,758
Olho D´água	1265,13	0,121	13,08	0,796
Olivedos	677,14	0,178	12,49	0,756
Ouro Velho	1131,74	0,162	12,30	0,787
Parari	1023,66	0,261	12,15	0,772
Passagem	990,37	0,156	13,04	0,791
Patos	1034,50	0,199	12,68	0,784
Paulista	922,97	0,276	13,18	0,780
Pedra Branca	1042,65	0,220	12,59	0,781
Pedra Lavrada	806,99	0,189	12,27	0,768
Pedras de Fogo	1277,29	0,191	12,81	0,786
Piancó	979,14	0,182	12,82	0,784
Picuí	827,26	0,202	12,55	0,775
Pilar	771,99	0,423	15,55	0,817
Pilões	933,87	0,165	13,13	0,788
Pilõezinhos	1017,51	0,146	12,62	0,792
Pirpirituba	789,55	0,234	12,54	0,769
Pitimbu	1309,35	0,168	11,80	0,771
Pocinhos	581,03	0,247	12,69	0,747
Poço Dantas	944,87	0,221	13,11	0,787
Poço Jose Moura	1123,88	0,140	12,70	0,793
Pombal	1046,55	0,186	11,71	0,756
Prata	1047,22	0,184	12,94	0,787
Princesa Isabel	960,04	0,193	12,59	0,782
Puxinanã	714,52	0,169	12,65	0,760
Queimadas	673,08	0,222	12,69	0,759
Quixaba	1040,88	0,197	12,69	0,783
Remígio	792,15	0,188	12,35	0,767
Riachão	1028,96	0,149	12,59	0,793
Riachão do Bacamarte	759,78	0,209	12,23	0,763
Riacho dos Cavalos-EMEPA	749,69	0,195	11,49	0,754
Riacho dos Cavalos-Jenipapeiro	1033,56	0,123	12,27	0,777
Riacho Santo Antônio	775,81	0,115	12,62	0,764
Rio Tinto	1335,12	0,166	12,53	0,780
Salgadinho	759,51	0,325	13,37	0,776
Salgado de São Felix	869,68	0,189	13,01	0,782
Santa Cecilia	710,74	0,130	12,58	0,753
Santa Cruz	1007,91	0,140	13,07	0,793
Santa Helena	1073,75	0,198	12,71	0,784
Santa Inês	1130,92	0,197	12,47	0,782

Estação	a	b	c	d
Santa Luzia	826,44	0,115	12,26	0,769
Santa Luzia-Riacho	879,42	0,168	12,52	0,779
Santa Rita	1432,37	0,109	12,00	0,797
Santa Teresinha	1279,76	0,126	12,57	0,793
Santana de Mangueira	1035,89	0,141	12,95	0,792
Santana dos Garrotes	894,08	0,260	13,15	0,777
Santo André	1111,54	0,192	12,87	0,786
São Bentinho	916,06	0,242	13,23	0,789
São Bento	1052,36	0,137	12,04	0,766
São Domingos	1229,55	0,086	12,90	0,785
São Domingos do Cariri	810,68	0,203	12,33	0,770
São Francisco	1102,56	0,104	13,06	0,796
São José Brejo do Cruz	1073,63	0,153	12,70	0,793
São João do Cariri	960,01	0,238	11,99	0,774
São João do Rio do Peixe	1308,82	0,134	12,71	0,793
São João do Tigre	884,30	0,148	12,28	0,777
São José da Lagoa Tapada	611,36	0,217	8,19	0,654
São José de Caiana	1170,24	0,182	12,43	0,785
São José de Espinharas	1018,40	0,203	12,61	0,783
São José de Piranhas	1131,80	0,161	13,05	0,786
São José de Piranhas-Arapuã	1216,80	0,125	11,84	0,799
São José de Princesa	706,63	0,219	9,72	0,702
São José do Bonfim	1174,17	0,170	12,56	0,787
São João do Sabugí	891,93	0,178	12,55	0,781
São José dos Cordeiro	1363,13	0,150	11,83	0,792
São Jose dos Ramos	889,30	0,199	12,80	0,784
São Mamede	1104,23	0,122	12,88	0,794
São Miguel Taipu	1122,24	0,150	12,96	0,792
São Sebastião do Umbuzeiro	900,38	0,192	12,15	0,777
São Sebastião de Lagoa de Roça	827,18	0,170	12,56	0,773
São Vicente do Seridó	816,00	0,212	12,36	0,771
Sapé	1035,41	0,181	12,52	0,783
Serra Branca	960,54	0,195	11,90	0,779
Serra da Raiz	1201,27	0,094	12,88	0,797
Serra Grande	1148,26	0,155	13,12	0,783
Serra Redonda	728,49	0,202	12,74	0,764
Serraria	1011,84	0,178	13,07	0,789
Solânea	964,27	0,131	13,04	0,793
Soledade	726,62	0,198	12,16	0,758
Soledade-Fazenda Pend.	1027,95	0,197	11,98	0,783
Sossego	639,63	0,230	11,99	0,749
Sousa	1070,64	0,203	13,11	0,782
Sousa - São Gonçalo	1399,11	0,119	13,14	0,797
Sumé	1025,27	0,168	12,25	0,786

Estação	a	b	c	d
Sumé - Fazenda Banana	1284,50	0,109	12,26	0,798
Tacima	918,70	0,188	12,23	0,779
Taperoá	1168,79	0,140	12,63	0,792
Tavares	1049,05	0,138	12,72	0,793
Teixeira	1240,90	0,174	13,07	0,789
Triunfo	1169,19	0,119	13,04	0,796
Triunfo-Pilões	1083,27	0,089	12,66	0,806
Uiraúna	1139,89	0,103	13,12	0,796
Umbuzeiro	841,69	0,157	12,70	0,776
Várzea	970,72	0,172	12,68	0,789
Vieirópolis	1011,67	0,113	13,05	0,795
Vista Serrana	1143,40	0,133	12,69	0,788
Zabelé	1091,58	0,145	12,64	0,793